

Master Thesis in Geosciences

Reservoir characterization and modelling of the Louriña Formation, Portugal

Paralic sandstone bodies

Mona Nyrud



UNIVERSITY OF OSLO

FACULTY OF MATHEMATICS AND NATURAL SCIENCES

Reservoir characterization and modelling of paralic sandstone bodies

The Lourinha Formation, Lusitanian Basin, Portugal

Mona Nyrud



Master Thesis in Geosciences

Discipline: Petroleum Geology and Geophysics

Department of Geosciences

Faculty of Mathematics and Natural Sciences

UNIVERSITY OF OSLO

01.05.2007

© **Mona Nyrud, 2007**

Tutor(s): Johan Petter Nystuen and Michael Heereman

This work is published digitally through DUO – Digitale Utgivelser ved UiO

<http://www.duo.uio.no>

It is also catalogued in BIBSYS (<http://www.bibsys.no/english>)

All rights reserved. No part of this publication may be reproduced or transmitted, in any form or by any means, without permission.

Acknowledgements

Firstly I would like to thank my supervisor Johan Petter Nystuen for making me interested in this particular master thesis and for his great support and guidance. I would also like to thank Michael Heeremans for his assistance and patience concerning modelling with the PetrelTM software.

The field work was greatly improved with guidance from Ivar Midtkandal and Liv Hege Lunde Birkeland and with collaboration with Samuel Etta. Thanks to you all.

I would also like to thank all the people who have contributed ever so slightly with insight or answers which have helped me achieve this result. Every detail matters. And finally a big thanks to all of my friends for motivation.

Oslo, June 2007

Mona Nyrud

LIST OF CONTENT

	Abstract	9
1	Introduction	11
2	Paralic Environment	12
	2.1 Coastal- and Delta Plain	12
	2.2 Deltas	14
	2.2.1 Tide-dominated Deltas	14
	2.2.1.1 Fly River Tide-dominated Delta, Papua New Guinea	16
	2.3 Estuaries	17
	2.3.1 Ord River Estuary, Australia	20
	2.4 Alluvial Fans	22
	2.5 Floodplain	22
	2.5.1 Soil	22
	2.6 Alluvial Ridge	23
	2.6.1 Levee	23
	2.6.2 Crevasse Channels and splays	24
	2.6.3 Fluvial Channels	24
	2.6.3.1 Braided Channels	25
	2.6.2.3 Meandering Channels	26
	2.7 Bars	26
	2.7.1 Point- and Scroll Bars	28
	2.7.2 Tidal Sand Bars	31
	2.8 Paralic Environment: Application to the Lourinhã Formation	32
3	Sedimentary Structures	33
	3.1 Ripples and Dunes	33
	3.2 Tidal Signatures	35
	3.2.1 Tidal Bundles and Paired Mud Drapes	35
	3.2.2 Bundle Sequences	37
	3.2.3 Flaser Bedding	37
	3.2.4 Reactivation Surfaces	37

3.2.5	Bidirectional Current38
3.2.6	Inclined Heterolithic Stratification38
4	Geological Framework	<u>40</u>
4.1	Structural Evolution40
4.2	Sub-basins42
4.3	Stratigraphic Overview42
5	Methods	<u>45</u>
5.1	Field Work45
5.1.1	Possible Source of Errors Related to the Field Work46
5.2	Petrographic Analysis46
5.2.1	Possible Source of Errors Related to Petrophysical Analysis47
5.3	Reservoir Modelling47
5.3.1	Possible Source of Errors Related to Reservoir Modelling48
6	Facies	<u>49</u>
6.1	Facies A: Through Cross-stratified Sandstone with Tangential or Angular Toesets51
6.2	Facies B: Planar Cross-stratified Sandstone with Tangential or Angular Toesets52
6.3	Facies C: Heterolithic Through Cross-stratified Sandstone with Tangential Toesets and Mudstone Drapes54
6.4	Facies D: Lower Stage Plane Parallel Stratified Sandstone with Mudstone Laminae56
6.5	Facies E: Upper Stage Plane Parallel Stratified Sandstone57
6.6	Facies F: Ripple Laminated Sandstone57
6.7	Facies G: Apparent Massive Sandstone59
6.8	Facies H: Extrabasinal Conglomerate59
6.9	Facies I: Intrabasinal Conglomerate60
6.10	Facies J: Mudstone61
6.11	Facies K: Siltstone62
6.12	Facies L: Paleosol62
6.13	Facies M: Soft Sediment Deformed Sandstone63

6.14	Facies N: Shell Bank63
7	Facies Associations and Architectural Elements	65
7.1	FA 1: Channel Infill Deposits66
7.1.1	FA 1.1: Abandoned Channel Fill Deposits66
7.1.2	FA 1.2: Lateral Accretionary Elements and Point Bar Deposits68
7.1.3	FA 1.3: Mid-channel Bars or Sandflat Deposits71
7.2	FA 2: Floodplain Deposits72
7.2.1	FA 2.1: Floodplain Fines73
7.2.2	FA 2.2: Paleosols73
7.2.3	FA 2.3: Crevasse Splay Deposits75
7.3	FA 3: Overbank Deposits77
7.3.1	FA 3.1: Levee Deposits77
7.3.2	FA 3.2: Crevasse Channel Sandstone Deposits79
7.4	FA 4: Inclined Heterolithic Stratification (IHS)80
7.4.1	FA 4.1: IHS Elements with Sporadically Rhythmic Sandstone-mudstone Laminae80
7.4.2	FA 4.2: Elements with Centimetre to Decimetre Thick Inclined Heterolithic Strata83
7.4.3	Discussion on Formation of IHS Deposits84
7.5	FA 5: Marine Deposits85
7.5.1	FA 5.1: Shell Banks85
8	Petrographic Analysis	87
8.1	Mineral Composition and Recognition87
8.2	Texture92
8.3	Interpretation96
9	Architectural Style	98
9.1	Architectural Style98
9.1.1	Connectedness99
9.1.2	Variations in Connectedness100
9.1.3	Architecture and Connectedness of the Upper Louriñha Formation101

9.2	Alluvial Architecture and Base-level Fluctuations105
10	Heterogeneities	108
10.1	Megascale Heterogeneity110
10.2	Macroscale Heterogeneity110
10.3	Mesoscale Heterogeneity111
10.4	Microscale Heterogeneity112
11	Depositional Environment	113
11.1	Processes113
11.2	Paleocurrent Directions114
11.3	Autigenic and Allogenic Processes115
11.4	Estuarine versus Deltaic Deposits117
11.4.1	Previous Studies on Tidally Influenced Deposits117
11.4.2	Recent Studies on Tidally Influenced Deposits119
11.4.3	Discussion of the Depositional Environment of the Louriña Formation121
11.4.4	Summary of Discussion on the Depositional Environment123
12	Reservoir Modelling	124
12.1	Parameters125
12.2	Stochastic Object Models129
13	Discussion: Reservoir Evaluation	134
13.1	Depositional Factors134
13.2	Diagenetic Factors136
13.3	Summary: Reservoir Evaluation137
13.4	Application as Analogue to Statfjord Formation, North Sea138
14	Conclusion	139
15	References	140
16	Appendix	147

Abstract

The Lusitanian Basin in Portugal is an Atlantic margin rift basin on the western side of the Iberian plate positioned north of Lisbon. The basin contains, among several other formations, the Upper Jurassic Lourinhã Formation which has been the object of this study. The Lourinhã Formation consists of tidally influenced fluvial deposits formed in a paralic environment. The succession includes several thin shell banks interpreted to represent marine flooding surfaces of limited duration. A total of 14 facies have been recorded which are grouped into 5 facies associations of channel fill deposits, floodplain fines, overbank deposits, inclined heterolithic stratification (IHS) and marine deposits. Intertidal flats have not been identified.

The paralic depositional environment is thought to be either an estuary or a tide-dominated delta, though due to little to no control in the third dimension within a rather small study area, a legitimate conclusion can not be drawn from the study. Mineral content and paleocurrent direction data indicate 1st order derived granitic detritus from the Hercynian Basement horsts in the northwest, which are areas presently exposed as the Berlengas and Ferilhões Islands. The burial depth of the Lourinhã Formation does not exceed 3 km.

The succession can be divided into 5 section (S0-S1) based on the characteristic architectural styles where lower and upper boundaries are set to either paleosols or flooding surfaces. The sand:gross ratio and connectedness of the sandstone bodies can be linked to base-level fluctuations as these have exerted a major control on the accommodation space created

A stochastic object modelling is performed with the use of PetrelTM software where the studied stratigraphic succession is divided into 4 zones with different input parameters of channel-belt geometries, i.e. the fluvial deposits, in addition to the sedimentary logs. With the generated models it is possible to evaluate the properties of a theoretical reservoir with relevance to connectedness and heterogeneity on different levels. The models imply a possible stacked reservoir with high connectivity in Zone 1 and 3-4, though a possible thin barrier between Zone 3 and 4. Zone 2 composes a barrier between Zone 1 and 3.

Thin sections from rock samples collected from the study area shows that the porosity, and likely also the permeability, in the sandstone bodies are generally poor and not of reservoir quality due to extensive carbonate cement and mud filled pore throats.

1 INTRODUCTION

The paralic environment composes the transitional zone between continental and shallow marine setting and includes deltas, estuaries and coastal plain to shoreline-shelf systems, commonly affected by both fluvial-, tidal- and wave processes. The paralic environment has a major relevance to petroleum geology as the sand supplied by rivers can generate mostly small ($< 10 \text{ km}^2$), but significant reservoirs, e.g. Statfjord Formation in the North Sea ($< 100 \text{ km}^2$) (Reynolds, 1999). However, due to the many subenvironments present in a marginal-marine setting the sand can be arranged in a series of geometries which can be very complex and difficult to predict, e.g. fluvial channel, distributary channel, crevasse channel and splays, tidal bars, tidal channels, tidal flats and valley fill (Reynolds 1999). Studies of these sandstone bodies are therefore vital to comprehend the setting in which they have been generated and to predict their geometry and spatial variations.

The Lourinhã Formation of the Lusitanian Basin in Portugal is characterized by a fluvial depositional system with tidal influence generated in probably deltaic- or estuarine paralic subenvironment. It is difficult to achieve a 3D control of the study area as well as the true size of the architectural elements present, but this is commonly also the case with well data from subsurface reservoirs.

The scope of this paper is to gather field data to determine the facies, facies associations and architectural style of the Lourinhã Formation. The data collected from the study area will be used to argue for depositional environment, base-level fluctuations and, in addition to empirical relationship between channel depth, channel width and channel-belt width from analogue studies, predict the fluvial sandstone body dimensions for input parameters in the reservoir modelling by PetrelTM software. The reservoir potential will be discussed based on the data collection at hand, where levels of heterogeneity compose major controls.

2 PARALIC ENVIRONMENT

The paralic environment includes several environments and subenvironments deposited at or near sea-level in coastal plain to shoreline-shelf systems and are thus very sensitive to changes in relative sea-level, both when it comes to fluctuations in the shoreline, which separates marine and continental deposits, and resultant depositional elements within subenvironments, i.e. architectural style. These environments are deltas and delta plains, coastal plain, estuaries and incised valleys with associated distributary channels, tidal channels, crevasse splays, floodplains, lakes, beaches, bars, bay-head deltas etc. (Emery and Myers, 1996). A paralic setting is characterized by interaction between a primary transport of sediments to the ocean and basinal reworking by waves, storms and tides, though in some cases the primary sediment transport may be landward. Both deltaic coasts with fluvial input and non-deltaic, linear coasts can be described in terms of paralic settings, based on the dominant reworking process which controls the shape and development of the coastline (Reading and Collinson, 1996). The deltaic coasts have been classified in terms of dominant process and put into a triangular diagram with fluvial-dominated-, wave-dominated- and tide-dominated deltas at end points, respectively.

A full account of the paralic environment is not the scope of this paper and given that the paralic environment is of such a large extent and include many subenvironments, only a few which have possible relevance to the actual study, i.e. the landward part related to fluvial systems, delta plains and estuaries with tidal influence, will be further attended to.

2.1 Coastal- and Delta Plain

The delta plain can be divided into upper- and lower delta plain. Lower delta plain is characterized by being affected by both fluvial and tidal processes while the upper delta plain is more characterized by alluvial processes. The fluvial channels will evolve into distributary channels on the lower delta plain. Distributary channels differ from fluvial ones in the following ways:”

- i) Influenced by basinal processes in terms of tides and waves

- ii) Saltwater wedge may penetrate lower parts
- iii) Switching and channel avulsion is more frequent than in a pure fluvial setting
as the delta progrades and changes its gradient
- iv) The distributary channel sand bodies have generally a lower width/depth ratio
as they are relatively short lived and do not easily migrate laterally”

(Reading and Collinson, 1996).

In interdistributary areas there are swamps and/or marshes, floodplains, tidal flats, lakes etc. In humid and tropical areas, saltwater and freshwater peat swamps are common on the delta plain, and organic detritus can substitute “mud drape” with “coal drape” in a tidal setting. Arid regions are more characterized by evaporites and abundant mud cracks (Dalrymple, 1992).

Tidal channels are common in tide-dominated deltas and estuarine settings where the tidal range is high. They are sourced from the sea and not by the fluvial system. They are large, sinuous channels with high degree of branching which spread out on the adjacent plains (Fig. 2.1). Some will drain back during ebb tide.



Fig. 2.1: A complex tidal channel system near the Ord River, Australia. From Google Earth™.

The coastal plain is the landward part from the shoreline and will lack major river systems like in a delta plain setting; a more linear coastline of strand plains and tidal flats can be expected.

2.2 Deltas

Deltas are characterized by progradation and form normally during relative sea-level fall or stillstand, but can also be formed during rising relative sea-level if the sediment discharge is large.

Galloway (1975) proposed a classification system for deltas based on dominant processes and suggested a triangular classification diagram with fluvial-dominated-, wave-dominated- and tide-dominated deltas at the three end points.

2.2.1 Tide-dominated Deltas

Tidal deltas tend to occur in narrow straits where the tidal current is strong (Klang-Langat delta, Malaysia) or in the heads of embayments where the tidal range is amplified. In the latter case the subaqueous part of the delta is characterized by tidal sand bars oriented with a high angle to the coastline. These tidal sand bars are best developed in the inactive areas of the delta where the fluvial discharge is small. The subaerial part of the delta has broad tidal flats and adjacent marshes or sabkha which are dissected by tidal high sinuous channels and large degree of branching. The tidal channels are particularly abundant in the inactive part of the delta plain. Progradation of the delta causes the distributary channels to erode and truncate the sand bars.

The abandoned part of the delta may undergo local transgression with estuarine trends like erosionally based and fining upward tidal ridges, flood-oriented cross-stratification rather than ebb-oriented and common shell accumulation. In any case the tidal sand bars will be overlaid by finer tidal flat sediments. The geometry of a tide-dominated delta is illustrated in Fig. 2.2 (Dalrymple, 1992).

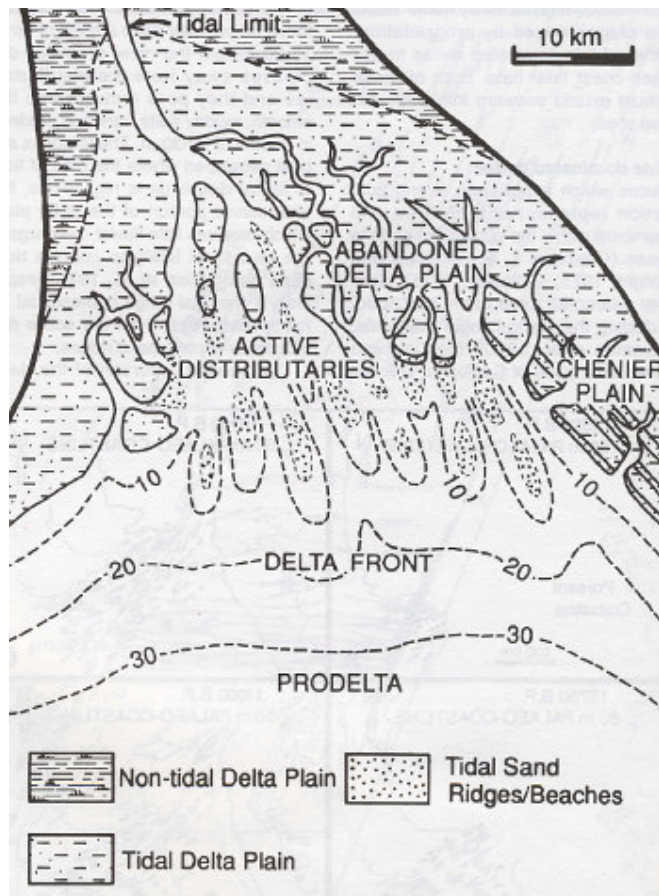


Fig. 2.2: The geomorphology of a tide-dominated delta. From Dalrymple (1992).

The deposits resulting from a tidally influenced delta should have clinoform geometry with clinoforms downlapping with a dip of $\sim 0,1-10^\circ$ onto a maximum flooding surface. The delta succession shows an upward coarsening and shallowing trend in facies due to progradation of the delta. The sand ridges or bars deposited will be eroded by distributary channels as well as from tidal currents. Deltas also tend to have large scale synsedimentary deformation like growth faults, mud diapirs, slumps and escape structures (Bhattachayra and Walker, 1992).

2.2.1.1 Fly River Tide-dominated Delta, Papua New Guinea

The Fly River delta is a classical modern tide-dominated delta positioned in the southeastern portion of Papua New Guinea (Fig. 2.3), where the climate is tropical and wet with seasonal variations. The tropical climate generates, by the high degree of chemical weathering, a great deal of silt and mud which is in suspension throughout the system. The river has a very low gradient which results in rapid deposition of coarser material in proximal areas, aggradation of channel and levees, and blockage of channels.



Fig. 2.3: Fly River delta, Papua New Guinea. From Google Earth™.

The Fly River delta has three main distributary channels merging into a tidal-fluvial channel. The tides are mixed semidiurnal and diurnal. The tidal range has a maximum at the transition from distributary to tidal-fluvial of 5,1 m during spring, i.e. macrotidal. The tidal influence extends 400 km inland. Though the main distributary channel is ebb dominated and connected to the river channel, distributary channels are subdivided into a series of ebb- and flood-dominated subchannels, separated by elongated tidal sand ridges.

Generally the deposits are heterolithic with sand and coarse silt and mud interbedded. Coarse-grained channel-floor deposits are mainly found in proximal areas. Here dunes can

also be found in channel reaches where the bed load has large enough grain size to reach the dune stability field. Mudstone-pebble conglomerate is commonly present directly above an erosional surface. Pieces of wood or shell fragments in more seaward areas can be found among these rounded mudstone-pebbles that have diameters of 0,5-1 cm.

Elongated tidal channel-bars or point bars form in channel segments. Both types of architectural elements can be characterised as low angular lateral accretionary deposits. These deposits are constituted of millimetre to centimetre thick inclined heterolithic stratification of mud and sand. Slump structures and ripples are common. Quasi-regular sandstone-mudstone cycles may be due to tidal variations, but this is not a clear tidal signature in the Fly River delta (Dalrymple *et al.* 2003).

2.3 Estuaries

The most accepted definition of an estuary is that of Dalrymple *et al.* (1992) who define it as “the seaward portion of a drowned valley system which receives sediments from both fluvial and marine sources and which contains facies influenced by tide, wave and fluvial processes. The estuary is considered to extend from the landward limit of tidal facies at its head to the seaward limit of coastal facies at its mouth”.

From this definition, it follows that an estuary can only form during transgression, and that it is affected by both marine- and fluvial processes and a mixture of these. Thus, estuaries can be divided into wave-, tide- and fluvial dominating estuaries.

A wave dominated estuary will characteristically have a sandy barrier at the outer part and a central basin of very low energy which accumulates mud. Where the fluvial process is strong, a small bay-head delta will prograde into the central basin of the estuary, often with bird-foot morphology, though this is not always the case.

The focus here will be on the tide-dominated estuary. Energy diagram, morphology and depositional elements of a tide-dominated estuary is shown in Fig. 2.4 a, b and c, respectively (Dalrymple *et al.* 1992). In this type of estuary the tidal processes dominate at the mouth of the estuary and elongated sand bars may develop with a variety of dunes

superimposed. Where these bars shift laterally a fining upward trend is expected. Due to the funnel shape the tidal current will increase in strength headwards generating extensive sandflats with parallel lamination. Further headwards, cross-stratification with mud drape may become more abundant. The tidal limit will lay possibly tens to hundreds of kilometers inland, above the tidally influenced fluvial system of straight-meandering-straight geomorphology (Dalrymple *et al.* 1992; Dalrymple, 1992). Inclined heterolithic stratification may be present in the tidally influenced meanders here. Since a tide-dominated estuary is sourced both by the river and the shelf, the grain sizes are coarsest at the mouth and at the head of the estuary (Dalrymple, 1992). The lower straight reach of the river has a net sediment transport headwards, while the inner straight part has a net sediment transport basinwards. Bay-head deltas are not present in tide-dominated estuaries, though tidally influenced bay-head deltas exists (Dalrymple *et al.* 1992). Adjacent to the axial estuary channel, tidal flats and marshes are present.

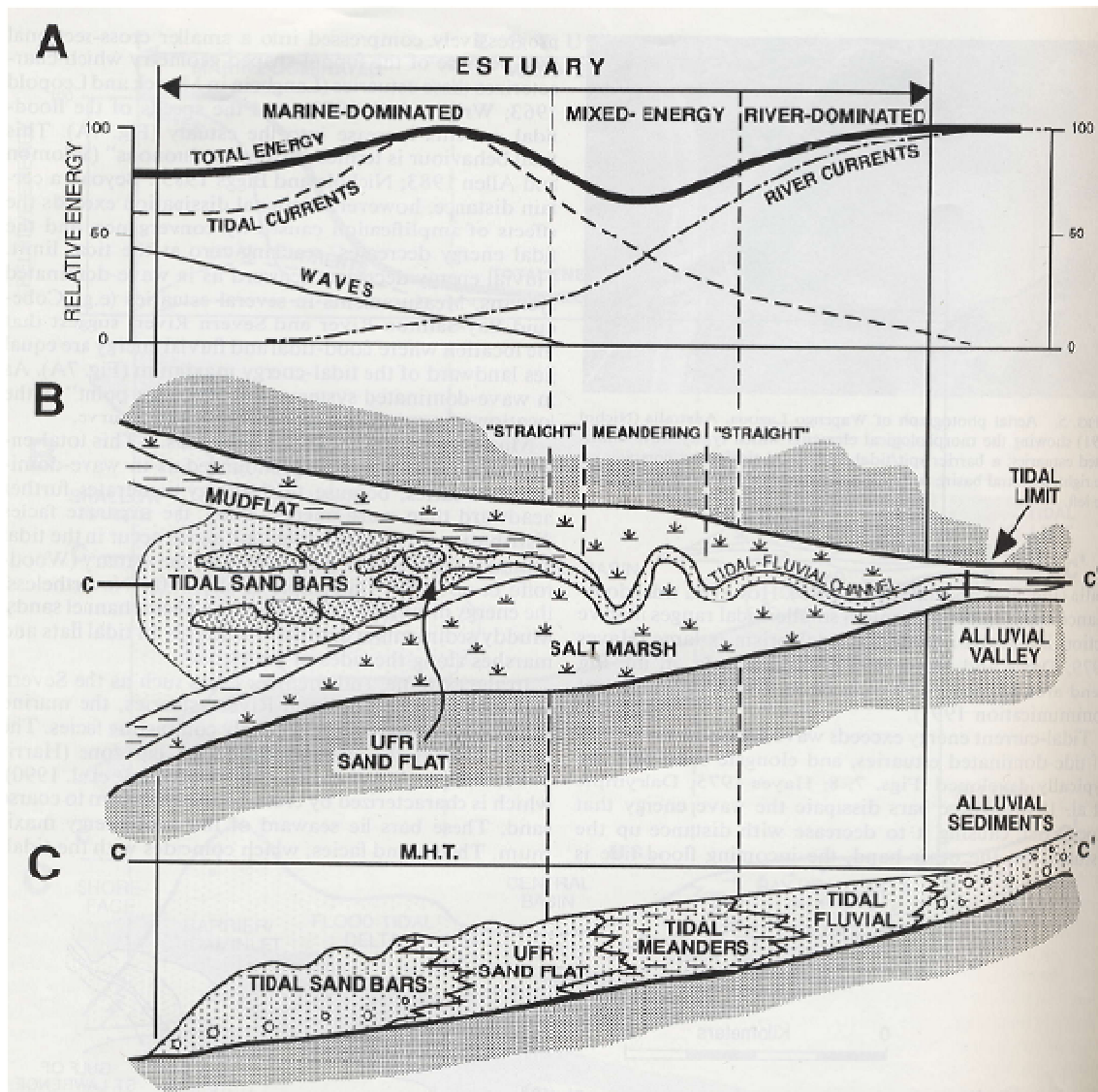


Fig. 2.4: Tide-dominated estuary A: The energy distribution of the marine-and fluvial components. B: Overview of depositional setting and distribution. C: A cross-sectional view along the axis of the estuary showing depositional elements. From Dalrymple *et al* (1992).

As the estuary is in a transgressive setting, there will be a landward shift of facies and a superposition of the deposits in Fig. 2.4 c. First there will be a general fining upward trend from sand or gravel to interbedded sands and mud of the inner estuary, which will be overlain by fine-grained parallel laminated sand and coarser cross-stratified sand from the elongated sand bars. Sand bars can be interbedded with mud flat or marsh sediments, and local erosion surfaces and deposits from tidal channels are expected. The latest stage in an

estuarine infill is a progradational upward-fining unit from tidal sand bars to parallel laminated sand and mud flat or marsh deposits on top (Dalrymple, 1992).

It should be noted that the morphological distinction between tide-dominated estuaries and deltas is not well documented (Dalrymple, 1992). Several debates in literature have addressed the recognition of ancient tide-dominated deltaic deposits versus estuarine deposits. This subject will be touched upon in a later chapter (Ch. 11.4).

2.3.1 Ord River Estuary, Australia

The Ord River lies within a hot, dry tropical climate with seasonal variation in discharge, resulting in a deficit in water balance most of the year. Its average tidal range is 3,80 m and average spring tide 5,15 m, though the geometry of the gulf amplifies the range to average 4,75 m and 6,60 m during spring tide. The lower region of the Ord River has funnel shaped geometry with elongated tidal sand ridges in its seaward portion. These ridges can be of 10-22 m in height, 2 km in average length and 300 m of width. Several bars are also present within the channel. Tidal sand ridges and distributary mouth bars are sandy deposits of high lateral continuity (Fig. 2.5).

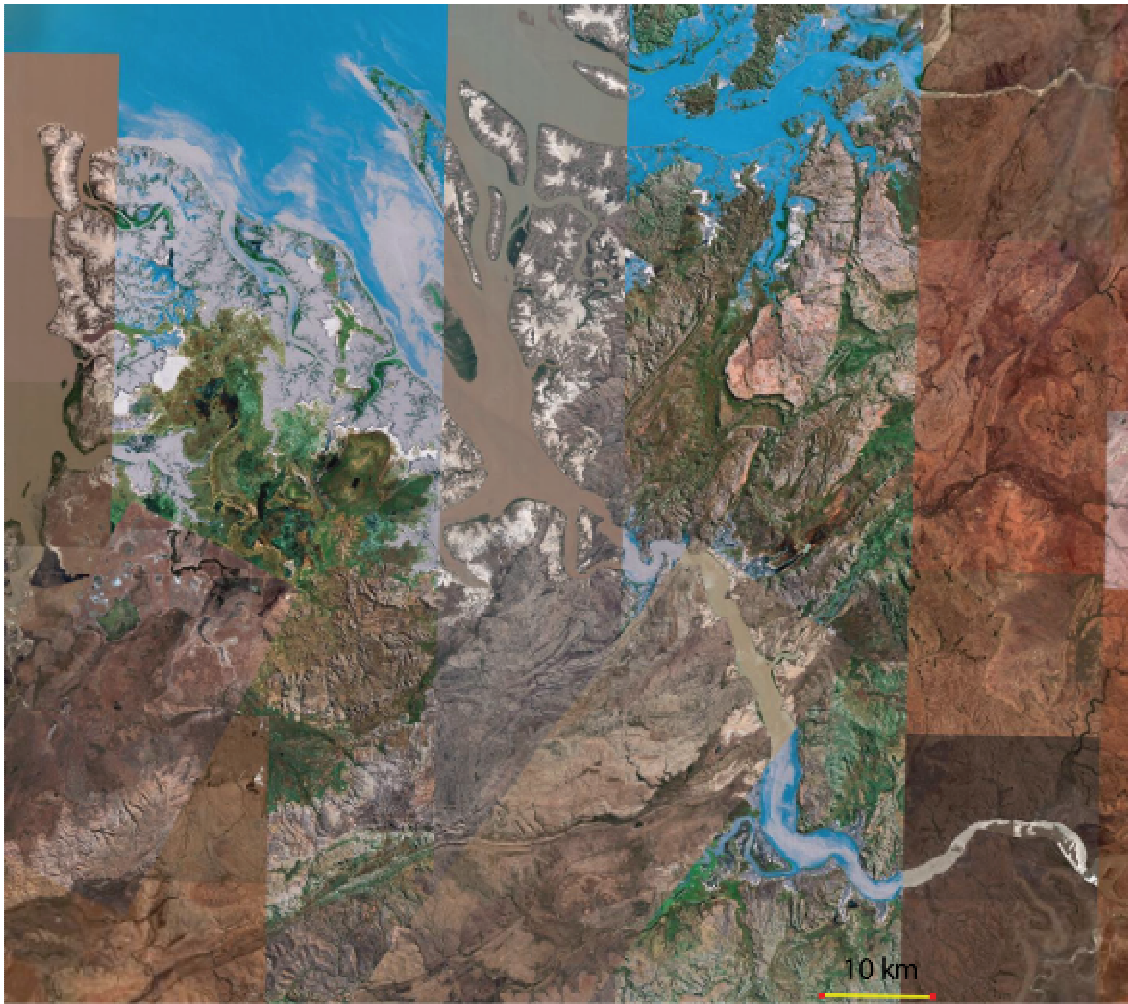


Fig. 2.5: The Ord River, Australia. From Google Earth™.

Bedforms indicate a flood-dominant current in the shallower parts, which will lead to clogging of the channel, but ebb-dominant current in the deeper parts. Mud-cracks and evaporites are common in the intertidal- to supratidal areas and adjacent plains. Tidal channels which branch out on the delta plain can deposit sandy material of 3-12 m thickness. Large scale bidirectional cross-stratification is common on the seaward side of the tidal ridges which grades landward into channel-fill deposits, with a dominant landward oriented cross-stratification. In the subaerial part burrowing and dessication structures are present.

2.4 Alluvial Fans

An alluvial fan is a distributary fluvial system where the fluvial system fans out from a point source, e.g. canyon mouth. On an alluvial fan avulsion occurs during events of flood and high discharge resulting in shifting of the depositional lobe. Most depositional units which have been interpreted alluvial fans are coarse-grained and poorly sorted, though this is not always the case, e.g. Kosi fan in India which grades from boulders to mud (Miall, 1992).

2.5 Floodplain

Floodplains lie adjacent to a stream channel and receive sediments during seasonal floods. Floodplains can be up to twenty times the width of the channel-belt (Bridge, 2003). Floodplain deposits consist normally of mud and silt deposited from suspension during flood events, though can have lenses or sheet of sand embedded in them, e.g. pond, lake with lacustrine deltas, crevasse splay deposits, and in addition coal and calcrete. Root structures are common in floodplain deposits. The geometry of floodplain deposits are mostly sheet-like (Miall, 1985).

2.5.1 Soil

Soil profiles can be recognized by horizons characterized by features like i) leaching leading to colour change and mottling due to presence or absence of iron minerals, ii) bioturbation, iii) root structures characterized by branching and often colouration, and iv) development of calcrete. Calcrete (caliche) forms by chemical or biochemical precipitation of micritic calcium carbonate from the groundwater when evaporation exceeds precipitation. As the carbonate becomes replacive and displacive, carbonate nodules form. This process is expected to take about 1000 years and up to 10 000 years for a well developed paleosol with calcrete nodules (Bridge, 2003), thus making this a very good correlation surface. Paleosol is the term applied to buried and ancient soil horizons.

2.6 Alluvial Ridge

Bridge (2003) described the alluvial ridge as a positive relief above flood basin lowlands with composition of “i) active and abandoned channels and bars showing accretion topography; ii) levees; and iii) crevasse splays and channels”, thus comprising the channel and near channel deposits (Fig. 2.6).

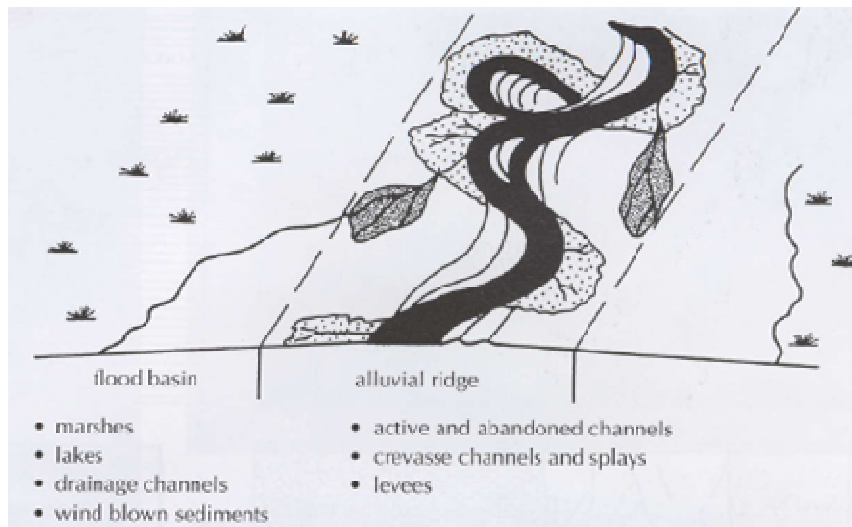


Fig. 2.6: The alluvial ridge and adjacent floodplain area. From Bridge (2003).

2.6.1 Levees

Levees develop discontinuously along the channel banks and can have a series of geometries, e.g. wedge-shaped, straight, sigmoidal, concave up, or convex up. Several minor strata sets of centimetres to decimetres thickness can build levees of decimetres to meters height and a width four times its associated channel. Levees will have finer material as it grows higher and wider and thus be transitional to the floodplain. Sandy levees can have planar lamination in flood generated strata sets: convolute lamination, ripple lamination, bioturbation, root structures, and can have a fining upward or coarsening upward trend representing abandonment or migration across the floodplain, respectively. Its facies can be similar to upper channel-bar deposits.

2.6.2 Crevasse Channels and Splays

Occasionally a crevasse event breaks through the levee, initiating a series of small crevasse channels and a sheet-like crevasse splay which expand over the floodplain. Crevasse channels are close to the main stream, but rather small and shallow relative to; though have channel geometry with concave-up, erosive channel floor (Miall, 1985). Crevasse channels are ephemeral channels which are active during floods. Their channel infill material consists generally of silt to sand and can be either upwards fining or upwards coarsening, depending on whether the succession represents the stage of abandonment or the infill stage during progradation and formation of a new channel course, respectively (Miall, 1985). Small scale cross-stratification and ripple cross-lamination are common sedimentary structures.

Crevasse splays have dimensions relative to the stream channel to which they are associated and can be of hundreds of meters to several kilometers long and wide near large rivers. Crevasse splay deposits can be difficult to distinguish from levees, particularly when concerning the distal part, though crevasse splays are normally coarser and thicker than levee deposits. Crevasse splay deposits can also consist of several strata sets. Commonly, medium scale cross-stratification and plane parallel lamination have climbing- and current ripple lamination superimposed which represent waning flow conditions. Mud cracks, root structures and bioturbation may be present (Bridge, 2003).

2.6.3 Fluvial Channels

A channel can be described by its depth, depth/width ratio and its sinuosity. The general shape of a channel in cross section will be a concave-up erosional base, often with a conglomeratic lag (Miall, 1985). The sedimentary channel fill is often of fining upward unit containing sand and sandstone facies with structures like i) massive or planar parallel lamination, formed from high velocity flows; ii) through cross-stratification, from migration of dunes; iii) planar cross-stratification, from migration of simple bars; and iv) ripple lamination due to waning flow. Large channels can have a multistorey fill including several erosional surfaces with sand and/or mud fill.

Though a general description can be given of a channel succession, fluvial channel units occur in different settings with different morphology and characteristics. The fluvial system comprises four types of main channels of different styles: i) braided, ii) meandering, iii) straight and iv) anastomosing, depending on grain size, total amount of transported material, proportion between bed load and suspended load, slope gradient, water discharge, discharge pattern and weather it is ephemeral or perennial (Bridge, 2003). Straight and anastomosing channel morphologies are rather uncommon and will not be discussed further here.

2.6.3.1 Braided Channels

Braiding of river channels normally occurs in coarse-grained to sandy bedload rivers of low sinuosity with weak non-cohesive banks, or when streams have variable discharge e.g. in connection with seasonal discharge or ephemeral flows. As bedload accumulates on the channel floor, longitudinal bars develop, thus split and redirect the river (Collinson, 1996; Miall, 1977). Different types of bars can develop in the downward accretionary- or lateral accretionary direction, generally with related cross-stratification in the accretionary direction, thus a bar can have a complex development of deposition and erosion and sets of cross-stratification obliquely to each other. The channel geometry of a braided river may be rather sheet-like as the width/depth ratio of these can be very large (Miall, 1985). Braided river systems do not normally have large floodplain areas associated with them, as the channel is not very stable and migrates laterally quite frequently. Nevertheless, these rivers carry a large amount of suspended load, particularly during flood stages. During extensive overbank flooding fine-grained material can be deposited above abandoned channel sandstone strata of the alluvial plain. In cases where the braided streams are due to variation in water discharge and not to grain size, floodplain deposits may be more common and extensive (Miall, 1977). Bridge (2003) disagreed with Miall (1977) regarding the mechanism of formation of floodplains and stated that “floodplains develop independent of channel pattern and in all alluvial valleys, on alluvial fans and on deltas”.

Deposits from braided rivers are expected to be rather coarse-grained with structures like cross-stratification from bar development and migration, imbrication of pebbles and stones and a lack of large finely-grained floodplain deposits and channel margins, in addition to rather high width/depth ratio of channel and resulting deposits (Miall, 1996).

2.6.3.2 Meandering Channels

The meandering river system is characterized by high amounts of suspended load, as well as sandy bedload (though possible some gravel). Meandering rivers flow with a high sinuosity in discrete belts on low gradient alluvial plains (Collinson, 1996; Emery and Myers, 1996). The meandering channel migrates within its belt by eroding its outer bank and depositing on its inner bank. The channel is rather stable as it commonly is surrounded by cohesive fine-grained material with well developed levees and thus do not braid easily. As the sinuosity increases channel avulsion will eventually occur, leaving an abandoned channel to be an oxbow lake. During flood or high discharge fine-grained material may be deposited on the floodplain, or levees may be broken creating crevasse channel and splays in which both can initiate avulsion (Collinson, 1996). Point bars are lateral accretionary bars associated with high sinuous channels and are discussed further below.

2.7 Bars

Bars in the fluvial environment are depositional forms, or architectural elements, which develop in different sizes on the channel floor or along the sides of the channel. According to geometry and position relative to the channel segment, bars are variously named as e.g. longitudinal-, linguoid-, transverse- lateral- and point bars. Miall (1977) suggested a simple classification of three types of bars of e.g. different geometry, grain-sizes, occurrence and internal structure (Table 2.1).

Table 2.1: Bar types and their characteristics. From Miall (1977).

Bar Type	Lithology	Internal Structure	Height	Length	Bedform Rank	Common Name	Occurrence
1) Planar massive bedded bars	Gravel	Planar stratified or massive. Imbrication	1m or Less	Several hundred meters	Mesoform	Longitudinal bars	Dominant bar form in gravel, rivers, e.g. proximal braided streams
2) Simple forest bars	Usually sand, rarely gravel	Planar cross-stratification	Typically 0.5 – 1m	Several hundred meters	Mesoform	Linguoid-, transverse-, lobate-, chute-bars	Dominant bar form in sandy braided rivers, rarely present in gravel rivers
3) Compound bars	Sand or gravel	Complex, with several cross-stratification types and internal erosion surfaces	Equal to channel bankfull depth	Hundreds to thousands of meters	Macroform	Point-, side-, lateral-,	Occur in all types of rivers, but best developed in sandy meandering systems

Large scale inclined strata can be associated with downward accretionary of bars in braided or unbraided rivers and can be recognized on a large scale by vertical changes in grain-size and sedimentary structures, where fining upward is a general trend and ripples and dunes are commonly superimposed bar strata. Tidal influenced bars can often be confused with intertidal-flats or coastal bays, as its upper part often contains relative large amounts of finer material (Bridge, 2003). An illustration of a simple braided channel with a downward accretionary bar and channel switching is shown in Fig. 2.7. The downstream portion of the bar has higher preservation value than the stoss side.

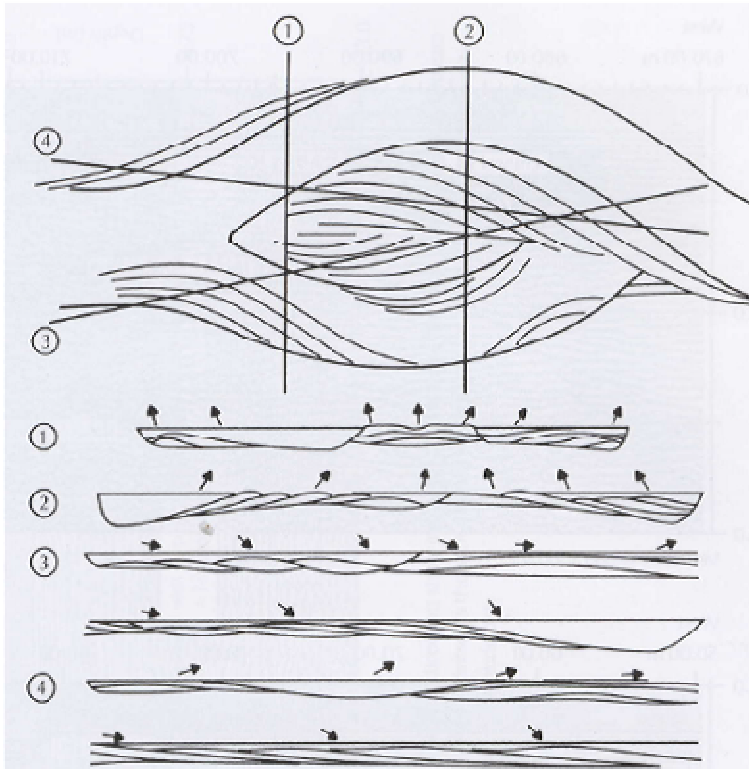


Fig. 2.7: Geometry of a downward accretionary bar with different cross-sections shown. From Bridge (2003)

2.7.1 Point- and Scroll Bars

Point bars are lateral accretionary bars which develop on the inner bank of a meandering river as helical flow creates a vertical circulation cell normal to the stream banks Fig. 2.8 (Boggs, 2001), where highest depositional energy is closest to the channel and decrease upwards due to shear stress, thus depositing a fining-upward element in general, though this trend is not always the present (Miall, 1978; Miall, 1977).

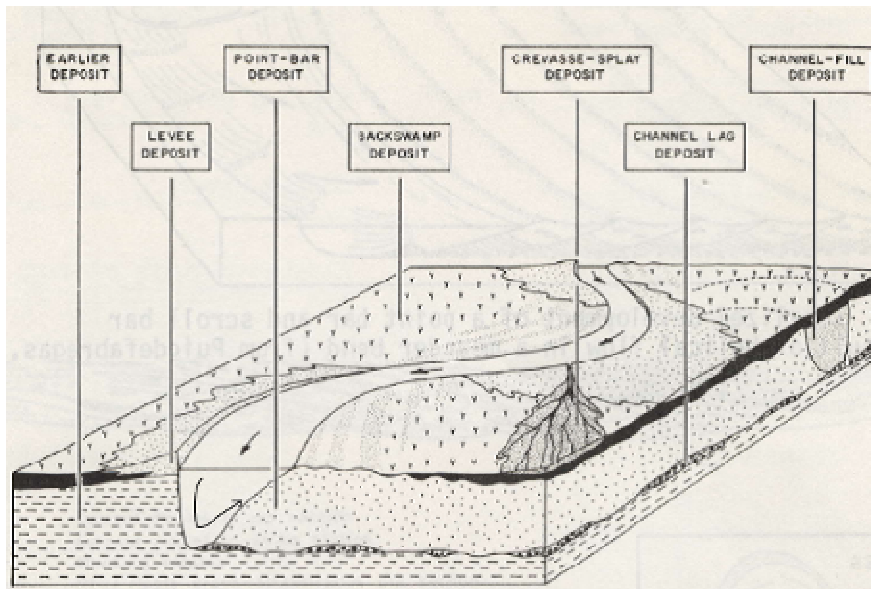


Fig. 2.8: A meandering stream with helical flow and point bar development. From Miall (1977).

The point bar has a distinct epsilon cross-stratification which terminates at base by downlapping onto the channel floor, and at top by offlapping and gradation into fine-grained floodplain deposits. The depositional surfaces have a dip towards the channel, usually with a low angle of less than 5° and rarely above 15° (Miall, 1978, Miall, 1977); however, higher dips, at least up to 20° , have been recorded (Miall, 2006; Puigdefabregas and van Vliet, 1978). Scroll bars are the ridges which develop on the top of a point bar as the meandering stream deposits its sediments on its inner bank (Fig. 2.9). The lows between the scroll bars are swales (Miall, 1977).

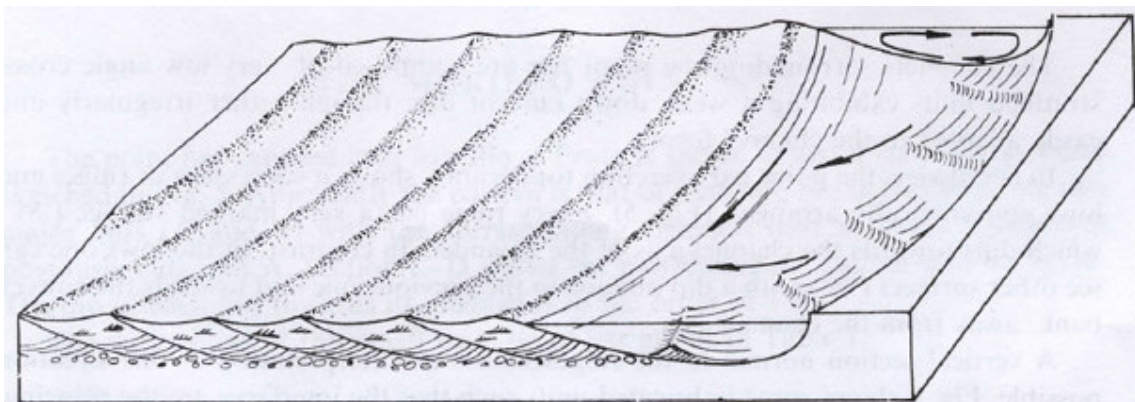


Fig. 2.9: A simplified model of depositional process of point- and scroll bars. From Puigdefabregas (1973).

The height or thickness of point bars approximates the depth of the channel, and the width of an actual point bar is about 1/3 the width of the channel creating it. The height of the compound cross sets are thought to be equal to the depth of the channel (Miall, 2006; Miall, 1996; Leeder, 1973).

A typical depositional development of a point bar may have a lag at its base, consisting of pebbles, mudstone- or siltstone-clasts and plant-debris. Dune formed in the lower part of the point bar can be expressed as large through cross-stratification, often with foresets dipping away from (Puigdefabregas, 1973) or obliquely to the palaeochannel axis, whereas ripples are more common in the upper part where the flow is weaker. The dip directions of the cross-stratification structures vary, but are usually in the downstream direction. Plane parallel laminations may also be present if the flow has occasionally reached the upper flow regime (Boggs, 2001).

Meckel (1975) summarized the vertical succession of point bars in the lower and upper delta plain of the Colorado tide-dominated delta as following:"

Basal contact: Sharp, erosional.

Texture and composition:

- 1) Grain size: pronounced upward fining from fine to coarse sand with pebbles in lower part to fine-very fine in upper part of deposits.
- 2) Sorting: Moderate to very well; no major stratigraphic variations.
- 3) Clay clasts: Both scattered and throughout the section and concentrated in well-defined beds.
- 4) Clay interbeds: Only a few at the very top.
- 5) Organic debris, both macerated and fragments, scattered throughout.
- 6) Basal lag of rounded clay clasts and wood fragments common near or at the base of the unit.
- 7) Granules and pebbles in lower part becoming common near the base.

Sedimentary structures:

- 1) Cross-stratification is dominant; medium-scale in lower and middle parts and small scale near the very top.
- 2) Massive and horizontal stratification may occur anywhere in the section.

3) Root marking common near the top.”

Meckel (1975) also noted that the point bars in the upper delta plain are thicker and coarser than the ones in the lower delta plain due to larger channel size and steeper gradient. Smith (1988) has compared modern point bar deposits in estuarine settings to the Athabasca oil sands in Alberta, Canada, as the oil sands mines there are all within meandering belts and large point bars. Fig. 2.10 shows a classification of point bar deposits in meandering rivers and estuaries based on proximal to distal position of the point bar and its degree of tidal influence.

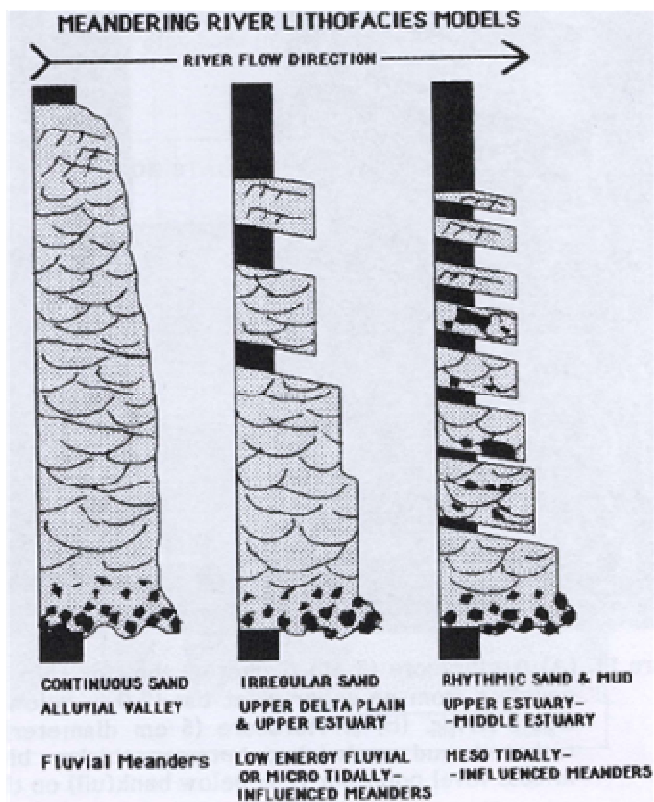


Fig. 2.10: Log profile of point bars in meandering rivers and estuaries with increasing tidal influence towards right. From Smith (1988).

2.7.2 Tidal Sand Bars

Tidal sand bars are large compound bedforms which develop within estuaries, tide-dominated deltas and on the shelf where the tidal range is large. These bedforms may range

from 1-20 m in height and be hundreds of meters wide. These bars are typically asymmetrical where the lee side can have angle of repose of $\sim 32-35^\circ$, or nearly zero, though commonly $\sim 5^\circ$. These deposits often form compound cross-stratification or large-scale cross-stratification with superimposed smaller dunes when the subordinate current has been weaker. The bars are composed of mainly medium to coarse sand with cross-stratification, though mud drapes and tidal signature may be present (Dalrymple, 1992).

2.8 Paralic Environment: Application to the Lourinhã Formation

As the Lourinhã Formation is continental though clearly affected by tidal processes (Ch. 3) it will belong to the paralic depositional environment. An important scope of this paper is to determine which subenvironment within the paralic setting the deposits represent. This is a challenging task. These challenges include among others estimating the relative position of the coastline at each stratigraphic level and by that conclude a transgressive or prograding system. This may be one of the main features to determine in the conclusion whether it has been a deltaic or estuarine system. Many of the topics and subchapters in this chapter will be further addressed in later chapters with immediate relevance to the study area and the Lourinhã Formation.

3 SEDIMENTARY STRUCTURES AND TIDAL SIGNATURE

3.1 Ripples and Dunes

Dunes are responsible for the most common sedimentary structure in rivers where cross-stratification is formed by the migration of these. Dunes and ripples are formed by the same process, though the two structures differ in size and grain-size as dunes are formed during higher rate of particle transport and in part also by higher flow velocity than ripples, according to the flow regime diagram (Harms *et al.* 1975).

Dunes and ripples form and migrate in the lower flow regime where the flow accelerates and erodes on the stoss side of the convex bedform and deposits on the lee side, as the flow decreases above the crest due to flow separation (Fig. 3.1).

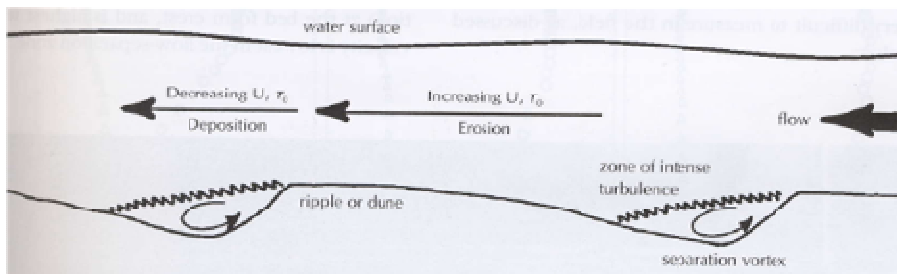
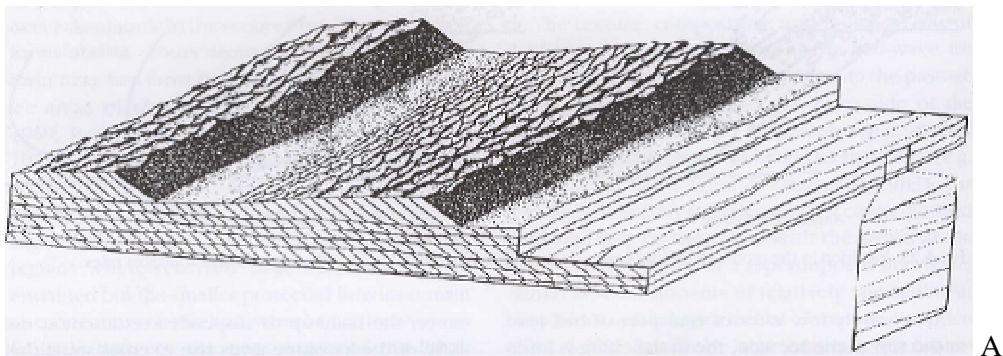


Fig. 3.1: A sketch illustrating the principle of formation and migration of dunes. From Bridge (2003).

Cross-stratification is formed as sediments are deposited on the lee side of the bedform. The stratification gets visible due to variation in texture or composition from: “i) general variations in bedload; ii) grain sorting during the process (avalanching); iii) settling of suspended material; and iv) modification of lee side after deposition” (Bridge, 2003). The cross-stratification can either be tabular or tangential to its lower boundary.

Ripples are defined to have a length less than 60 cm and a height of less than 4 cm and form in very fine- to medium-grained sand only. Ripple length is equal to the lee side flow separation flow and downstream erosion zone, and height/length ratio is dependent on the bed-load transportation rate, thus insensitive to water depth (Bridge, 2003). Ripples can be either symmetrical or asymmetrical, thus representing bidirectional wave ripples or unidirectional current ripples, respectively.

Dunes develop from ripples as sediment transport rate increases and are defined by the same boundary as the ripples as its lower boundary, i.e. higher than 4 cm and longer than 60 cm. The dune size generally increases with flow depth, in contrary to ripples, and is close to zero for the transitional stage to ripples and to upper flow regime plane beds. The dune bedform is also known as sand waves, megaripples, transverse bars and linguoid bars. They can be classified into 2D- and 3D dunes based on the form of their crest line. 2D dunes (sand waves, bars) have long and straight crest lines, which are formed at the transition stage from ripples to dunes, whereas 3D dunes have sinuous crest lines and are formed at higher transportation rates. 2D dunes will show plane stratification in a vertical section parallel to the crest line. Additionally, the lower boundary of 2D dunes will be a nearly planar surface of erosion in both sections, thus the cross-stratification of 2D dunes is also termed planar cross-stratification (Fig. 3.2 A). 3D dunes have more through-shaped erosion surfaces, thus the cross-stratification of 3D dunes are commonly termed through cross-stratification (Bridge, 2003) (Fig. 3.2 B).



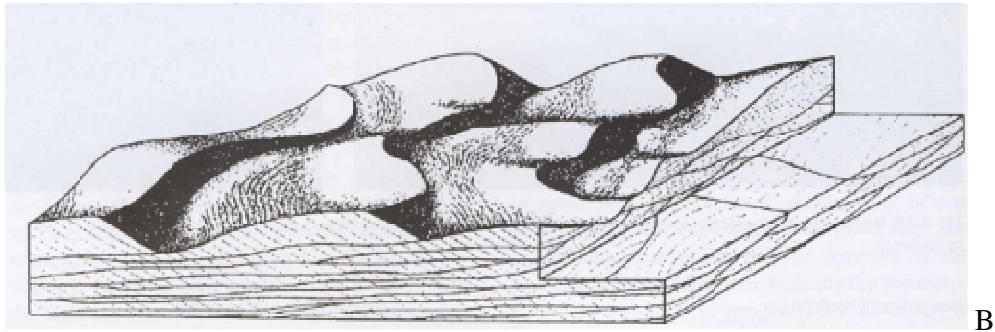


Fig. 3.2: **A:** The uppermost figure shows straight crested 2D dunes and its associated planar cross-stratification. **B:** The lowermost figure shows sinuous crested 3D dunes and their associated through cross-stratification. From Harms *et al.* (1975).

3.2 Tidal Signatures

According to Nio and Yang (1991) there are 4 unique features that can only be the result from tidal processes; “i) mud couplets or paired mud drapes; ii) lateral bundle/toeset thickness variation; iii) diurnal bundle thickness variations; and vi) reactivation surfaces”. Shanley *et al.* (1992) emphasised the need for several structures to be present within the strata in order to determine the influence of tidal current activity. Visser (1980) claimed that double mudstone drapes are diagnostic of a subtidal depositional environment and that bundle sequences also are diagnostic for the tidal environment, reflecting different phases of the moon.

3.2.1 Tidal Bundles and Paired Mudstone Drape

Paired mudstone drapes, or double mud drapes, occur where sandstone laminae are separated by thin, mm, draping of mud or fine organic material (“coal drape”). The double mud drape represents the two slack-water stages in a daily tidal cycle between the dominant- and subordinate current. Double mud drape is a characteristic feature of subtidal environments as this depositional setting experiences two slack-water stages, whereas intertidal areas experience only one, thus receive only a single mud drape, according to (Thomas *et al.* 1987; Visser, 1980).

Double mud drapes often occur in cross-stratified sandstone of migrating dunes, with alternating foreset and toeset thickness. The dominant current will deposit a sandy foreset of a few centimetres thickness. The following first slack-water stage leaves a mud drape which often will be eroded at the top of the lee side during the subordinate current stage as the lee side then becomes the stoss side, i.e. a reactivation surface. The subordinate current will deposit a new sandy foreset, thought to be thinner than the one deposited during the dominant current, and this sand layer may have ripples climbing up the foreset. The second slack-water mud drape has a higher preservation value than the first one, as it forms at the dominant current's lee side and can often be traced to the crest of the dune or ripple structure (Fig. 3.3). The mud drape couplet is visible since the dominant current deposits thicker foresets than the subordinate current. Mud-layer couplets are separated by sand deposited during the event of the dominant current, i.e. a *tidal bundle*. A tidal bundle is bounded below by the mud drape after the subordinate current, i.e. the second slack-water stage, and above by the mud drape after the dominant current stage, i.e. the first slack-water stage (Visser, 1980).

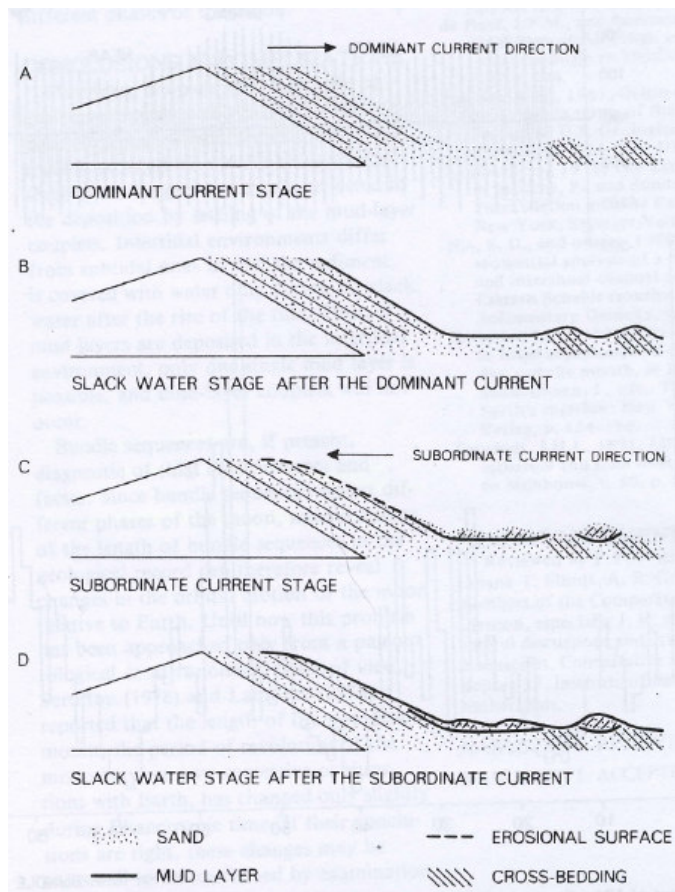


Fig. 3.3: The formation of double mud drapes and bundles in a subtidal setting. A: Dominant current stage where thickest sandy foreset is deposited. B: First slack-water stage depositing a mud drape. C: subordinate current stage, where erosion of first mud drape and possibly dominant stage sandy foreset occur, with deposition of a thinner sandy unit. D: Second slack-water stage with mud drape. From (Visser, 1980).

Single mud drapes within a fluvial system can represent fluctuations on the energy level in the stream, e.g. during a single flood cycle or alternating wet and dry periods and are thus not unique to the intertidal environment.

3.2.2 Bundle Sequence

A bundle sequence (terminology after Visser, 1980) represents the different moon phases, thus has a tidal signature and can be distinguished by the lateral variation in the thickness of the bundles, where the thick bundles represent the high tidal ranges around spring tide, and the thin bundles represent the low tidal ranges around neap tide (Visser, 1980). Normally such a sequence will have 26-28 bundles, representing a semi-diurnal (14,7 days neap-spring cycle) tidal regime. Due to the orbit of the Moon and the tilt of the axis of the Earth a diurnal (once a day) component is added to the tidal spectrum some places and may be dominant where the semidiurnal tide is small. A diurnal cycle will have 14 tidal bundles.

3.2.3 Flaser Bedding

Flaser bedding occurs in heterolithic channel fill, where daily tidal cycles drape sandy or silty ripples with mud. Fluctuating hydraulic conditions result in erosion of the ripple crests, leaving only the lower part of the ripple and mud between ripple sets preserved (Boggs, 2001, Shanley *et.al.* 1992).

3.2.4 Reactivation Surfaces

Reactivation surfaces are minor erosion surfaces which are gently dipping and slightly convex upstream of cross-stratified strata. Reactivation surfaces are present in fluvial, marine and tidal environments and can be due to fluctuation in stream flow in fluvial systems or reversal of flow due to tides, i.e. erosion of the lee side where the lee side becomes the stoss side (Shanley *et al.* 1992). Nio and Yang (1991) claimed that the occurrence of dominant flow reactivation surfaces together with those of subordinate currents is unique for the tidal environment. The rate of erosion will increase with increased strength of the subordinate

current and reactivation surfaces of different form and geometry will be formed. 5 different reactivation surfaces are suggested by Nio and Yang (1991) depending on erosion, preservation of bundles and mud drape, development of back-flow ripples, dip of the reactivation surface and flaser development.

3.2.5 Bidirectional Current

Palaeocurrent measurements or structures showing a bidirectional current, with one dominant- and one subordinate direction, is a good tidal indicator. Such structures can be herringbone structures or ripples climbing up-dip on sandy foresets, indicating a dominant direction of migrating dunes and a subordinate direction (Nio and Yang, 1991).

3.2.6 Inclined Heterolithic Stratification (IHS)

Due to the amount of mud found in tidally influenced systems, Inclined Heterolithic Stratification (IHS) is commonly found in relation to these, e.g. tidally influenced point bars, tidal channel deposits, deltaic distributary channels with tidal influence or lower delta plain levee deposits.

Thomas *et al.* (1987) suggested a genetic unbiased terminology of Inclined Stratification (IS) and Inclined Heterolithic Stratification (IHS) regarding particularly lateral accretionary strata like point bars, though also other inclined strata like Gilbert-type deltas. This terminology could be used for inclined deposits independently of its depositional process and environment in which it was formed. IHS is proposed for: “i) deposits with initial or depositional dip; ii) of lithologically heterolithic composition, often with alternating coarser- and finer-grained units; iii) and with a wide variety of thicknesses”. IHS has in several cases been used to describe tidal deposits, e.g. Shanley *et al.* (1992), tidally influenced point bar deposits; and Rebata *et al.* (2006), deposits within a tidal channel.

Thomas *et al.* (1987) emphasised, however, that IHS is not meant to be applied to tidal bundles, although mention that fine members of IHS often has been referred to as mud drapes or equivalents in the previous literature. The finer members of IHS are mainly related

to flood events and ephemeral streams in the fluvial system. Thus, tidally influenced point bar deposits can be classified as IHS, while any double mud drape or bundles present within these need to be described by its own terminology.

4 GEOLOGICAL FRAMEWORK

4.1 Structural Evolution

The Lusitanian Basin extends in length ~300 km north of Lisbon and in width ~150 km, including its offshore extension (Azeredo *et al.* 2002), while its onshore area has a length of ~250 km and a width of ~100 km. It is bounded to the east by Hercynian basement rocks and to the west by a series of basement horsts which are today visible as Berlengas and Ferilhões islands offshore Portugal (Wilson *et al.* 1989) (Fig. 4.1 a). The faults and diapiric structures have a dominant trend of north-north eastern – south- south eastern direction north-north eastern – south-south western- and a subordinate north eastern-south western direction (Leinfelder and Wilson, 1989) (Fig 4.1 b).

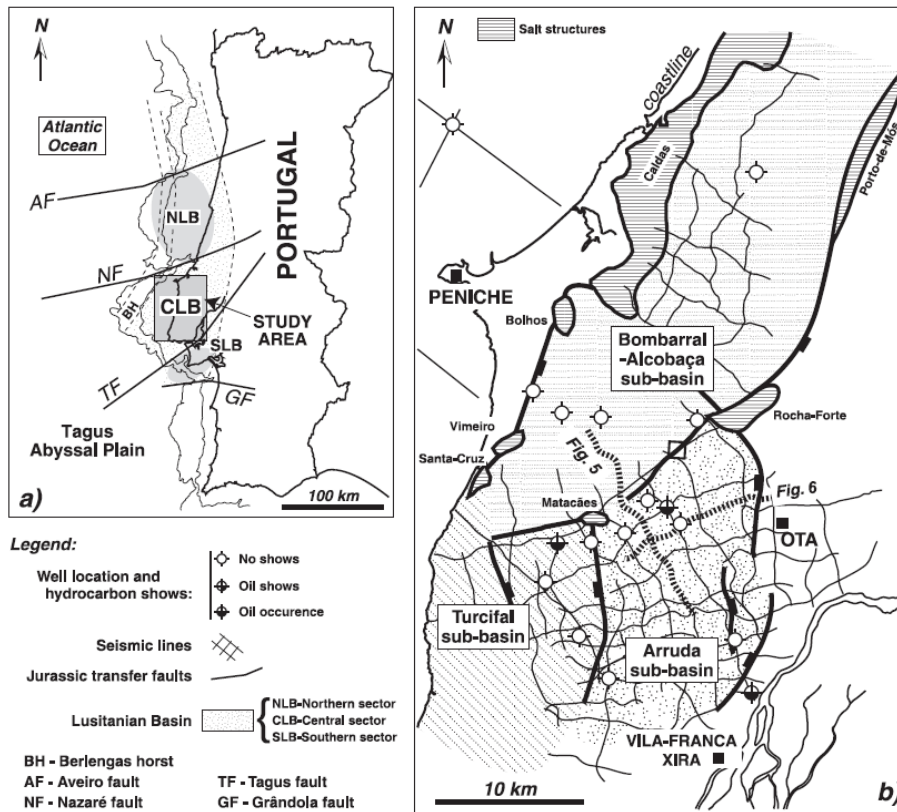


Fig. 4.1: a) The position of the Lusitanian Basin in Portugal today with its boundaries and offshore extension included. b) The Central Lusitanian Basin in detail with faults, diapiric structures and sub-basins included. From Alves *et al.* (2003).

The basin is a narrow Atlantic margin rift-basin which evolved as a response to Mesozoic extension, i.e. the break-up of Pangea (Rasmussen *et al.* 1998). The Iberian plate was at this time positioned in a focal position between Tethys Ocean and what was to be the Atlantic Ocean and was thus strongly affected by the rift events associated with the opening of Central- and North Atlantic (Wilson *et al.* 1989) (Fig. 4.2 a-d). There are four rift phases from Late Triassic to Early Cretaceous; Late Triassic; Sinemurian-Pliensbachian (Lower Jurassic) (Rasmussen *et al.* 1998); Stapel *et al.* 1996); Oxfordian-Kimmeridgian; and Tithonian-Barremian (Latest Jurassic-Earliest Cretaceous) (Rasmussen *et al.* 1998), though they can be considered as two main episodes, or cycles, of rifting; Late Triassic and Late Jurassic (Azeredo, 2002; Wilson *et al.* 1989; Leinfelder, 1987). As the opening of the Central Atlantic and the related rotation of the African continent progressed, the Iberian rift had a northward propagation resulting in shallowing of the basin towards north (Leinfelder, 1987). The basin experienced inversion and further halokinesis during Cenozoic (Rasmussen *et al.* 1998).

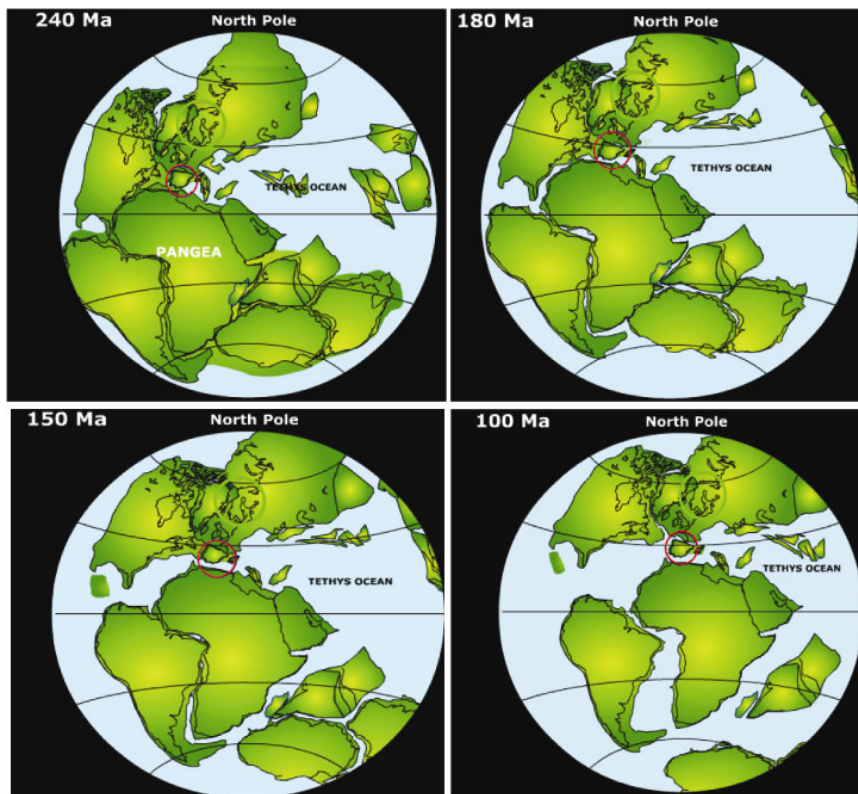


Fig. 4.2 a-d: Development of the opening of the Atlantic Ocean from 240 to 100 MA. The Iberian plate is marked with a blue circle. From Kullerud (2003).

4.2 Sub-basins

A change in the basin configuration occurred in Late Jurassic. The central part of the Lusitanian Basin developed several sub-basins where the sub-basins are either bounded by faults or halokinetic structures. The halokinetic structures evolved over reactivated Hercynian basement faults in areas where evaporites of the Dogorda Formation, deposited after the first rift phase, are thick (Alves *et al.* 2003; Leinfelder and Wilson, 1989; Wilson *et al.* 1989). The Turcifal and Arruda sub-basins are fault-bounded half-grabens. The Bombarral-Alcobaça sub-basin is bounded by the Torres Vedras-Montejunto anticline and the Caldas diapir to the east and west, respectively. The Caldas diapir follows the Louriñha-Caldas fault that bounds the Bombarral-Alcobaça sub-basin onshore just to the east of Louriñha. The Torres Vedras–Montejunto lineament also separates the two sub-basins Turcifal and Arruda from Bombarral-Alcobaça (Alves *et al.* 2003). These sub-basins were rapidly subsiding during the Late Oxfordian and Early Kimmeridgian in association with the rifting and rejuvenation of the faults at this time (Wilson *et al.* 1989). The Torres Vedras – Montejunto and Caldas diapiric structures was initiated during Late Jurassic (Leinfelder and Wilson, 1989) and resulted in largely salt controlled subsidence of the Bombarral-Alcobaça sub-basin (Alves *et al.* 2003) (Fig. 4.1 b).

4.3 Stratigraphic Overview

After the initiation of rifting in Late Triassic red clastics and evaporites were deposited as the Silves and Dagorada formation, respectively, following carbonate and shale deposits throughout Early and Middle Jurassic after a global sea-level rise. A Callovian-Oxfordian hiatus lead to karstification of the previous carbonate deposits before overlain by freshwater carbonates of the Cabaços Formation. After a new relative sea-level rise, fully marine deposits of hemipelagic shale of the Montejunto Formation, siliciclastic shales and marls of the Abadia Formation, and cross-stratified ooid grainstone of Amaral Formation were deposited before the fluvial Louriñha and Torres Vedras formations (Hill, 1989; Leinfelder and Wilson, 1989).

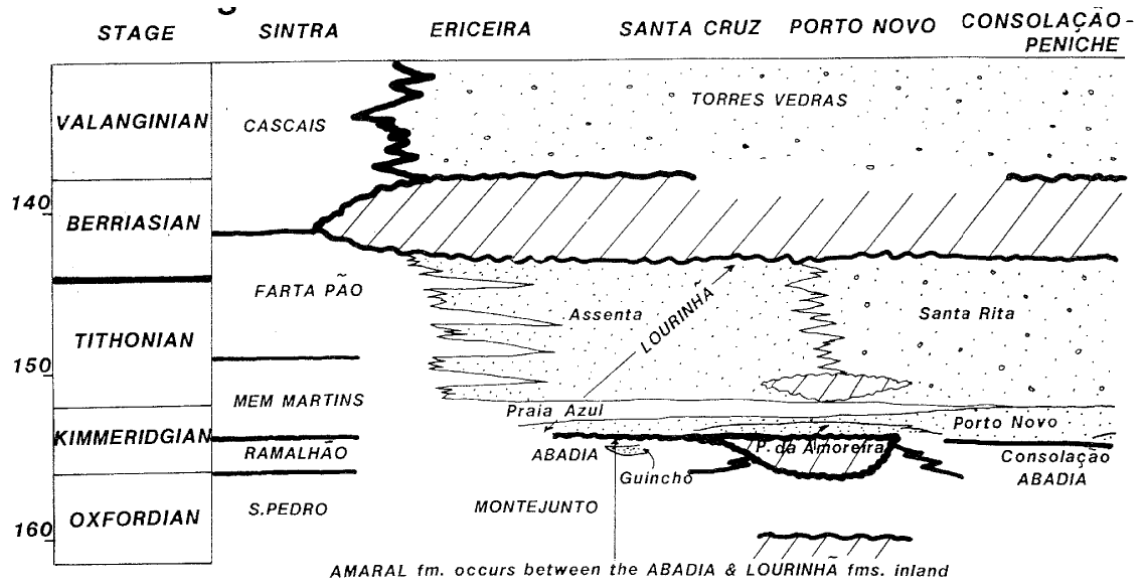


Fig. 4.3: A stratigraphic summary from the Late Jurassic-Early Cretaceous in the Lusitanian basin. Our field area lies just south of Consolação, towards Porto Novo. From Hill (1989).

The Lourinhã Formation consists of the following members: Praia de Amoreira, Porto Novo, and Assenta or Santa Rita. The lowermost member, Praia de Amoreira, is thought to be of mid-to-late Kimmeridgian age. The Lourinhã Formation is thought to extend into Earliest Cretaceous. Praia de Amoreira is mud rich with only small channel deposits and is interpreted to be the distal deposits of low-relief alluvial fans. The apexes of the fans are thought to be ~15 km northwest of today's coastline, i.e. by the Hercynian horst blocks (Hill, 1989).

Porto Novo is a fluvial meander deposits with larger scale palaeochannels. The fluvial system of the member may have coexisted somewhat further east with the deposition of the distal alluvial fans. The youngest members of the Lourinhã Formation are the Assenta and Santa Rita members which are finer- and coarser-grained, respectively (Fig. 4.3). The Assenta Member is present south of Santa Cruz and the Torres Verdes-Montejunto anticline, whereas the Santa Rita Member is found to the north and east. The development of different facies styles can be due to active salt diapirism. This relation between stratigraphy and structural development is supported by a local unconformity below the Santa Rita Member west of the Vimeiro diapir, and "channel" dominated facies style rather than "overbank" dominated facies style here. The dominant facies style may indicate higher gradient of the

fluvial system, with a sub-basin subsiding more slowly than the basin as a whole and thus promoting downcutting instead of aggradation (Hill, 1989).

Leinfelder and Wilson (1998) have interpreted the upper Lourinhã formation to represent fluvial/deltaic deposits interfingering with marine limestone and marls of the Farta Pão formation to the south (e.g. Vila-Franca, Sintra). Deltaic sediments, of probably Late Kimmeridgian to Earliest Tithonian, are present at the base of the formation (Leinfelder and Wilson, 1989). The Lourinhã formation is deposited in the late post-rift stage of the Lusitanian basin, as it covers all the sub-basins. The deposits are consequently not thought to be affected by basin tectonics or major topographic differences at this stage (Leinfelder and Wilson, 1989), though Hill (1989) has recorded facies changes possible due to diapirism. Palaeocurrent data show a regional trend of transportation towards southeast (e.g. Hill (1989)).

5 METHODS

5.1 Field Work

The field work was done in the period of 26.09.06-16.10.06 in a succession belonging to the upper part of the Lourinhã Formation in the Lusitanian Basin positioned on the western coast of Portugal, ~50 km north- northwest of Lisbon. The work was done in collaboration with master student Samuel Etta. The work was supervised by Johan Petter Nystuen, Ivar Midtkandal, Michael Heeremans and Liv Hege Lunde Birkeland.

The study area was along a ~2,5 km long cliff wall extending from Pai-Mogo to Aria Branca. The strata dip gently towards south such that a total of 150 m of the stratigraphic column were studied. Lithological logs were made of the whole stratigraphic column and locally in areas of interest with focus on sandstone bodies. The logs record grain size, sedimentary structures, bed thicknesses and palaeocurrent measurements where this is possible. In total 26 logs were made of which 8 logs, extending over 12 sheets, represent the stratigraphic column coded as “framework”, e.g. framework_0, in addition to a sheet number, e.g. FW 1/12. The number increases as the logs positions are further south. 13 logs represent some of the characteristic architectural elements present in the field area not represented by the framework logs. These are coded according to which section they are positioned within and a log number which position them further, e.g. S2_P1. A map of the log position is illustrated in appendix A.

The logs are important in documenting and determining the facies, facies associations, architectural elements and architectural style. The paleocurrent measurements were almost exclusively measured from the azimuth of cross-stratifications, with the exceptions of possibly two measured on depositional surfaces.

In total of 19 rock samples were taken from sandstone units and a marine flooding surface with the purpose of making thin sections for a petrographic study. The red numbers in appendix B indicates the location at which the sandstone samples are taken from. Several pictures were taken for documentation and for visual aid while writing the paper.

5.1.1 Possible Source of Errors Related to the Field Work

True thickness of the stratigraphic column

Since the area has a tilted stratigraphy, the framework logs, which represent the stratigraphic column, are done in a zigzag pattern across the cliff wall. The stratigraphic level at top of one log is therefore traced to the base of a new log position. This stratigraphic level is not always prominent and easily traceable, thus possible errors, predicted to be less than 3 meters, should be expected at each “jump” between these logs. Possible errors can also occur where the terrain makes it difficult to do accurate thickness measurements, though these errors are expected to be rather small.

Sand:gross ratio estimates

The sand:gross calculations are based on the sand proportions in the logs. However, with the exception of the stratigraphic framework log, log positions are strategically chosen to record sandstone bodies. Even though this is taken into account and an attempt to minimize the error is done through closer evaluation of Appendix B this may result in optimistic sand:gross ratio values some places.

Quantifications of size of the architectural elements

Several places quantification of the different architectural elements is attempted. Due to the tilting of the stratigraphy the larger elements are rarely completely exposed in 2D outcrop and the quantifications of these are only estimates. With only partially exposed geometry of channels and overbank deposits in outcrop and no data from the third-dimension, the quantifications or estimates of e.g. palaeochannel size and degree of sinuosity may be of limited value. This is also pointed out as a general method problem by Bridge (1985).

5.2 Petrographic Analysis

Thin sections were made from the 19 rock samples collected from the study area. By looking at these in a microscope it is possible to identify the minerals the rock consists of, the maturity of these minerals, degree of diagenesis (e.g. mechanical and chemical compaction)

and porosity. This information can provide information about e.g. the source area and burial history.

When using Cross Polarized Light (XPL), or crossed Nichols the interference of colours occur due to different velocities of the light along different axis of the mineral. This interference does not occur in glass, fluids or cubic minerals, which are isotropic and have same velocity properties in any direction. This interference is unique for each mineral thus can be applied for mineral identification.

A statistical valid volumetric value of the different minerals and pore space is made with the aid of a counting device. This device applies a grid to the thin section in which the occurrence of a mineral or pore space at the intersection points in the grid are registered. 9 channels will register alkalifeldspar, plagioclase feldspar, leached feldspar, mica, quartz, pore space, calcite crystals, mud and organic matter. More than 500 points are counted for each chosen thin section to assure statistical validation. Only a few thin sections from representative sandstone bodies will be chosen to make petrographic study from.

5.2.1 Possible Source of Errors Related to Petrographic Analysis

Petrography:

Due to the lack of thorough training within the line of optic mineralogy mistakes can be made in recognizing the mineral. The minerals which can be easily mistaken for each other are orthoclase and quartz, in addition to heavily leached feldspar which contains secondary minerals and quartz with needle inclusions of other minerals or fluid inclusions. This can affect the volume calculation of the individual minerals, though hopefully not to a great extent. The pore volume should be rather accurate as blue epoxy is easily recognizable in plane polarized light (PPL).

5.3 Reservoir Modelling

The software PetrelTM (Schlumberger) was used to do a stochastic reservoir modelling of the succession studied. The logs were used as input and Fluvial Facies synthetic Well Logs were

interpreted from these which were later upscaled to give a single value to the cells in a 3D grid.

The area to be modelled was determined with relevance to the length of the study area, which is ~2,5 km. This will compose the width of the modelled area, while the length were extended an equal length, i.e. 2,5 km, in the northwest and southeast directions. Thus the area for modelling is 2,5 * 5 km and has a direction with its long axis roughly along the palaeocurrent direction (Ch. 11.2).

The succession was divided into 4 zones (see Fig. 12.1), in accordance to the architectural style (Ch. 9). The 4 zones were modelled with different parameters of channel amplitude, wavelength, width, depth and sand:gross ratio. The main architectural element is Fluvial Channel, though an addition of crevasse splay architectural element were included with fan geometry in Zone 2 as it is the main geometry within this section.

5.3.1 Possible Source of Errors Related to Reservoir Modelling

Cell size

If the grid cells are oversized the upscaling of the logs and the modelling result can be coarse and inaccurate. The area modelled is small and should have grid cells accordingly.

Parameters

The basis for determining the size of the architectural elements and thus the parameters in which the modelling rely upon, is observations during field work and supporting literature on the subject. Within the study area the elements present are commonly only partially exposed and a 3D control on the geometry is absent. Miall (2006) pointed out the uncertainties of measuring or estimating channel size, even with 100% exposure. The lack of 3D control also results in poor knowledge about type of channels present in the Lourinhã Formation. This may cause large uncertainties and errors if the empirical data and equations are applied to a different channel type than the ones the data and equations are derived from, e.g. braided- versus sinuous streams or fluvial- versus distributary channels.

6 FACIES

TABLE 6.1: List of facies present in the Louriñha formation of the Lusitanian Basin, Portugal.

<i>Facies</i>	<i>Description</i>	<i>Grain size</i>	<i>Interpretation</i>
A	Through cross-stratified sandstone with tangential or angular basal boundary. Metres thick. Minor erosive lower boundary.	Fine- to medium-grained sandstone with little to no mud.	Migration of 3D dunes. Bed-load traction in lower flow regime
B	Planar cross-stratified sandstone commonly with sandstone-sandstone amalgamated surfaces.	Medium- to very coarse-grained sand. Little to no mud.	Deposition from migration of 2D dunes.
C	Tangential through cross-stratified sandstone with single and double mud drapes. Variations in thickness of sandy foresets.	Primarily very fine- to very coarse sandstone. Secondary mud or “grounded” organic matter (coal drapes).	Migration of 3D dunes with tidal influence. Tidal signature of double mud drapes, tidal bundles and tidal bundle sequences. Tidally influenced fluvial deposits.
D	Plane parallel-stratified sandstone with mudstone lamina. Sandstone-mudstone lamina alternating with sandstone.	Mainly fine- to medium-grained sandstone. Secondary mud to silty mud	Deposition from suspension in lower flow regime with regular variations in energy. Continuous sedimentation
E	Plane parallel-stratified sandstone.	Fine- to medium-grained sandstone. Little to no mud.	Bed-load traction in upper flow regime deposits.

<i>Facies</i>	<i>Description</i>	<i>Grain size</i>	<i>Interpretation</i>
F	Ripple laminated sand with normal ripples, climbing ripples and ripples climbing up foresets of cross-stratified foresets. Asymmetrical	Very fine- to medium-grained sandstone	Lower flow regime deposition of current ripples
G	Apparent massive sandstone	Fine- to coarse-grained sandstone	Rapid deposition from suspension in upper flow regime or extensive burrowing by organisms.
H	Extrabasinal conglomerate with basement derived pebbles. Matrix supported. Erosive or plane base. Interbedded with facies B and C	Pebbles in a medium- to very coarse sandstone matrix. Pebbles < 1cm	Fluvial channel or in-channel high energy deposits. Basement derived pebbles.
I	Intrabasinal conglomerate of rounded mudstone clasts. Matrix borne with occasional clustering. Commonly occur at base of beds otherwise composed of facies D	Mudstone pebbles and fine- to medium-grained sand matrix pebbles < 2 cm pebbles 4-8 mm	Tidal channels or crevasse channels cutting into floodplains. Short transportation distances.
J	Mudstone. Sheet geometry. Can be > 10 meters thick. Thin layers of siltstone or shell banks imbedded.	Mud and silt	Background sediments deposited from suspension during flood events
K	Siltstone. Decimetre thick. Sheet geometry, lateral extensive, grey colour, burrowed.	Siltstone which may contain some very fine sand	Distal crevasse splays, levees or other overbank sediments
L	Paleosol. Red root structures (often green) with calcrete nodules	Mud to very fine sand	Soil development and exposure of 1000 - 10 000 years

<i>Facies</i>	<i>Description</i>	<i>Grain size</i>	<i>Interpretation</i>
M	Soft sediment deformed sandstone	Very fine sand to coarse sand. Usually with mud interbedded	Rapid deposition creating water escape structures; loading; or tectonic activity stirring the sediments
N	Shell bank. Siltstone containing shell fragments or shell fragments generating shell bank conglomerate.	Silt to very fine sand and shell fragments < 3 cm of size	Marine flooding surface

6.1 Facies A: Through Cross-stratified Sandstone with Tangential or Angular Toesets

Description

Facies A is composed of through cross-stratified sandstone with tangential or angular toesets, consisting of fine- to medium-grained sand with little or no mud- or organic material draping, i.e. rather homogeneous or minor heterolithic. Though this facies may include some very thin single mudstone drapes, this is not the main feature of this facies and is only a subordinate characteristic. However, the foreset boundaries are enhanced by these grain size variations and the cross-stratification is difficult to distinguish where the variations are small. Mudstone drapes are more common and thicker in toesets than in the foresets in this facies. Extrabasinal pebbles may be present in foresets together with mud drape.

Individual through cross-stratified beds vary in height from decimetre to several decimetres, though the bed thickness is normally above ~>20 cm. Bed sets composed of several cross-stratified beds can be a few meters thick in which the amplitude of the cross-stratification tends to decrease towards the top. Several beds contain sand-sand amalgamated surfaces where traces of finer material are present along some surfaces. In outcrop view some deposits of this facies appear clean with good sorting, and the cross-stratification or amalgamation is not always clear due to little variation in grain size.

Interpretation

Through cross-stratification is formed by migration of 3D dunes which can have varying sinuosity of their crests and develop at higher flow velocities than 2D dunes where parameters like grain size and depth are equal. During migration of 3D dunes the sand is transported up the stoss side by traction and deposited at the crest where the bed-shear stress diminishes and flow separation occurs. The differentiation of 3D from 2D dunes is related to the growth of three-dimensional separation vortices on the lee side as the shear stress increases within the turbulent outer layer (Miall, 1996). They commonly form in channel deposits or channel associated deposits like bars, but can form anywhere where bedload transport occurs in lower flow regime, e.g. in crevasse splays.

Where mud is found in toesets, mud is clearly present in the depositional system. Thus, the lack of mud in the foresets is probably due to small preservation potential of mud when mud may have been deposited at foresets during low energy conditions, but been eroded by increasing subordinate current energy. The current may also have been strong enough to keep the mud in suspension and not vary much over short time periods to give rise to settling of mud at all.

6.2 Facies B: Planar Cross-stratified Sandstone with Tangential or Angular Toesets

Description

Facies B (Fig.6.1) consists of tabular cross-stratified medium to very coarse sandstone with intermediate to very little mudstone present. The dune height can vary a great extent from decimetres to ~1 meter. Thicker units composed of several beds of 2D dunes are present, but rare. This facies occurs as compound beds; interstratified with through cross-stratification in composed beds; as a component in thicker beds together with extrabasinal conglomerate with planar base; or in single thin beds in complex compound sandstone bodies.

Amalgamated surfaces, indicating closely spaced single events, are commonly present.



Fig.6.1: Planar cross-stratified sandstone in a compound bed. Some mudstone drapes are present, mainly in the toesets, though this is rare.

Interpretation

Planar cross-stratified sandstone results from migration of 2D dunes which have straight crests and is a transitional stage between ripples and 3D dunes in lower flow regime (Bridge, 2003). During migration of 2D dunes the sand is transported up the stoss side by traction and deposited at the crest where the bed-shear stress diminishes, indicating avalanching of sand down foresets.

Cross-stratified sandstone with a planar base is not a common facies in our field area, as most cross-stratification is from 3D dunes. Some 3D dunes may have very low sinuous crests where the dune structures can be discussed whether represents 3D or 2D dunes, thus be through cross-stratification or planar cross-stratification. Also some of the larger dune structures may in fact be from 3D dune, though they appear planar in a limited outcrop.

6.3 Facies C: Heterolithic Through Cross-stratified Sandstone with Tangential Toesets and Mudstone Drapes

Description

This facies is heterolithic tangential through cross-stratified, very fine- to very coarse sandstone with single- or double mud drapes in foresets and toesets (Fig.6.2). Most of the facies is fine- to medium-grained sandstone. The beds occur both in small scale of height less than 2 decimetres and larger scale of several decimetres. These cross-stratified strata are frequently interbedded with most other facies, or they compose ~1-3,5 meter thick bed sets. Such compound beds are found in several architectural elements, though mostly present in channel shaped units and within horizontal to subhorizontal bed sets of several meters in thickness. These sandstone units have an erosive to slightly erosive lower boundary and a traceable lateral extent of less than 100 meters. Internal amalgamated surfaces are present within this facies.

Double mud drapes are recognized by alternating thinner and thicker sandy foresets bounded by mudstone lamina, in which the uppermost mud drape is commonly more developed and better preserved than the lowermost one. The amounts of sand deposited at toesets are usually thin to non existent, resulting in mergence of the double mud drapes.

Some places a clear repetitive trend also occurs in the intervals between the double mud drapes, i.e. thickness of the bundles, where the distance regularly and gradually varies from millimetres-centimetres to several centimetres within single dunes.

In some cases double mud drapes can not be determined as they show no great variation in the thickness of the sandy foresets or a mergence of the mud drapes at toesets. These mud drapes are termed *single mud drapes* and can coexist with double mud drapes in a single cross-stratified unit or composed beds.

Interpretation

The tangential cross-stratified sandstones are formed by migration of 3D dunes of varying sinuosity from high sinuous to nearly straight crests, while the double mud drapes are interpreted to be deposited during first and second slack-water stage in a subtidal setting and

are known to be one of the structures which alone represents tidal influence (Nio and Yang, 1991). The double mud drapes will be separated by a tidal bundle.

The variations within the distances between the double mud drapes, or the thicknesses of the tidal bundles, are thought to represent one tidal bundle sequence deposited during one moon phase, where thinner and thicker bundles, i.e. the densely- and more widely spaced double mud drapes, represent deposition around neap flood and spring flood respectively (Visser, 1980) (Fig.6.2).

However, due to the relative low preservation potential of mud drapes, there is not always clear double mud drapes, but rather only single ones. Single mud drapes can be formed by other mechanisms than tidal current variations, e.g. flooding or seasonal to daily variations in current flow, though when they occur in cross-stratified sandstone at such regular frequencies and among such amount of double mud drape, it is reasonable to assume tidal origin also when encountering single mud drapes in foresets or toesets.

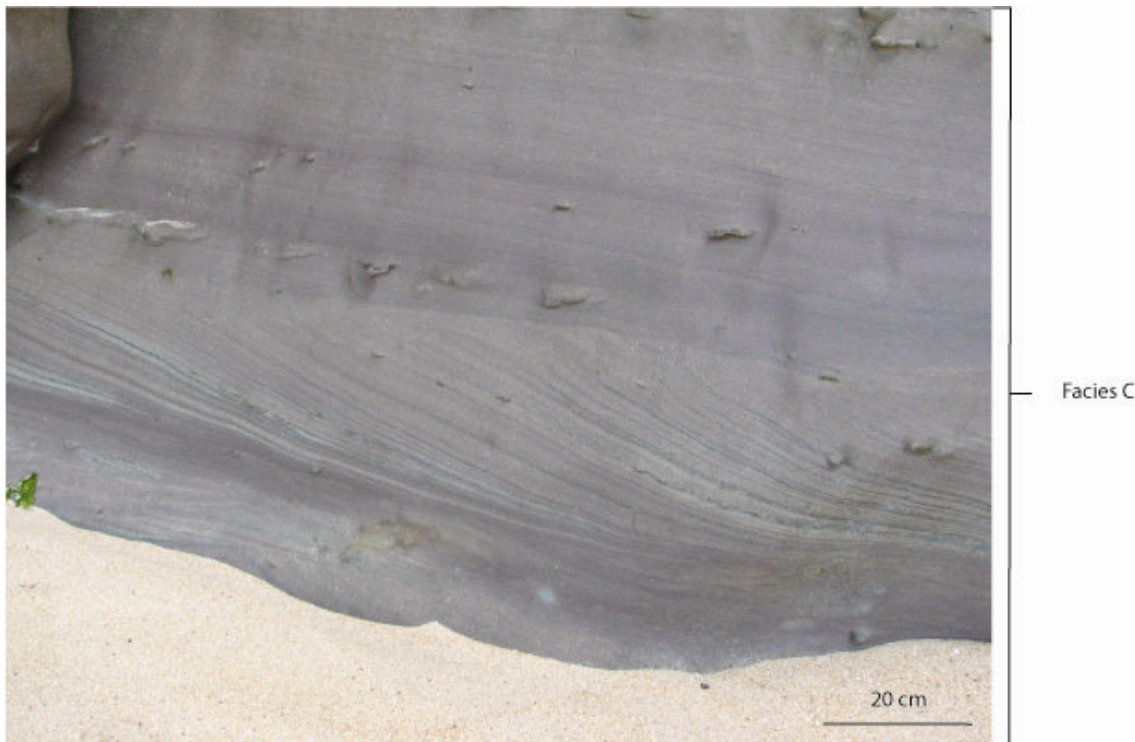


Fig. 6.2: Large scale through cross-stratified sandstone with single and double mud drapes. The variations of thicker and thinner bundles reflect sedimentation during spring and neap tide, respectively.

6.4 Facies D: Lower Stage Plane Parallel Stratified Sandstone with Mudstone Laminae

Description

Facies D consists of fine- to medium-grained sandstone containing millimetres thick mudstone laminae of varying density. The mudstone lamination generally composes centimetres thick groups of sandstone-mudstone laminae occurring with varying density, thus occurring at centimetres to few decimetres thick intervals in sandstone beds of ~1 meter thick. This facies occurs in several sandstone bodies, which in general are a few meters thick and have a lateral extent of 10-60 meters. The beds are subhorizontal; have irregular lower- and upper boundaries; or slightly concave-up beds within the area they are exposed (Fig. 6.3). The beds have commonly minor erosive lower boundaries, often with somewhat coarser-grained or conglomeratic (intrabasinal) base. Occasionally rhythmic variations can be observed in the sandstone-mudstone laminae.



Fig. 6.3: Sandstone unit with extensive sandstone-mudstone laminae (Facies D).at Aria Branca. The bed is 1-1,5 meters thick.

Interpretation

The sandstone-mudstone variations are thought to result from fluctuations in the energy levels where the sand is deposited by traction or suspended load while the mud settled from suspension in the lower stage of lower flow regime. Gradational contacts indicate continuous

sedimentation rather than closely spaced single events which would be represented by amalgamated surfaces.

The rhythmic variations are probably due to the tidal variations where the low and high density of the grouped sandstone-mudstone laminae represents neap- and spring flood respectively.

6.5 Facies E: Upper Stage Plane Parallel Stratified Sandstone

Description

Facies E; fine- to medium-grained sandstone with plane parallel-stratification, is fairly uncommon, but present at base of some beds. Very low angle cross-stratified sandstone may appear parallel stratified in outcrop and these two subfacies can thus be wrongly interpreted for each other.

Interpretation

Plane parallel stratified very fine- to medium-grained sandstone form during high energy current flow in the upper flow regime, and can be deposited during flood stages in main fluvial channels, crevasse channels or splays. The facies type can, however, be misinterpreted in the field since the stratification in outcrops can resemble very low angle stratification and the strike view of planar cross-stratification.

6.6 Facies F: Ripple Laminated Sandstone

Description

Facies F consists of current ripples (asymmetric unidirectional) (Fig. 6.4) and climbing ripples (ripple cross-lamination) in very fine- to medium-grained sandstone which is commonly positioned on top of beds with dune structures. In addition, facies F is recorded as the dominating facies in decimetres to several decimetres thick beds with minor erosive bounding surfaces which occasionally are sand-sand amalgamated surfaces. Burrows or/and rootlets are commonly present in facies F.



Fig.6.4: Thin sandstone bed with ripple lamination (Section 1, log: FW_0). Pencil for scale. (Photo: I. Midtkandal)

Ripple lamination can generate lenticular bedding when occurring in sandstone lenses in silty or muddy matrix, and wavy when occurring as the main sandy feature with minor mud present.

Ripples found together with cross-stratified sandstone are present on the stoss side of the dune bed form, or as ripples climbing up the lower part of foresets of the larger sand structure.

Interpretation

Ripple lamination forms in the lower flow regime by currents of lower flow energy than those forming dunes. The ripple lamination thus often represents a waning flow when superimposed on dunes in a single bed. The opposite succession of dune stratification and current ripple lamination indicates an increase in the current's magnitude. Climbing ripples

(ripple cross-lamination) implies rapid deposition from suspension, like on a floodplain, on a point bar or river deltas (Boggs, 2001).

Ripples climbing up foresets indicate a subordinate current to the one generating the dune structures, which can be interpreted as a subordinate tidal current, or in a unidirectional flow system, where flow separation at the crest line of dunes may give rise to a backflow in the vortices formed (Allen, 1984).

6.7 Facies G: Apparent Massive Sandstone

Description

This facies consists of fine- to coarse-grained sandstone which contains no clear structures, thus appear massive. Commonly these beds are quite thin; not thicker than a few decimetres and seldom compose thicker beds. In some beds only burrows may be present while it otherwise appears massive.

Interpretation

Massive sandstones may have been formed from high energy currents in upper flow regime where sand falls out from suspension; or originated from very intense burrowing, which have destructed any original structures present. These beds can be present in crevasse plays where the current may be quite strong at its initial stage, or other near channel elements which can experience strong currents during flood.

6.8 Facies H: Exstrabasinal Conglomerate

Description

Facies H consists of subangular basement derived clasts of crystalline quartz, feldspar, dark minerals etc. The exstrabasinal clasts are generally less than 1 cm in diameter and embedded in a medium- to very coarse-grained sandstone matrix. This facies can be found as i) centimetres to decimetres thick plane strata in thicker composed beds with minor occurrences of angular cross-stratified sandstone (2-3 meters), alternating with tabular plane cross-stratified medium or coarse sandstone (facies B) which lacks pebbles; or ii) as a

granule or pebble lag at erosive bases and amalgamated surfaces in channel shaped units where facies H alternates with through cross-stratified sandstone (facies A and C).

Interpretation

The extrabasinal pebbles are assumed to originate from the basement horsts north-west, i.e. now exposed in the Berlengas and Ferilhões islands, or the Hercynian basement rocks in the east of the field location. The poor roundness of the pebbles indicates a relative proximity to the source area. Pebble lag in channels form during high discharge. Pebbles may also accumulate on bars in channels, which is likely the case in the first case described above (i).

6.9 Facies I: Intrabasinal Conglomerates

Description

This facies is composed of rounded clasts of mudstone and organic fragments of intrabasinal origin, embedded in fine- to medium-grained matrix. The intrabasinal conglomerates are either matrix- or grain supported and develop different characteristics.

Intrabasinal conglomerate is present at base of- or at amalgamated surfaces in channel shaped depositional units, where the mudstone clasts are clearly derived from the immediate substrate in which it cuts into, e.g. paleosols. Where the current has cut into well developed paleosols, rather large (< 2 cm) mudstone clasts have been concentrated into clusters and given rise to grain-supported conglomerate beds some places.

Intrabasinal conglomerate may also compose beds of < 0,5 m in thickness which contains small mud clasts (~4-8 mm) in a fine-to medium-grained matrix and contains in addition large fragments of coal fragments. The base of such beds is associated with “ball and pillow” loading structures and minor soft sediment deformation some places, though any primary internal depositional structures are not visible. Intrabasinal conglomerate of these characteristics commonly occur in association with Inclined Heterolithic Stratified units (Thomas *et al.* 1987). They also occur at base of units otherwise consisting of facies D.

Interpretation

The intrabasinal conglomerate is formed from break up of mudstone beds and/or incorporation of organic matter originated within the floodplains of the basin. Some places the source of mudstone clasts is eroded from the mudstone beds just below, in which the mudstone clasts are fairly large and have same lithological characteristics as the bed below, e.g. colour and texture.

Intrabasinal conglomerates which have smaller mud clasts and are deposited on top of e.g. sandstone beds indicate somewhat longer transport, though not necessarily a great distance as mud clasts get easily rounded during transport. This sort of deposition is likely to occur related to a slightly eroding stream-, tidal-, or crevasse channel, or crevasse splay near an eroding crevasse channel.

6.10 Facies J: Mudstone

Description

This facies consists of fine-grained material of silt and clay of red, grey or mottled colour. It can occur in units up to several tens of meters thick and ten to hundreds of metres in lateral extent with sheet geometry. Smaller units are also present where sandy architectural elements embedded within are frequent. Thin layers of siltstone, shell banks or very fine sand can be embedded in this facies. However, these beds can be difficult to discover and trace due to scree material which tend to cover these areas of the cliff wall. No major sedimentary structures are usually present or visible in the mudstone, though lamination, burrows and root structures occur.

Interpretation

This facies can be thought of as “background sediments” representing finer floodplain material deposited from suspension during flooding of the main stream.

6.11 Facies K: Siltstone

Description

This facies consists of decimetre thick siltstone beds which are found mostly interbedded in thick units of mudstone or as thin beds in sandstone units. Sporadically lenses of rippled, very fine sand are embedded in silt, thus generating lenticular bedding. When alternating with mudstone, siltstone beds generally have hundreds of meters lateral extent with sheet geometry. In this way, siltstone beds form horizons of coarser material within the background sediments, thus causing stratigraphical marker horizons. The siltstones are usually gray of colour, burrowed and possibly with some laminae when preserved.

Siltstone is probably also an important constituent in areas which are not reached to be observed closer, but only estimated from a distance; typically those areas composed mainly of mudstone (facies J) with several smaller beds of fine sand and silt

Interpretation

These minor siltstone beds in background sediments and compound sheet elements can be interpreted as distal crevasse splays, levee deposits or overbank deposits in general. When occurring within sandstone units a temporarily waning of the flow, migration or abandonment of channels or bars is plausible.

6.12 Facies L: Paleosol

Description

This facies consists of fine-grained units of sheet geometry of dark red finer material, commonly of clay and silt, though possibly very fine sand, with calcrete nodules. Green traces of rootlets are frequently present. Paleosol can be a few metres thick, where the paleosol horizon overlies mudstone facies (facies J) with a transitional base and is generally eroded on top beneath overlying sandstone units. Paleosol beds also occur as thin, some decimetres thick units, between sandstone beds. Paleosols are often found at beach level, where the total thickness is difficult to determine. Paleosols are associated with large rootlet of green colour from reducing conditions.

Interpretation

Paleosol is not a depositional feature, but soil development resulting from long term subaerial exposure, > 10 000 years (Bridge, 2001), with very little disruption and additional sedimentation.

The blue/green colourings of root traces are rizcretions which are calcrete precipitation formed in reducing conditions along decaying rootlets (Bridge, 2003).

6.13 Facies M: Soft Sediment Deformed Sandstone

Description

This facies is characterized by very fine to coarse sandstone frequently interbedded with clay disturbed by soft sediment deformation. Beds of facies M can be recognized by the chaotic internal structure of the sediments where the layers or original sedimentary structures are deformed. This facies occur only locally within beds of other facies.

Interpretation

Soft sediment deformed sediments can form in several ways in which the most widespread is related to water escape structures under rapid deposition, often of clayey material with high primary porosity and low permeability; loading; and tectonics which may stir the sediments.

6.14 Facies N: Shell Bank

Description

This facies is composed of mudstone or siltstone units less than 1 meter thick which contain a great deal of marine shell fragments. The shell banks can range from matrix supported conglomerate to grain supported conglomerate consisting nearly exclusively of shell fragments. The fragments can be up to 3 cm in diameter. The layers are difficult to trace extensively southwards due to the slight regional dip of the whole succession that eventually leads to disappearance of the layers into the beach and the ocean. Northwards, it has been possible to trace some of the layers tens to few hundred meters before it loses its thickness

or extend into an unreachable area high up on the cliff wall. About 4 or 5 of these layers are registered.

Interpretation

Shell banks are thought to represent flooding surfaces of greater marine influence than the tidal influence. Other possible interpretations for these are lagoonal settings or beach zone for the grain supported shell banks.

7 FACIES ASSOCIATIONS AND ARCHITECTURAL ELEMENTS

TABLE 7.1: Table of facies associations and their respective architectural elements. The facies are listed in accordance to the frequency of their appearance in the elements.

Facies Association	Description	Architectural elements	Description	Facies
FA 1	Channel fill	FA 1.1	Abandoned channel fill	C,A,H,F,I,J,E, B
	Deposits	FA 1.2	Lateral accretionary elements/point bars	A,B,E,I,F,C,J, D
		FA 1.3	Mid-channel bars/sandflats	D,C
FA 2	Floodplain Deposits	FA 2.1	Floodplain fines	J
		FA 2.2	Paleosols	L
		FA 2.3	Crevasse splays	A,B,F,J,G
FA 3	Overbank Deposits	FA 3.1	Levee	B,A,F,E,G,K,J,
		FA 3.2	Crevasse channel	B,A,D,F
FA 4	Inclined Heterolithic	FA 4.1	IHS elements with sporadically rhythmic sand-mud lamina	D,G,M
	Stratification (IHS)	FA 4.2	Elements with centimetre to decimetre thick inclined heterolithic strata	E,G,J,K,A,B,C, F,I,M
FA 5	Marine Deposits	FA 5.1	Shell banks	O

7.1 FA 1: Channel Fill Deposits

Channel fill deposits are generally high energy deposits related to the deposits occurring in the main stream channel. It is within FA 1 we expect to find the majority of sandy deposits. FA 1 is thus the most important facies association as concerns petroleum reservoir in a fluvial system. Architectural elements within FA 1 are abandoned channel fill (FA 1.1), lateral accretionary bars or point bars (FA 1.2) and mid-channel bars or sandflats (FA 1.3). The presence of large sand filled abandoned channel elements in the study area are also indicated by the extension of less erosive rocks into the Atlantic Ocean beyond the beach and which are visible during low tides.

7.1.1 FA 1.1: Abandoned Channel Fill Deposits

Description

Abandoned channel fill deposits, or abandoned channel fill, can be of sandstone, mudstone or a mixture of the two depending on the abandonment history. Most commonly the channel infill is multistorey and complex with internal reactivation surfaces associated with conglomeratic lag (facies H and I) alternating with through cross-stratified sandstone (facies A and C). Upward fining trends are common with the uppermost strata frequently dominated by ripple laminated fine sandstone, thus indicating a waning flow. Some few examples of abandoned channels are filled with mudstone (facies J), or a mixture with sandstone beds (facies E, B and A or C) embedded in mudstone (facies J).



Fig. 7.1: Two examples of abandoned channel fill (FA 1.1) consisting of a mixture of sandstone and mudstone.

Abandoned channel fills (Fig. 7.1) are characterized by a symmetrical or asymmetrical, erosive and concave lower boundary, whereas the upper boundary can be conformable to sharp towards overlying floodplain fines or transitional with levee deposits, depending on the process of avulsion and abandonment. FA 1.1 is juxtaposed to elements of the same facies association (FA 1), e.g. point bars, as well as levee deposits (FA 3.1) or floodplain fines (FA 2.1).

The abandoned channel fills have low width/depth ratio, which are typical for meandering streams, with recorded thickness and widths of 3-10 meters and < 40 meters, respectively. These numbers are, however, somewhat misleading as the exposure is usually not extensive enough to allow measurements of the larger structures which are partially visible. The largest partially exposed stream channel is estimated to be ~300 meters wide, based on its association to the point bar (see Ch. 6.1.2), and a minimum depth which equals the height of the point bar, i.e. 12 meters.

Interpretation

Rapid abandonment of the channel will result in a channel fill not associated with the stream channel itself, but merely other facies associations (FA 2 and FA 3) filling in the space the channel has created.

Channel fill with compound amalgamated surfaces with pebble lag characterizes multistorey infilling from durable channels experiencing repeated erosion and infilling episodes. In contrary, singlestorey channel fill indicates a solitary channel infilling event (Komatsubara, 2004). Channels in the field area are almost exclusively multistorey filled, with the exception of small scale channels cutting into bars (FA 1.3) and some crevasse channels (FA 3.2).

7.1.2 FA 1.2: Lateral Accretionary Elements (LA) and Point Bar Deposits

Description

Point bars deposits, or point bars, are characterized by epsilon cross bedding with sigmoidal reactivation surfaces dipping towards the stream channel (Fig.7.2). The point bar is a fining upwards succession with intrabasinal conglomerate (facies I) at base followed by upper plane parallel-stratified- or low angle cross-stratified sandstone (facies E), a main component of planar- and through cross-stratified sandstone (facies A and B), and ripple laminated sandstone at top (facies F). The large scale sigmoidal reactivation surfaces are often associated with centimetres to decimetres thick mudstone (facies J) marking these surfaces. Internal reactivation surfaces are numerous but barely visible due to lack of grain size variations resulting from good sorting. Moderate grain size variation in foresets also makes the sandstone appear massive some places. Nevertheless, foresets with double mud drapes (facies C) are observed locally, particularly in the vicinity of the stream channel. Large fossilized tree trunks have been trapped at base of the clinothems in the transition to the river channel where also mudstone laminae (facies D) are present.

Minor lateral accretionary elements tend to be somewhat more heterolithic with occasional mudstone laminae (facies D), low amplitude dunes (facies A), and sporadically soft sediment deformed muddy sandstone (facies M) at base. The accretionary elements may lack ripple lamination (facies F) and plane parallel stratified sandstone (facies E), but have clear sigmoidal geometry and lateral association to abandoned channel fill (FA 1.1). Minor lateral accretionary elements are commonly < 5 meters of width and <1,5 meters of height.

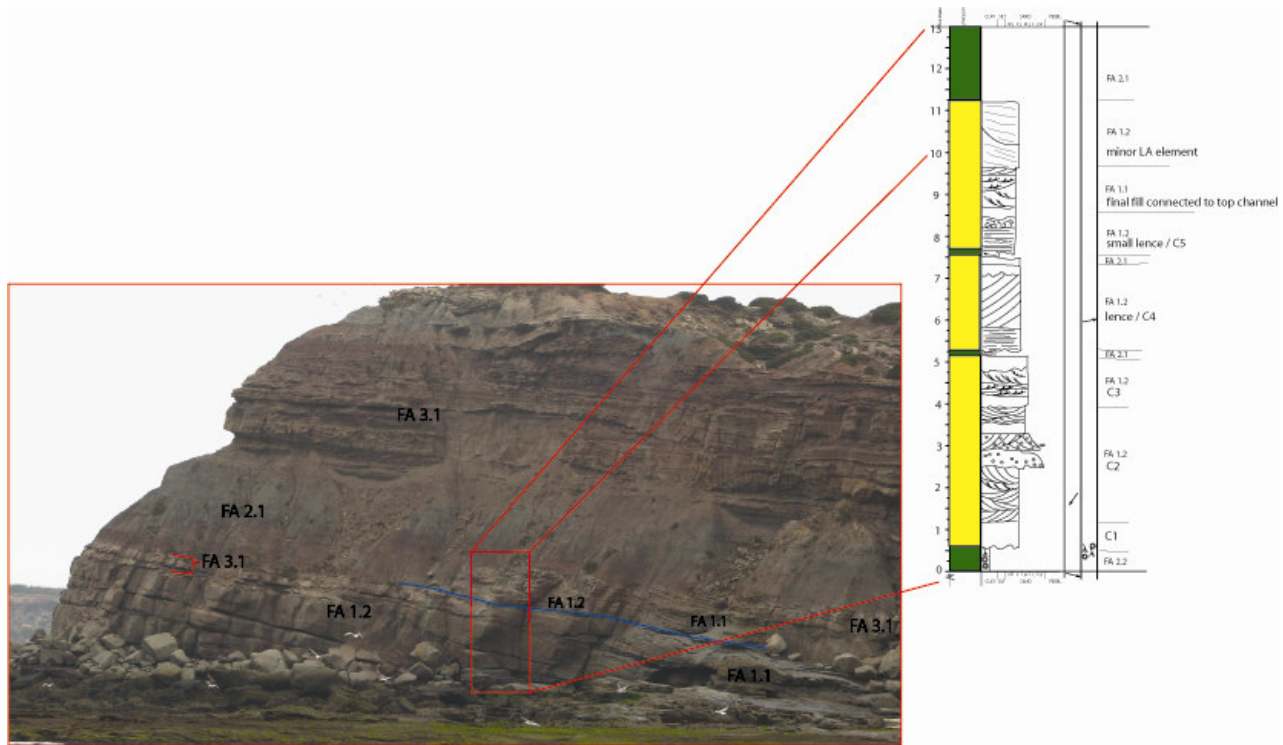


Fig. 7.2: Point bar element of approximately 100 meters wide and 12 meters thick. Levee elements (FA 3.1), Abandoned channel fill (FA 1.1) and floodplain fines (FA 2.1) are also present identified. The log illustrated is S2_P5.

The lower bounding surface of the point bar units is erosive, as it corresponds to an old channel base. Point bars and minor lateral accretionary elements underlie mostly an unconformable upper boundary of deposits of same facies association (FA 1), e.g. a new channel-bar complex, though a conformable boundary to levees (FA 3) or floodplain fines (FA 2) is also possible. Laterally the point bars are associated with abandoned channel fill (FA 1.1) on one side and floodplain fines on the other (FA 2).

The large point bar present is measured to be ~100 wide and 12 meters high, in which both dimensional parameters can be used to calculate the bankfull width of the palaeochannel it is associated with. This palaeochannel is estimated to have been ~250-350 meters wide. An extended perspective of the point bar elements is obtained in third dimension, where up to 2 meter thick beds, which thin towards north, are embedded in floodplain fines (FA 2.1) in an overlapping pattern which resembles “en echelon” patterns. These sandstone beds consist of medium- to very fine-grained sand with mudstone drape (facies J), sandstone-mudstone laminae (facies D) and occasional cross-stratification with mud drapes (facies C).

Interpretation

The clinothems and lenses present in this depositional element have a characteristic sigmoidal geometry bounded by mudstone draped reactivation surfaces representing lateral accretionary surfaces. The geometry in 3D view and its association to a stream channel exclude the possibility of a small delta, e.g. bay-head delta in an estuary. This element is therefore interpreted as a rather large point bar deposited in a meandering belt.

Furthermore, the point bar element is interpreted to be a section through the upstream or downstream part based on the overlapping geometry visible in 3D and the position of the channel, which has a continuation into the sea, though lacking reoccurrence in outcrops further north.

Helicoidal flow development in sinuous streams leads to erosion of the outer bank and deposition on the inner bank. The helicoidal vertical circulation cell normal to the stream banks will experience a velocity decrease due to shear stress as it passes obliquely over the point bar (Miall, 1992; Miall, 1977), thus generating lateral accretionary bars and lateral migration of the channel across the floodplain.

The helicoidal current develops due to the curvature in the stream channel and will therefore become more developed in the downstream half of each meander bend. In general, the point bar deposits show a fining upward trend, though the upstream part may deviate from this and have local upward coarsening successions (Miall, 1977).

“En echelon” pattern may represent the tail (downstream part) of the point bar, as indicated in Fig. 7.3, or possibly the upstream part. Bluck (1971) has, recognized “en echelon” patterns in the upstream portion of point bars, though these are of coarse material representing gravel bars.

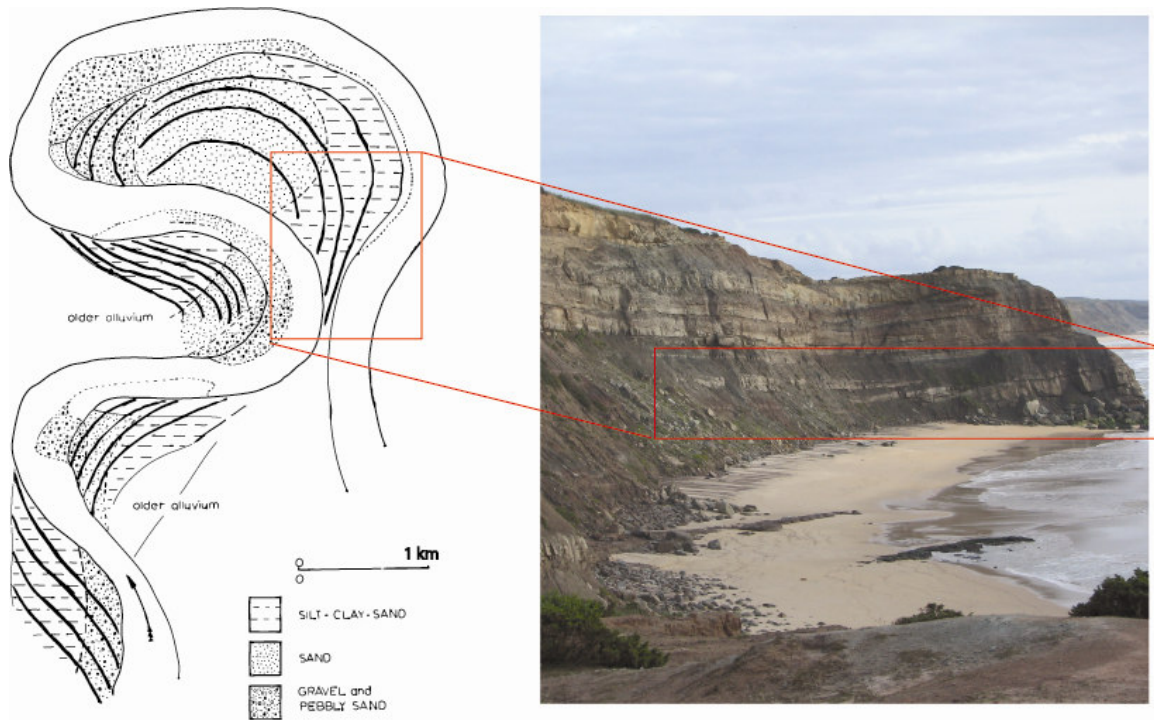


Fig.7.3: An “en-echelon” pattern in the third dimensional geometry of the point bar is interpreted to represent the tail in the downstream portion. The picture is compared to a drawing of a point bar made by River Endrick, Scotland, UK (from Bluck,1971).

Lateral accretionary elements can be formed in a range of fluvial settings; not only in association with meandering channels, though that is the expected case for the larger LA element discussed here, but not for minor LA deposits.

7.1.3 FA 1.3: Mid-channel Bar Deposits or Sandflats Deposits

Description

Mid-channel bar deposits, i.e. mid-channel bars, or sandflats, that could be downstream accretionary bars, lobate bars or compound bars (Bridge, 2003; Miall, 1977) are characterized by 1-5 meter thick beds of subhorizontal geometry. The bar morphology is characterised largely by high amplitude, ~0.5 meters, tangential through cross-stratified sandstone dunes of low sinuous crests to near planar through cross-stratified sandstone dunes with double mud drapes (Fig. 7.4) (facies C) and tidal bundle sequences, though some plane

parallel stratified sandstone beds with mudstone laminae (facies D) may also be present. Ripple lamination (facies F) may occur in the upper part of the bar succession. Numerous internal reactivation surfaces are present within the beds. Their lower boundary is erosive towards underlying floodplain fines (FA 2.1), or elements of the same facies association (FA 1). The upper boundary is conformable to overlying floodplain fines (FA 2.1) or levee deposits (FA 3.1), or erosive to elements of the same facies association (FA 1). The bars are laterally associated with levee deposits (FA 3.1) and elements of FA 1. Some minor singlestorey channel fills (FA 1.1) and minor lateral accretionary elements (FA 1.2) can cut into the bar forms, but are frequently camouflaged due to small grain size variations.

Bar elements with double mud drapes compose tidal bundle sequences containing seemingly ~14 tidal bundles.

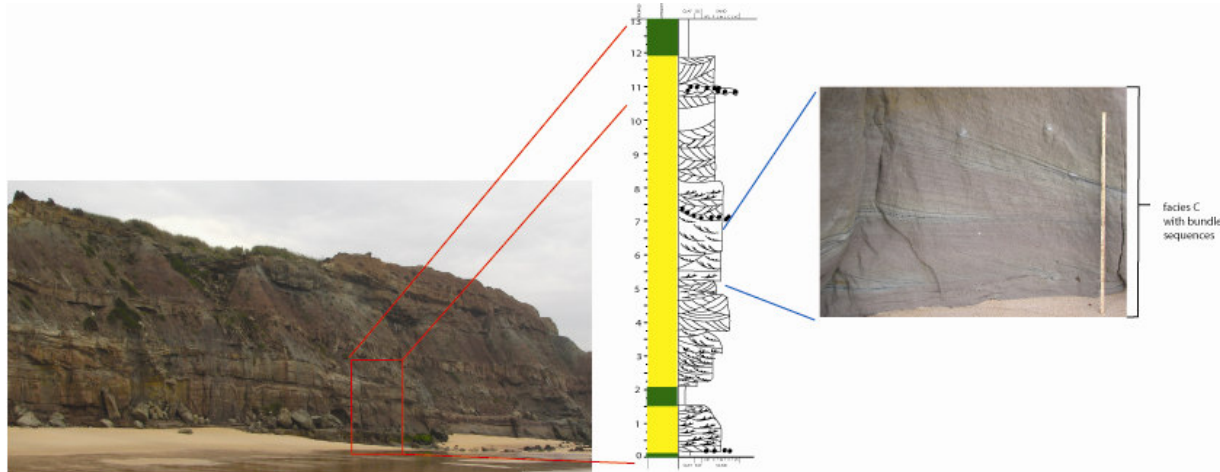


Fig. 7.4: Element of mid-channel bar with tidal bundle sequences of thinner and thicker bundles thought to represent the moon cycle and thus neap- and spring tide, respectively. The measuring stick is 1 meter long. The log shown is S3_P1.

Interpretation

The interpretations of mid-channel bar elements are based on the large dune structures with well developed tidal signatures, indicating deposits within a channel, as well as apparent position in channels due to its lateral association with abandoned channel fill and levee. Additionally, the bars are flat topped and lateral extensive within few hundred meters.

Mid-channel or sandflats may be classified as “simple foreset bars” or “compound bars” from Miall (1977) (see Table 2.1). These bed forms have their dominant occurrence in sandy

braided channels or sandy meandering. Fig. 2.7 shows several possible cross sections through a compound bar.

A tidal bundle sequences containing seemingly ~14 tidal bundles are thought to origin from a diurnal tidal, i.e. one daily, oscillation or a mixed tidal oscillation. A semidiurnal phase will record two tidal floods per day which results in ~28 bundles during one moon phase or bundle sequence.

7.2 FA 2: Floodplain Deposits

The floodplain lies adjacent to the alluvial ridge (Fig. 2.7) and is primarily subaerially exposed, except when receiving predominantly fine-grained sediments during flooding of the river or sand through crevasse events. FA 2 is the main facies association composing the background sedimentation in which sandstone bodies are embedded. Deposits of FA 2 can be up to several tens of meters thick and hundreds of meters in lateral extent, with observable extent only limited by the size of the actual outcrop. Elements of FA 2 are mainly fine-grained (FA 2.1 and FA 2.2), though sandy lobes of crevasse splays (FA 2.3) are also included as architectural elements in this facies association, because lobes and splays commonly extend onto the floodplain and reach beyond the proximal sand-rich overbank deposits where the floodplain facies association originates.

7.2.1 FA 2.1: Floodplain Fines

Description

Floodplain fines are composed of mudstone (facies J) which constitutes the majority of the background sedimentation. Floodplain fines occur with sheet geometry where the lateral extent can reach hundreds of meters and thickness of the units reaches tens of meters. Since floodplain fines compose the background sedimentation, this facies association is bounded below, above and laterally to any other facies associations. The lower boundary is exclusively conformable while the upper boundary is generally erosive, with the exception of a transitional boundary to paleosols (FA 2.2).

Interpretation

During flooding events water will reach above the river banks and spread out on the floodplain depositing mud and silt from suspension. Between these flooding events the floodplain will be predominantly subaerially exposed which give room for growth of vegetation, burrowing and paleosol development.

7.2.2 FA 2.2: Paleosols

Description

The paleosol component (Fig. 7.5) of this facies association is equal to the paleosol facies (facies L), though it is generally primarily deposited as mudstone facies (facies J), from which the paleosols have developed by pedogenic processes. Well developed paleosol units can be up to a few meters thick, ~3 meters, with a transitional lower boundary to floodplain fines (FA 2.1). Paleosol units also lie above or in between units of overbank deposits (FA 3) or crevasse splays (FA 2.3), in which they are commonly less developed. The upper boundary is erosional beneath elements of FA 1, FA 3 or crevasse splays (FA 2.3). The paleosols are laterally limited in outcrop view where they are commonly eroded away or disappear due to the regional dip. Paleosols are, however, laterally persistent over hundreds of meters to kilometres originally.

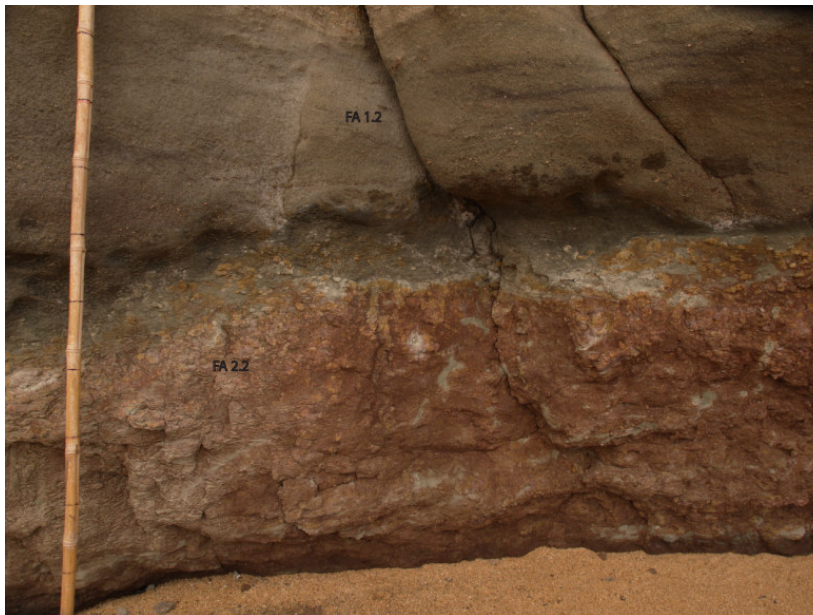


Fig. 7.5: Paleosol development (FA 2.2) below the large scale point bar (FA 1.2). Black lines are marked at every 10th cm interval on the stick. (Photo: I. Midtkandal)

Interpretation

Paleosols are recognized by calcrete nodules, red colouring and green root structures. Paleosols represent long term (1-10 ky) subaerially exposure and soil formation with development of calcrete nodules and greenish root traces, rhizoliths, where calcrete have precipitated in a reducing environment around rootlets. Paleosols are not a depositional feature but a result of soil formation. Mature soils form where there is little or no accumulation and erosion of sediments and where burrowing, pedogenic activity and fluctuating moisture operate during several thousands of years (Bridge, 2003). Demko (2004) differs between floodplain/overbank paleosols and paleosols which develop at unconformable boundaries of long term erosion and non-deposition. The latter paleosols are generally more developed than the first. The strata above and below such an unconformity may represent different environments. The surface may be associated with base-level fall and formation of incised valleys, thus creating a subaerial unconformity and sequence boundary (Zaitlin *et al.* 1994). Paleosols formed in this setting commonly occur on interfluvies (Emery and Myers, 1996; Zaitlin *et al.* 1994).

Paleosols of this origin are initially laterally extensive and can be utilized as a chronostratigraphic horizon for correlation purposes.

7.2.3 FA 2.3: Crevasse Splay Deposits

Description

Crevasse splay deposits, or crevasse splays (Fig.7.6), are usually composed of sandstone beds with small to medium scaled cross-stratification (facies A, B), with climbing- and/or current ripple lamination (facies F) commonly superimposed. Mudstones (facies J) are locally present between crevasse splay sandstone beds. Apparent massive sandstone (facies G) beds occur. Desiccation cracks at base of sandstone beds, root structures and burrows are not uncommon. The thicknesses of crevasse splay deposits vary, depending on single- or multistorey lobes and distance to the river channel. Composited proximal bedsets can be up to few meters thick, with several internal erosional surfaces and amalgamated surfaces present. However, generally singlestorey crevasse splay deposits are less than 1m meter thick. The lateral extent is up to a few hundred meters in outcrop.



Fig. 7.6: Crevasse splays (FA 2.3) and crevasse channel (FA 3.2) elements. The base of the crevasse channel is indicated by a red dashed line. The elements to the right are only partially exposed and are thus of uncertain facies association. Samuel Etta for scale (left).

Crevasse splay sandstone units have mildly erosive lower- and conformable upper bounding surfaces adjacent to river channel and proximal overbank levee deposits (FA 3.1). Distally the boundaries are conformable to finer-grained floodplain deposits (FA 2.1) of the same facies association. Proximal to the main stream channel, the thicker strata sets of crevasse splays are usually sandy, whereas the grain size commonly decreases to very fine sand and siltstone (facies K) by increasing distance away from the source channel. The thickness also decreases in distal direction into the floodplain, thus giving the depositional element a wedge-shaped geometry which fingers into floodplain fines (FA 2.1). Crevasse splays are laterally bounded to crevasse channels (FA 3.2), levees (FA 3.1) and elements of its own facies associations (FA 2.1 and FA 2.2).

Interpretation

Distal crevasse splays are recognized by thin sandstone or siltstone sheets embedded in floodplain mud and its association with crevasse channels, composing units of “steerhead” geometry. Proximal crevasse splay deposits are more difficult to identify as they may

resemble levee deposits in some cases, but have in general thicker and coarser strata (Bridge, 2003). However; compound crevasse splay strata sets representing superimposed lobes or splays are uncommon.

Crevasse splays expand onto the floodplain from a system of crevasse channels which break through the levee or bank of the stream river. Normally the crevasse splay will experience a waning flow both stratigraphically upwards and laterally away from the stream- and crevasse channel (Bridge, 2003).

7.3 FA 3: Overbank Deposits

Deposits of FA 3 are mainly sandy deposits in the immediate proximity to the stream channel, in which architectural elements of levee and crevasse channel are included. Though proximal crevasse splays also can be incorporated into FA 3, the crevasse splay element is included in FA 2, though occasionally interbedded with FA 3.

7.3.1 FA 3.1: Levee Deposits

Description

Levee deposits, or levees (Fig.7.7), are composed of decimetre thick, 0.1-1 meter, beds of tabular planar cross-stratified- and through cross-stratified sandstone (facies B and A), plane parallel stratified sandstone (facies E), ripple laminated sandstone (facies F), apparent massive sandstone (facies G), and sandstone with mudstone laminae, which are frequently bioturbated. Occasionally these facies are interbedded with mudstone (facies J) and siltstone (facies K). The levee elements appear rather planar in their geometry but are slightly wedge shaped and thin away from the channel they are associated with. Levee strata compose bed sets with a thickness of ~13 meters and are laterally extensive within distances of ~300 meters in outcrop. The lower boundary of levees is slightly erosive towards underlying floodplain fines (FA 2.1), architectural elements of FA 1, or elements of same facies association (FA 3.2). The upper boundary may be conformable when overlain by the depositional units of the facies associations just mentioned above. Small crevasse channels, with concave up erosion surfaces of ~3 meters width and < 1 meter thick, commonly cut

through the levee deposits thus appear embedded within. Laterally, levee deposits will be associated with abandoned channel fill (FA 1.1.) at one end and pinch out into floodplain fines (FA 2.1) at the other.



Fig. 7.7: Thick levee complex (FA 3.1) on top which extends hundreds of meters. The red line marks a concave-up erosional base which is interpreted to be a crevasse splay cutting through the levee complex. Smaller levees deposits are also present in this figure and are marked with red arrows.

Interpretation

The depositional units interpreted as levees have characteristics of thin beds of siltstone to sandstone with some mudstone in between. These beds have near planar geometry and compose compound bedsets. The interpretation of levee deposits is also highly associated with the lateral relationship to an abandoned channel. Levee bedsets insinuate a highly aggradational succession with near planar beds with little erosion at base. The bedsets are locally cut by crevasse events which is thought to be the case in Fig. 7.7

Levee deposits can have a great variety of facies incorporated and differ greatly from site to site. Levees grow during submergence by major flood where suspended material will be deposited when the turbulent flow ceases. Minor floods may not cover the levees or only locally. Finer material will be deposited further away from the channel. Crevasse events will break through the levees giving rise to crevasse channels and splays (Collinson, 1996).

The preservation potential for levee deposits depends greatly on migration- and avulsion history of the river channels in which it is generated from, in addition to the valley confinements. A wide meander belt can lead to well preserved levees. Low velocity currents in the stream channel will also be reflected in slow-moving, little erosive waters spreading out in the floodbasin and thus generate fine-grained levees and floodplain deposits (Ferguson, 1999).

7.3.2 FA 3.2: Crevasse Channel Sandstone Deposits

Description

Crevasse channel sandstone deposits, or crevasse channels (Fig. 7.6), contain plane parallel stratified sandstone with local mudstone or coal laminae (facies D), through or tabular cross-stratified sandstone with little or no mud drape in foresets (facies A and B), and ripple laminated sandstone (facies F). Larger coal fragments may be found at base. Crevasse channels are characterized by their small cross sectional size and shallow depth of up to ~50 and 5 meters, respectively, as well as their association with crevasse splays and levee deposits.

Crevasse channels have channel geometry defined by their concave erosive lower boundaries. Crevasse channels differ from other channels with their winged sides composed by crevasse splays. They overlie floodplain fines (FA 2.1), crevasse splays (FA 2.3), or architectural elements of same facies association (FA 3). The upper boundary of FA 3.2 units is conformable to floodplain fines (FA 2.1), abandoned channel fill (FA 1), or elements of the same facies association (FA 3).

Interpretation

Crevasse channels are mostly recognized by their association with crevasse splays which gives the units “stepped” geometry in cross section (Fig. 7.6), and their relatively small sizes compared to the stream river cross sections. When viewed from an oblique angle or along the axis of the crevasse channels, they are more difficult to identify. Sand-sand or sand-mud amalgamated surfaces may be present where a crevasse channel sustained for some time, thus recording multiple crevasse events. Thickness variations are not expected to be great over short distances (tens to few hundred meters) along the axis, but will thicken and thin towards channel and floodplain respectively on a larger scale.

Crevasse channels are ephemeral channels which break through the levees during flooding and branches out on the floodplain with an associated crevasse splay lobe. Crevasse channel deposits normally represent a waning flow, characterized by ripple lamination superimposed on cross-stratified sandstone. Slow avulsion processes of the stream channel through the crevasse channel may occur and thus give rise to continuous active growth of a crevasse

channel, forming a reversed facies development, from current ripple lamination at the base to cross-stratified sand dunes on top. Intervals of sand and mud laminae (facies D) or mudstone (facies J) interbedded with cleaner sandstone may indicate several minor crevasse events superimposed where sandstone-mudstone laminae represent the waning flow on top of each event with a continuous sedimentation. Where mud is deposited between high energy flow events, amalgamated surfaces may have been formed with sandstone to sandstone contacts with discontinuous mudstone laminae between.

7.4 FA 4: Inclined Heterolithic Strata (IHS)

Inclined heterolithic stratification (IHS) (Thomas *et al.* 1987) occurs on millimetre to meter scale, but differ from Visser's (1980) bundles. The IHS facies association represents the more heterolithic units in the study area. The IHS units include e.g. lateral accretionary- (FA 1.2), levee- (FA 3.1) and channel infill elements (FA 1). IHS has, however, been put into its own facies association because it is thought to represent a somewhat different depositional environment than the previous mentioned facies associations.

The elements of FA 4 can be separated into general characteristics of *IHS elements with sporadically rhythmic sandstone-mudstone laminae* and *elements with centimetre to decimetre thick inclined heterolithic strata*.

7.4.1 FA 4.1: IHS Elements with Sporadically Rhythmic Sandstone-mudstone Laminae

Description

Sandstone-mudstone lamination (facies D) is present within 2-3 meters thick and *ca* 50 meters wide sandstone beds of low dip to slightly concave-up geometry beds with undulating base. Sandstone-mudstone laminae are also present intermittently where otherwise centimetres to decimetre scale heterolithic strata prevail. A rhythmic trend is commonly present in the laminae.

The rhythmically stratified sandstone-mudstone laminae are arranged in up to 10 cm thick groups of internal mm thick laminae that are separated by *ca* 1-3 cm thick sandy layers

(Fig.7.8). On a larger scale of some decimetres, <0,5 meters, there are variation in the mud/sand ratio in the beds. These variations generate intervals of grouped sandstone-mudstone laminae interbedded with 5-15 cm thick sandstone of most commonly massive (facies G) or plane parallel stratified (facies D) with no or little mud.

Interpretation

The sandstone-mudstone variation creating the laminae is thought to have resulted from fluctuations in the energy levels, though continuous deposition, where the sand is deposited by traction currents or suspension, whereas the mud settled from suspension. The rhythmic variation is probably due to tidal cyclicity where the grouped sandstone-mudstone laminae are produced by the daily tidal fluctuations and the alternation with sand is due to the monthly variation in the tides of neap- and spring flood (Rebata *et al.* 2006). The higher order of variability in the sand/mud ratio may represent seasonal variations of e.g. wet and dry periods.



Fig.7.8: Sandstone-mudstone lamina (facies D) of with cm thick sporadically rhythmic variations which can be interpreted to represent neap- and spring tides where higher amount of sand would represent spring floods.

These deposits are found in elements of concave-up channel geometry with locally thin dune structures at base and a lateral association with levee deposits. The deposits may thus represent abandoned channel fill or very low energy current channel fill.

Where FA 4.1 is present within the sandier beds of FA 4.2, it may signify periods of lower energy currents and fluctuations with continuous deposition. Intertidal flats with sandstone-mudstone laminae have been recorded within mixed flats, commonly the middle region of the intertidal flats (Boggs, 2001).

7.4.2 FA 4.2: Elements with Centimetre to Decimetre thick Inclined Heterolithic Strata

Description

Centimetres to few decimetres (up to 0,3 m) thick heterolithic strata can be composed of a great variety of facies where the sandstone mainly has structure of parallel stratification (facies E or facies D), tangential or through cross-stratification (facies A, B or C), apparently massive (facies G) and occasionally ripple lamination (facies F) and soft sediment deformation (facies M). Interbedded with sandstone are mudstone (facies J), siltstone (facies K) and intrabasinal conglomerate (facies I) (Fig. 7.9).



Fig. 7.9: Element on top with centimetres to decimetres thick Inclined Heterolithic Stratification (FA 4.2). (Photo: M. Nyrud).

Elements of FA 4.2 are generally found at the uppermost stratigraphic level in the study area. These elements show a high degree of amalgamation and aggradation laterally and vertically, which occasionally makes it difficult to separate the geometry of one element. However; several channel downcuts and infill and sigmoidal accretionary surfaces are distinguishable. Moreover, a subhorizontal element of thin alternating sandstone, siltstone and mudstone beds are included in this facies association.

Interpretation

The elements of this facies association are interpreted to be e.g. point bars/lateral accretionary elements, abandoned channel fill and levees, associated with channel infill and overbank deposits. These elements and facies associations are already defined above in their own facies associations, but due to their strong heterolithic character they are distinguished from previously described facies associations and included in this new facies association; IHS.

7.4.3 Discussion on Formation of IHS Elements

Inclined heterolithic stratification (IHS) is traditionally interpreted to represent depositional elements related to tidal channels or strong tidally influenced deposits within fluvial-deltaic systems, e.g. point bars of distributary rivers and tidal bars (Rebata *et al.* 2006; Thomas *et al.* 1987). Tidal channels are marine sourced and will spread out on the intertidal flats of the delta- or coastal plain with increased branching and reduced power inland. Tidal channel related deposits indicate a position within the intertidal flat, i.e. very close to the coastline.

The tidal channels can spread onto the intertidal flat directly from the coastline or diverge from the fluvial distributary channel onto the flat. Evaporites are expected to form on an intertidal flat in an arid climate. The nature of the intertidal flat also varies with amount of sand present. The amount of sand depends firstly on the presence of a marine source of sand, though channels which diverge from a distributary channel may be sourced partially fluvially. Further the amount of sand on the intertidal flat tends to increase from the supratidal area towards the lower intertidal region. Intertidal flats have thin planar beds often with sedimentary structures like ripple laminated sand, tidal rhythmites, bidirectional current indicators, mud drape and wavy-, lenticular- and flaser bedding. Additionally shell fragments and intraclasts may be present in higher energy areas, e.g. channels (Boggs, 2001).

However; the IHS deposits do not necessarily origin from tidal channels, but can also form in fluvial distributary channels which record high tidal influence. The tides reach further inland in fluvial channels since they have lower gradients than the surrounding areas. The IHS units may thus be deposited above the intertidal flat.

FA 4 may therefore represent either tidal channels or intertidal flat, or highly tidally influenced fluvial distributary channels and floodplain. The thin subhorizontal beds and the bed containing abundant sandstone-mudstone laminae may be interpreted as intertidal flat sediments; though have not been due to the concave-up geometry of the latter and the lack of other intertidal indicators like shell fragments, abundant peat/coal and evaporites.

7.5 FA 5: Marine Deposits

The field area has vast amount of marine indicators from numerous and well developed tidal signatures giving a proximity to the marine coast, thus placing the field in a paralic setting. Occasional beds with shell fragments are other indicators of marine influence. FA 5 includes the architectural elements of shell banks.

7.5.1 FA 5.1: Shell Banks

Description

The shell bank architectural element is composed of its equivalent facies (facies N) (Fig. 7.10). Shell bank units are commonly less than 1 meter thick siltstone beds with fragmented marine mollusc fossils, embedded in floodplain fines (FA 2.1). Shell banks can be traced laterally some hundred meters, <300 meters, before they dip into ground or into unreachable areas of the cliff wall.

One bed which contain only some fragmented pieces of shells differs somewhat from this description as it is composed almost entirely of mudstone clasts and large coal fragments with very little silt matrix. This bed is not laterally traceable and underlies a channel shaped unit.

Interpretation

These shell banks are thought to represent marine flooding surfaces, based on marine shell fragments and the association of fossil assemblages. The shell banks contain fragments of thin oyster shells; possibly of genus *Gryphaea* which are common in Jurassic rocks (Doyle, 2004). *Gryphaea* are, in its adult stage, epifaunal and adapted to soft substrate in calm environments with little or only temporarily high sedimentation rates (Gahr, 2005). Moreover; *Corbulomima* benthic mollusc association have been registered in the marine environment of Kimmeridgian age in the Lusitanian Basin (Fürsich and Werner, 1986). This association represent similar calm environment with small infaunal bivalves adapted to silty, soft substrate (Gahr, 2005).

About 4 flooding surfaces are recorded in the study area. Flooding surfaces can be applied as chronostratigraphic horizons and can be utilized for correlation.

The deviating unit may better be classified as an intrabasinal conglomerate bed as the broken shell fragments, large coal fragments and mud clasts present insinuate allochthonous deposition and not an *in situ* (autochthonous) marine shell bank. This is also supported by its position near the base of a channel in which it appears to compose a basal lag. The presence of large pieces of coal in addition to intrabasinal mud and well fragmented shells signifies continental deposits of both the intrabasinal conglomeratic bed and the overlying channel.

A)



B)



Fig.7.10 A & B: Two illustrations of the shell bank facies association (FA 5 of facies N) interpreted to represent marine flooding surfaces. Pen for scale.

8 PETROGRAPHIC ANALYSIS

A petrographic analysis can give a better understanding of reservoir sandstones in terms of mineral composition, texture and porosity and possibly utilize this to get information about source area, burial and fluid flow properties of the sandstone bodies.

8.1 Mineral Composition and Recognition

The main components of the sandstone bodies in our study area are quartz, feldspar (alkali feldspar, plagioclase and leached feldspar), mica and calcite, in addition to organic matter and mud. The clastic grains are angular to sub-angular, thus showing a very low maturity and indicating a short transportation distance. In general, the sorting is rather good in most sandstone samples of larger sandstone bodies, though a poorer sorting exists within crevasse splays and extrabasinal conglomerate.

Quartz:

Quartz grains are characterized by lack of colour in plane polarised light (PPL) and their black, grey to white colour in cross polarized light (XPL) and lack of cleavage.

Both single crystals, i.e. monocrystalline quartz, and grains made from a number of crystals with different orientations, i.e. polycrystalline or composite quartz, are present in the thin sections. The boundaries between individual crystals in composite quartz are sutured. Also some composite quartz grains with apparent banding are present within the extrabasinal conglomerate. The presence of composite quartz and particular banded composite quartz is an indication of metamorphic source (Adams *et al.* 1984).

Within some of the larger quartz crystals there are inclusions present. These inclusions are small needles of different minerals or fluid inclusions, commonly oriented along lines. Fluid inclusions may indicate a low-temperature source like a hydrothermal vein (Adams *et al.* 1984).

There is no evidence of quartz cementation or overgrowth in our samples.

Feldspar:

Feldspars are grouped into alkalifeldspar ((K, Na)AlSi₃O₈), which includes e.g. orthoclase and microcline; and plagioclase ((Na, Ca)(Al, Si)AlSi₂O₈), which has the end members albite and anorthite. Plagioclase is recognized by its sharply defined striations of albite twinning pattern of either single or double lines. Microcline feldspar is recognized by a cross-hatched pattern, “tartan” twinning, of somewhat diffuse lines or patterns of perthitic intergrowth. Perthitic intergrowth occurs from lamellae of Na- rich feldspar in K-rich feldspar. Orthoclase can appear quite homogenous and difficult to differentiate from quartz, though weathering by leaching may be an indication (Adams *et al.* 1984). Other indications may be the presence of cleavage which is not present in quartz.

Leaching is chemical weathering due to meteoric flushing of feldspar, and mica, resulting in dissolution of these and precipitation of authigenic kaolinite. The reaction is expressed by:



i.e. feldspar + water = kaolinite (clay) + cations

(Bjørlykke, 1998)

Precipitation of diagenetically formed authigenic kaolinite can have a highly reducing effect on the permeability of the sandstone as kaolinite clay particles commonly block the pore throat between grains. On the other hand, kaolinite may have a positive pore space preserving effect during deeper burial where it coats quartz grains and thus prevents grain-to-grain contact, dissolution and quartz overgrowth (Bjørlykke, 1998).

A majority of the feldspar shows evidence of leaching without any additional structures, though plagioclase and microcline are commonly distinguishable. Plagioclase feldspar tends to be more abundant than alkalifeldspar. Original perthitic structure may show as selective leaching within the grains.

Feldspar is formed in and is frequently a large constituent in igneous and metamorphic rocks (Adams *et al.* 1984).

Mica:

Micas are sheet silicates which are easily broken down during weathering. Mica minerals in the sandstones are characterized by thin, long grains with internal cleavage running parallel with its long axis. The mica grains are recognized by their shape and bright colours in XPL. The mica group includes muscovite and biotite as the most common minerals. These are difficult to distinguish in XPL, but easy in plane polarized light (PPL) where biotite is brown while muscovite is colourless.

Micas commonly form in igneous and metamorphic rocks.

Calcite:

Calcite is recognized by a higher order of pinkish/greenish interference colours and the rhombohedral shape of the cleavage pattern. Calcite occurs both as larger crystals and as cement filling original pore space between grains. Cementation is a porosity reducing process related to chemical compaction where calcite is precipitated from supersaturated pore fluids.

Mud:

Mud includes both the silt and clay fraction. The fraction of clay is below the resolution of visibility in the microscope so the individual grains can not be differentiated. The mud thus occurs as clearly fine-grained material of brown patches in PPL and a combination of brown, green and pink in XPL (Fig 8.1). Mud is also commonly found in the pore throats though not within the larger pore space.

Chlorite is a sheet mineral which is common in sedimentary rocks as an alteration product from e.g. leaching of e.g. mica and feldspar. Chlorite has a bluish-grey interference colour in XPL and pale brown to green in PPL. It is, however, very difficult to identify chlorite accurately since it is within the silt and clay fraction and not always resolvable in the microscope. Due to the large amount of leached feldspar in the samples it is possible that a large amount of the mud present is chlorite originating from the break down of mica and feldspar. An XRD (x-ray diffraction diagram) analysis of the samples would be helpful in determining the amount of chlorite present. This has been chosen not to be done in the present study, due to priority of time.

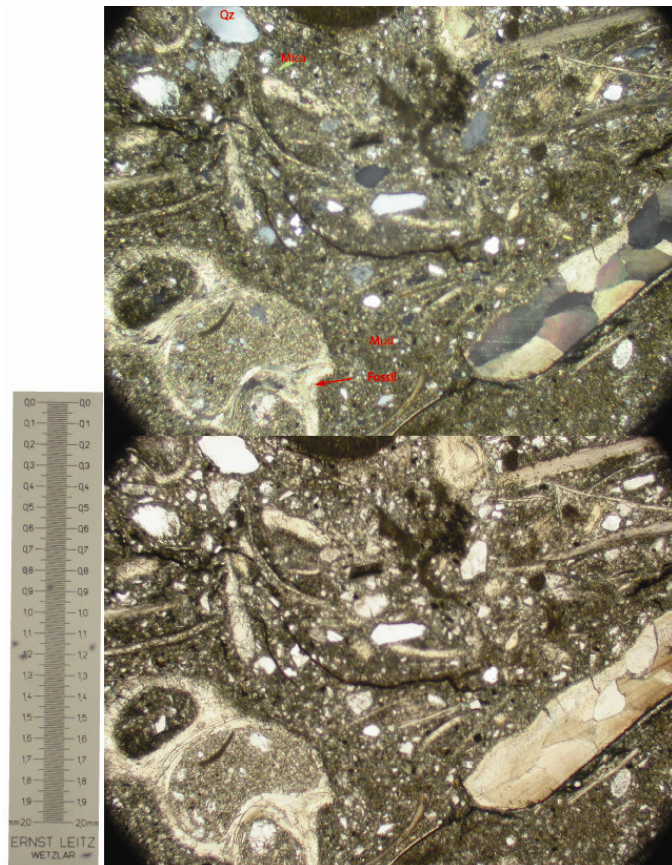


Fig.8.1: Thin section of a shell bank. Top: XPL. Bottom: PPL. The fine grained mud appears as of brown matrix in PPL and a combination of brown, green and pink in XPL. The grain size is too small to see individual grains on this magnification level.

Organic matter:

Organic matter is brown in PPL and dark brown in XPL, or black if it is burned organic matter (charcoal). Little to no changes in colour is visible when the sample is rotated. It is more easily recognized in PPL than in XPL, though better distinguished from biotite in XPL if doubt occurs, as biotite shows bright colour in XPL.

Pore space:

The samples are filled with blue epoxy to easier identify the pore space. The blue colour is visible in PPL, but not in XPL since it is a substance with isotropic properties. The pore throats between the larger pores are occasionally blocked, though this varies from sample to sample. Grain-to-grain contact is frequent.

Point counting:

TABLE 8.1: Table of the point counting results of the samples 15, 6, 9, 12 and Im.

Sample:	15	6	9	12	Im
Observer:	Mona Nyrud	Mona Nyrud	Mona Nyrud	Mona Nyrud	Samuel Etta
No. of points:	564	700	722	519	507
Facies:	Channel element (FA 1.1)	Mid-channel Bar (FA 1.3)	Exstrabasinal Conglomerate (facies H)	Lateral accretionary, IHS (FA 4.2)	Point bar (FA 1.2)
Minerals:					
Quartz	24,2 %	27,7 %	45 %	37,3 %	28,4 %
Plagioclase feldspar	0,5 %	2,2 %	0,8 %	1,1 %	2,5 %
Alkali feldspar	3,1 %	6,7 %	6,5 %	4 %	22 %
Leached feldspar	14%	20 %	12,4 %	16,3 %	2,1 %
Mica	1,9%	3,7 %	0,9 %	1,5 %	8,2 %
Calcite	22,6 %	14 %	11,7 %	1,9 %	26,7 %
Mudstone	23,3 %	5,1 %	8,3 %	2,5 %	0,7 %
Organic Matter	4,7 %	2,7 %	0,6 %	12,5 %	1,9 %
Pore Space	5,3 %	17,6%	13,4 %	22,5 %	7,5 %

The calcite percentage estimated by point counting largely represent how cemented the sample is. Table 8.1 also indicates the relationship between the amount of mud and calcite and the porosity percentage, in addition to a general overview of the amount of each mineral component.

8.2 Texture

Sample 13 represents a fine-grained channel fill facies association (FA 1). This sample is characterized by a relatively large amount of charcoal and only moderate amount of calcite cement and mudstone. This gives optimistic values concerning the porosity, but mudstone is largely present in the pore throats, thus reducing the permeability. The pores appear rather large and some places the grain-to-grain contact is moderate. Little calcite cement is observed. The sorting is good and the grains are sub-angular and more seldom angular.

Sample 14 represents crevasse splay element (FA 2.3). This sample is largely characterized by a large amount of mudstone, much organic matter and very low porosity. In areas of the thin section where the grain size is within the middle- to upper sand fraction primary pore space is nearly completely filled with calcite cement, thus indicating high primary porosity and initial fluid flow. Other parts of the thin section containing minerals in finer sand fraction to silt fraction are dominated by mudstone, though with some porosity still preserved (Fig. 8.2). The permeability is poor. The sorting is moderate to poor.

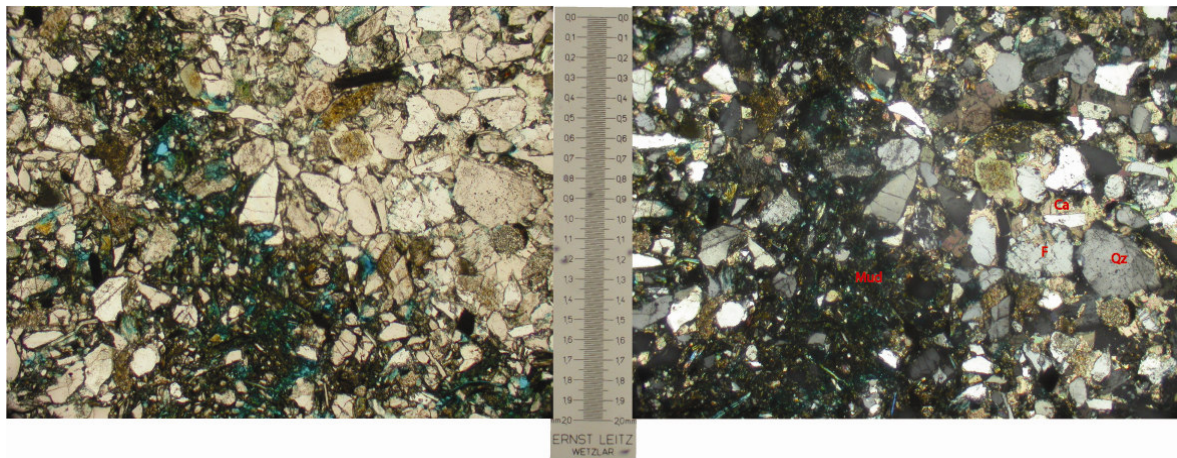


Fig. 8.2: Thin section of sample 14. Left: As indicated by the blue epoxy, porosity is present within the area containing small grains and mud. (PPL). Right: Irregular carbonate cement, surrounding the grains, are present in the areas of coarser material. (XPL).

Sample 15 represents a supposed channel element (FA 1). This sample has a high amount of calcite, ~23 %, and is thus well cemented. Cement, in addition to mud (~23 %), have reduced the primary porosity significantly to only ~5 %. The pores are small in size but

densely spaced. The connection between the pores is, however, not very optimistic due to the amount of mudstone which is commonly present in the pore throats. The sorting is moderate.

Sample Im represent the point bar facies association (FA 2.1). This sandstone appears well sorted in mesoscale and in microscale. Viewed under the microscope it is clear that calcite cement has reduced a large amount of the primary porosity. These samples are more abundant in mica than other samples. The mica grains tend to have their long axis oriented parallel to the stratigraphic level in which they occur (Fig. 8.3).

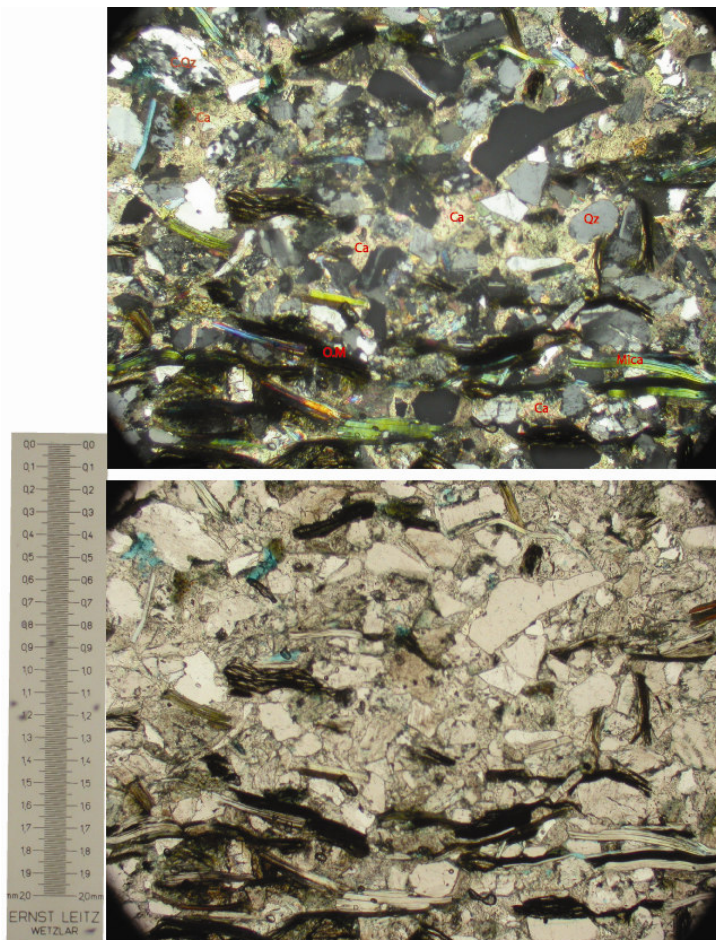


Fig. 8.3: Thin section of sample *Im*, point bar element. Top: The pinkish carbonate cements is irregular and surrounds the grains. Elongated fragments of organic matter and mica are oriented with its long axis perpendicular to the stratigraphic direction. (XPL). Bottom: Same image (PPL). Virtually no porosity is present.

Sample 6 is a representative sample for elements composed of mainly cross-stratified sandstone with mud drapes (facies C) taken from an architectural element interpreted to be a

mid-channel bar (FA 1.3). The sample shows evidence of some calcite cement, though this is highly subordinate. Mudstone is seldom present as large clasts, but mainly in pore throats and as partial fill in pore space (Fig. 8.4). This may reduce the permeability severely. The present porosity has been estimated to be around ~18 %. The grains are angular to sub-angular and are moderately sorted.

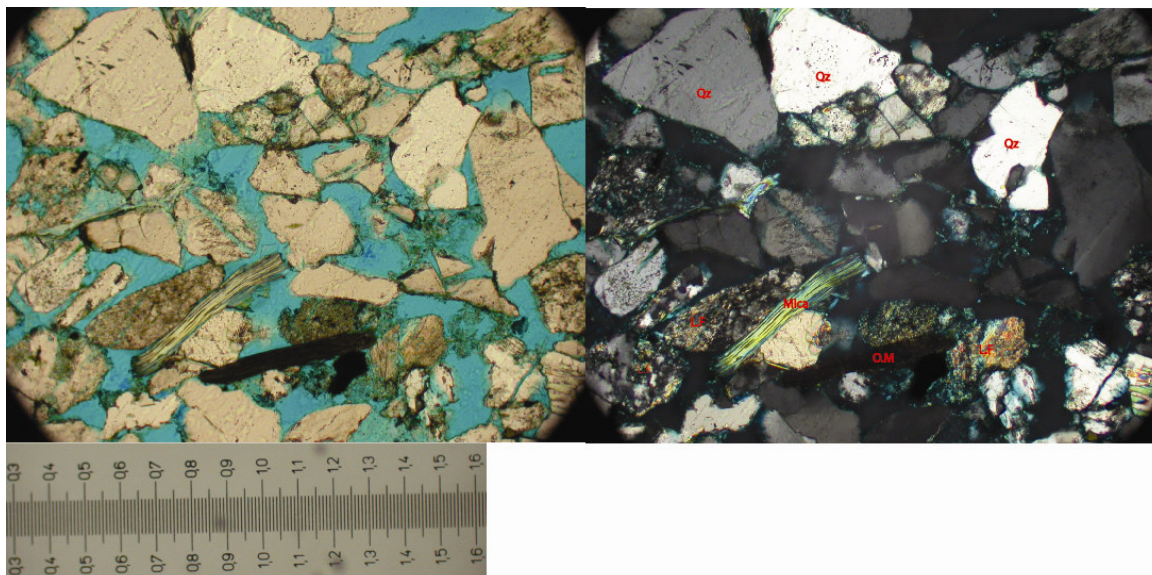


Fig.8.4: Thin section of sample 6. Left: The porosity is fairly good, but mud is present in the pore throats (PPL). Right: Same image with XPL.

Sample 9 represents the facies extrabasinal conglomerate (facies H) and is taken from an architectural element thought to represent a bar (FA 1.3). The high amount of quartz, 45 %, probably represents an anomaly due to the size, and thus the volume, of quartz pebbles as quartz is more resistant than softer minerals. Occasional feldspar grains are equally large, but generally smaller and fewer. Little, but some calcite cement and mudstone is present. Pore throats contain mud to a lesser extent than in sample 6. The porosity is ~13 %, which is mainly composed of some large pores. The permeability appears optimistic. The grains are angular to sub-angular, though larger grains (very coarse sand and pebbles) may be better rounded than the intermediate (sand). The sorting is poor.

Sample 12 represents a sandstone bed within a lateral accretionary element of IHS facies association of amalgamated channel elements (FA 4/ FA 1.2). This sample has a very large

amount of charcoal or dark, possibly organic, mud of which commonly coats the mineral grains (Fig. 8.5 top). The porosity is high, ~ 23 % (Fig. 8.5 bottom left), with barely any calcite cement present (Fig 8.5 right) and rather poor grain-to-grain contact. Since only some mud is present here the sample is expected to have both good porosity and permeability values. The sample is well sorted with angular to sub-angular grains. Within some grains the leaching of feldspar and mica has created secondary porosity.

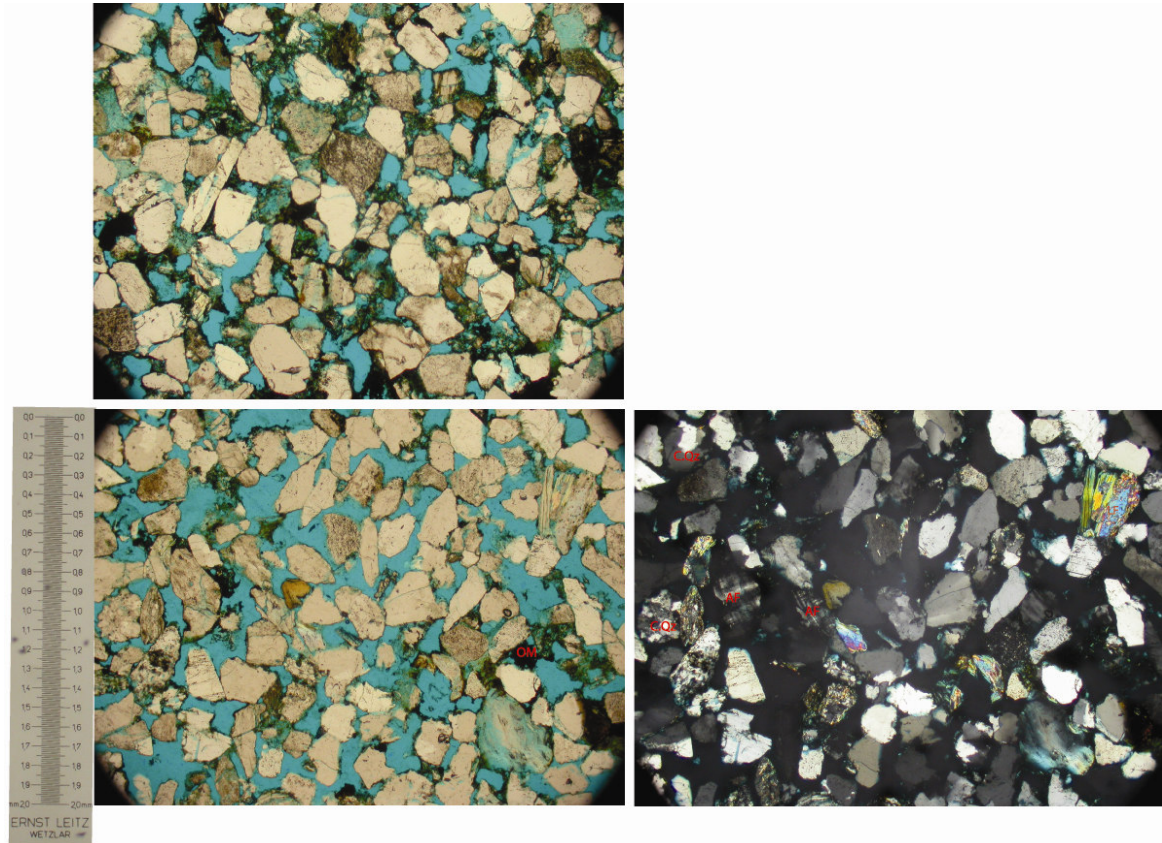


Fig. 8.5: Left: Top: Thin section of sample 12 where mud and organic matter/mud are present in the pores and pore throats which reduces the porosity and permeability. (PPL). Bottom: A cleaner area of same thin section of sample 12 as above. Less mud and organic matter/mud is present. (PPL). Right: same area as left lowermost image with XPL. Little to No carbonate cement is present in this sample.

Sample N represents an abandoned channel element (FA 1.1). This sample has a larger amount of mica than the other samples and contains some mudstone clasts. The moderate to poor sorting is emphasized by increase of calcite cement where larger grains dominate. This can be from better primary porosity and permeability, thus better initial fluid flow. Areas with smaller grains commonly have mud in the pores and pore throats. The minute variations in the grain size seem to be along the stratigraphic level on microscale.

8.3 Interpretation

Source area:

The minerals composing the sandstones constitute mainly of quartz and feldspar in addition to some mica. The calcite is largely secondary precipitated cement, though possibly a small amount is primary. The main constituents are derived from igneous, e.g. granitic or metamorphic gneissic rocks. Further indications of metamorphic origin are the composite grains of quartz with sutured boundaries and quartz pebbles with apparent banding. The grains are angular to sub-angular, a feature which indicates a short transportation and 1st order derived detritus from the source rocks. Thus the sandstones appear to originate from mechanical weathering of closely positioned igneous or metamorphic rocks. It is therefore reasonable to assume the source rocks are the Hercynian Basement at the basin's margin in the east and north-west; preferably north-west considering the palaeocurrent data (Ch. 11).

Such an interpretation is also supported by Bjørlykke (1983) which pointed out that rift basins are characterized by low mineralogical maturity as the sediment is often derived from erosion of the uplifted horsts of crystalline basement. The mineral composition also reflects a source of crystalline basement and is commonly rich in feldspar.

Diagenetic processes:

There are 4 diagenetic processes that are responsible for reducing the primary porosity in the sandstones:

- 1) Mechanical compaction due to increased burial and overload burden, which includes rearrangement and deformation of the grains.
 - 2) Chemical compaction from precipitation of calcite or quartz cement in pore space
 - 3) Chemical compaction from precipitation of expanded hydrous minerals like kaolinite from leaching of feldspar and mica
 - 4) Both mechanical and chemical compaction as a result of pressure solution which increases the compaction and precipitation of cement
- (Bjørlykke, 1983).

The first three points are present even during early diagenesis at shallow burial and are evident in the thin sections. Point 4 indicates deeper burial and later diagenetic processes

where grains experience such pressure from overburden that dissolution occurs at their boundaries. Sutured grain boundaries occur by this process where the mechanical compaction is prominent.

The amount of chemical compaction varies greatly from sandstone to sandstone. The amount of calcite present is highly connected with the porosity as this is the primary cement. Quartz cement has not been identified. The solubility of quartz increases with increasing temperature and can be about 100 ppm in seawater at 100 °C opposed to about 6 ppm at surface temperature. This increase in solubility can lead to supersaturation in the pore water with respect to quartz, and precipitation of quartz cement (Bjørlykke, 1983). Quartz cement is therefore associated with deep burial (approximately 3 km depth) and late diagenesis.

Porosity and Permeability:

The porosity is greatly affected by the calcite cement and is generally poor, while the permeability is significantly affected by mud present. Most samples of main sandstone bodies, i.e. mainly channel fill (FA 1), does not show very poor sorting and presence of mudstone. The mudstone is mainly intergranular and moderately present in the pore space, and may be from secondary processes like leaching of feldspar and mica and not from the original depositional processes. Fluvial sediments will be flushed by meteoric water after deposition, but in a hypothetical case of later submarine burial of the studied succession the leaching effect may be reduced due to less flux of meteoric water (Bjørlykke, 1998). This factor could improve the permeability within the sandstone. Leached feldspar grains may also have been derived from strongly weathered zones in the hinterland area.

Burial:

The study area does not show any evidence of late mechanical or chemical diagenetic processes and thus indications of deep burial. Some places the grains even show moderate rearrangement, i.e. mechanical compaction due to weight of overburden, by the poor grain-to-grain contacts. There is abundant calcite cement which forms at even early diagenesis, but no evident quartz cement to indicate deeper burial and later diagenesis. Thus the Lusitanian Basin succession at the present study area has probably been buried at shallower depths than 3 km.

9 ARCHITECTURAL STYLE

9.1 Architectural Style

Fluvial architecture can be defined as “the three-dimensional geometry and interrelationship of the deposits of channel, levee, crevasse splay and floodplain and other subenvironments of the fluvial depositional system” (Emery and Myers, 1996); or “the geometry and internal arrangement of channel and overbank deposits in a fluvial sequence” (Miall, 1978).

To determine the architectural style is to evaluate the interaction between the different architectural elements and the background sediments both laterally and vertically in reservoir scale with focus on position, orientation and connectedness of the elements, i.e. whether the elements are isolated, laterally stacked or compartmentalized, or vertically stacked or compartmentalized. By considering the architectural style and elements in 2D outcrops it is attempted to determine the fluvial style and predict the orientation of sandstone bodies in 3D and thus estimate the connectedness of the reservoir sandstone bodies, which is one of the key parameters in determining if a fluvial reservoir is producible as it affects the recovery factor. Further, architectural style is frequently the basis for sequence stratigraphic studies, e.g. base-level fluctuations in a fluvial setting, and are utilized to simulate 3D sandstone body geometry using a stochastic approach in modelling.

The architectural style and connectedness of the sandstone bodies are important to evaluate in the pre-modelling phase to be able to do a realistic prediction in the third-dimension. Marine flooding surfaces and paleosols are horizons which represent significant time intervals and are thus suitable for correlation purposes. There are three marine flooding surfaces, represented by shell banks, and three paleosol horizons in the study area which intersect one or several logs. In addition to their relevance as chronostratigraphic surfaces and correlation levels they may also signify alternation in the fluvial style in consequence of base-level fluctuations and transformation from low sinuous channels to channels of higher sinuosity, or lateral shifting of the meander belt.

9.1.1 Connectedness

Larue and Hovadik (2006) defined geobody or sandbody as “units which has optimistic values of parameters that differentiate the ability for fluid flow in reservoirs, e.g. permeability, porosity, facies”; and their connectivity as “the percentage of the reservoir that is connected”. The connectedness is a function of sand:gross ratio, and not net:gross ratio as for connectivity, and whether the reservoir has a 2D- or 3D fluvial architecture.

2D fluvial architecture

2D fluvial architecture or 2D fluvial reservoirs are characterized by i) straight, parallel channels in map view with little variation in orientation and no permeable conduits connecting them; ii) or layered sheet reservoir sandstone separated by laterally extensive impermeable mudstone in cross sectional view, i.e. be respectively laterally or vertically compartmentalized on reservoir scale.

Consequently the connectedness for 2D reservoirs are predicted to be very low below the point of percolation threshold at a sand:gross ratio of 66 % , though thought to approach 100 % above this point. The predicted connectedness of a 2D reservoir is based on an “S-curve” (Fig. 9.1 A) which plots the connectedness versus the sand:gross ratio. This curve illustrates that for sand:gross values greater than 75 % the connectedness is >95 %; while between 50-75 % the connectedness can vary greatly from 0-100 % (Laure and Hovadik, 2006).

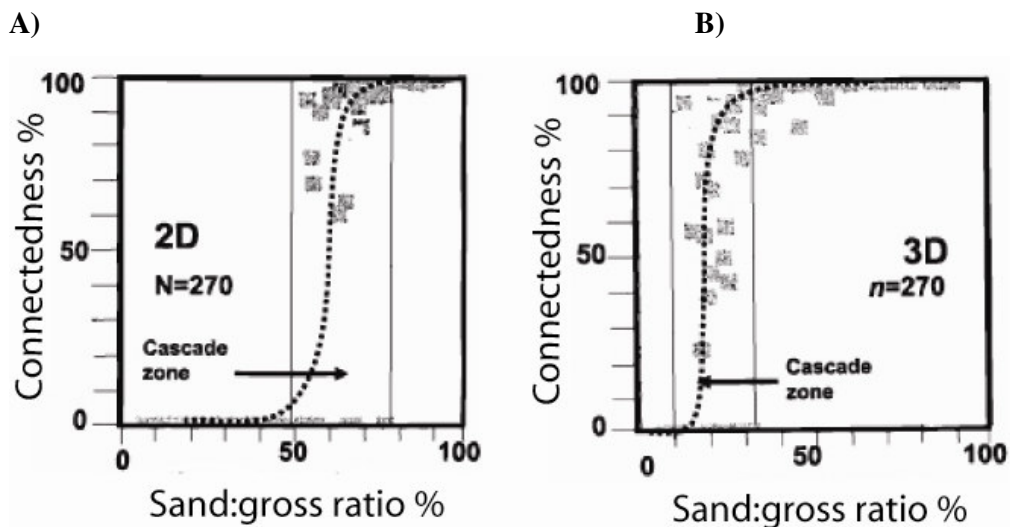


Fig. 9.1: A) 2D S-curve applied to predicted connectedness from sand:gross ratio. B) 2D S-curve applied to predicted connectedness from sand:gross ratio. From Laure and Hovadik (2006).

3D fluvial architecture

3D fluvial architecture or 3D fluvial reservoirs are characterized by multistorey and multilateral organization of architectural elements which compose channel-belt- or channel complex deposits, including e.g. point bars and overbank deposits, and will thus have in general a higher connectedness than 2D reservoirs. These reservoirs are generated from more sinuous, non-parallel and migrating channels, commonly containing bars. In practise; a 3D fluvial architecture based on the architectural style in 2D outcrop view gives high possibilities of predicting connectedness in the unknown third direction rather than continuation of the 2D outcrop, which would be the case of a 2D architectural style.

The predicted percolation threshold for 3D reservoirs or channel complex deposits is at sand:gross ratio of 25 %. The 3D “S-curve” (Fig. 9.1 B) is positioned further to the left in the diagram in comparison with the 2D diagram. A 3D reservoir is considered to have highly connected elements at sand:gross ratio of 30 % and a zone of great variation in connectedness between sand:gross values of 10-30 % (Laure and Hovadik, 2006).

9.1.2 Variations in Connectedness

There are several factors which differentiate the two fluvial architectural styles which are responsible for enhancing and degrading, respectively, connectedness of fluvial reservoirs.

There are mainly three factors which are responsible for enhanced connectedness at lower sand:gross ratios i) conduits between the main channel elements, e.g. crevasse splays and levees; ii) genetic cluster of elements, i.e. channel complexes from laterally stacked elements of e.g. abandoned channel fill, point bars, and levees; and iii) low aggradation rates which are associated with preservation of higher sand:gross ratios and lateral channel amalgamation causing deposits of great width/thickness ratio, i.e. more laterally extensive deposits (Laure and Hovadik, 2006). The factors i) and ii) are typical for 3D fluvial architecture, while the latter, iii), is a relevant factor for both architectural styles.

Factors which can reduce the connectedness of the reservoirs are, i) straight parallel channel

geometry which tends to follow the 2D pattern and not intersect in map-view or third dimension, thus generating lateral compartments; ii) continuous mudstone between thin, laterally extensive reservoir units, generating a 2D, stratified reservoir with vertical compartments; and iii) local heterogeneous impermeable units, e.g. mudstone drape coats in otherwise amalgamated channel units, continuous mudstone beds in channel fill, or inclined heterolithic units (Laure and Hovadik, 2006). The two first, i) and ii), characterize 2D reservoirs, while the latter, iii), can occur in both 2D and 3D reservoirs.

9.1.3 Architecture and Connectedness of the Upper Lourinhã Formation

The field area can be roughly divided into 5 sections (S0-S4) (Fig. 12.1) which can be studied more closely as they differ in sand:gross ratio, facies, dominating facies associations, tidal influence and architectural style (appendix A and B).

Section 0

Section 0 lies in the northernmost part of our study area, Pai Mogo, at which limited data are achieved because this section is represented by only one log. The section is bounded below by a paleosol horizon and its upper boundary to Section 1 is set to the first occurring marine flooding surface (16,5 m). The log represents vertical stacking of 3 channel fill elements (FA 1) which also appear laterally aggrading within several hundred meters in both directions. The log shows initially ~65% sand with some tidal influence. The tidal influence is clearer in very fine- to fine-grained sand then in medium-grained sand. This may signify a weak tidal current which is not capable of reducing the dominant current sufficiently for mud to be deposited when it transports coarser sand.

Due to the lack of data in both directions it is difficult to determine the fluvial and architectural style more closely, though the channel infills are vertically stacked and appear multilateral, thus predicted to be a 3D reservoir with high connectedness.

Due to the mainly fluvial character of the multi-stacked channel sandstone bodies and the tidal affect this section is thought to represent deposits close to the alluvial plain where the tidal influence in the stream channel has been weak. The reduced strength of the tidal current may indicate a relative large distance to the coastline.

Section 1

The lower boundary of Section 1 is put at the first marine flooding surface recorded in the study area, and the section is bounded at top by a paleosol which underlies a large point bar element. Above this point the sand:gross ratio and architectural style change. Within Section 1 two marine flooding surfaces have been recorded.

Section 1 has architectural elements of thin crevasse splays and minor crevasse channels, with the exception of one partially exposed, thicker wedge shaped sandstone element (Log FW_1b, 43-51 m) thought to be compound crevasse splays or levee, which extend north to a larger crevasse channel or small stream channel. Some of the crevasse splays are laterally extensive within few hundred meters, but are in general isolated in background mudstone with little vertical communication visible in 2D. Section 1 is mainly composed of mud with a sand:gross ratio of ~32 %.

Tidal influence is present, but still quite subordinate. The lack of extensive tidal structures in this section can be due to i) the elements present in this section are not likely to record clear tidal signatures as it is floodplain (FA 2) or overbank (FA 3) associated elements rather than channel deposits (FA 1); ii) the tidal influence has not been present or significant here. However, some crevasse channels have recorded tidal structures showing that the deposits are within the range of the tidal currents. Moreover, tidal structures are probably present to a larger extent in the associated river channel sandstone unit.

The connectedness in this part of the stratigraphy is extremely poor in cross-sectional view and may remain equally poor in the 3D extension, thus implying that a vertical compartmentalization is present. However, there are possibilities for better connectedness in the third-dimension, if the outcrop view is cut through a floodplain area parallel to subparallel to a stream channel. The sinuosity and meandering characteristics of this system may be minor as it fails to occur within the stratigraphic interval of Section 1, possibly indicating a straighter channel in a stable belt and thus suggesting lateral compartmentalization in this interval. The magnitude or the fluvial style of the stream channel is difficult to determine based on the architectural elements recorded. However, according to the sequence stratigraphic model of Shanley and McCabe (1993) these thick

floodplain deposits with isolated sandstone units are likely to also include isolated fluvial belts, thus representing a 2D reservoir.

Section 2

Section 2 is almost exclusively composed of a large point bar and its associated channel deposit, in addition to some minor channel depositional units and their related levees and lateral accretionary elements. The section is bounded below by a paleosol horizon whereas the upper boundary is set to a shell bank bed. The tidal influence is not present within the point bar, but is significant in the associated channel element, thus indicating tidal currents travelling up along the stream channel. Some decimetres thick mudstone layers are also present in the point bar-channel transition. Heterogeneity is therefore present in this section, but barely in the point bar element itself where the sandstone is quite clean.

The architectural elements here indicate a high sinuous, meandering stream channel with both vertical and lateral amalgamation of elements and a sand:gross ratio of ~45-50 %. Thus high connectedness and a channel complex in the third-dimension with several large point bars are expected. The width for the composite sandstone body of point bar and channel deposit are calculated to around 400-500 meters or more (Ch 6.1.2). The thickness of the point bar is logged to be around 12 meters. Thick mud directly above the sandstone body may represent a vertical barrier to sandstone bodies of the overlying section. It is difficult to evaluate the vertical connectedness in the third dimension here.

Section 3

The architectural elements in Section 3 may signify a stable sandy braided stream river of probably minor sinuous fluvial style. Considering the extensive levee complex which has developed and the thickness of the levee deposits (~10 meters), the stream river is most likely without a considerable meandering belt. The sinuosity is, however, difficult to determine more closely as the three-dimensional geometry is not visible. A minor meandering system including minor point bars appears, however, to be present at top of this section.

The section has a high degree of lateral stacking of several mid-channel bars and levee complex extending over several hundred meters. Vertical stacking of e.g. bars is also present resulting in increased thickness, few tens of meters, for composed sandstone units. The

amount of sand in this section is ~65-70 % and thus the connectedness is expected to be good also in the third-dimension even though the stream channel seems somewhat less sinuous than the channel sandstone bodies in the underlying section. Channel complex deposits are indicated by the lateral stacking, vertical stacking of bars and a composite and extensive levee complex with local indications of down cutting elements within.

Section 4

Section 4 is both laterally and vertically amalgamated to Section 3 as the regional dip has diminished considerably from the initial dip in Pai Mogo. The deposits have, nevertheless, been separated into two sections as they appear to represent somewhat different facies associations and architectural style.

Section 4 represents the uppermost stratigraphic level within the study area. It is characterized by a prominent increase in tidal influence from the underlying section with dominant IHS facies association (FA 4). This section has also an increased aggradational character upwards in the stratigraphy where single elements and their geometry can be difficult to separate as they are frequently cut. This results in high lateral and vertical amalgamation in the upper part, which appears to extend beyond the outcrop in both cases. Sandstone bodies in the lower part of this section are less connected vertically, but have some lateral amalgamations of elements, e.g. channel infill and levee units. Sand:gross ratio is estimated to be ~40 % in this section.

The deposits here may resemble tidal channel and intertidal flat deposits based on e.g. the heterogeneity and structures like sandstone-mudstone laminae which are common on intertidal flats. This would place the depositional environment within the intertidal flats of the lower delta plain or adjacent to an estuary, being intersected by marine sourced tidal channels. However, no clear intertidal mud or intertidal flat indicators have been recognized, e.g. evaporites, dessication cracks and shell fragments. Thus these deposits most likely represent a fluvial distributary channel system, which are closer to the coastline than previously; hence the deposits likely have experienced stronger tidal influence.

The sandstone bodies in Section 4 are well connected and can be considered as a 3D reservoir with channel complex reservoir sandstone bodies. The section has, however, reduced reservoir quality due to the amount of mud present.

9.2 Alluvial Architecture and Base-level Fluctuation

It is difficult to make a sequence stratigraphic analysis or apply sequence stratigraphic concepts to such a short stratigraphic column within a small study area. The regional dip of the strata also makes the correlation somewhat difficult and limits the outcrop extent of the architectural elements. Moreover, the facies do not change greatly as virtually all sandstone bodies contain tidal signature, though to some different extent.

Nevertheless, there have been recorded 4 marine flooding surfaces and changes in the architectural style within the stratigraphic column. The changes in alluvial architecture may be interpreted to represent changes in the base-level rise or fall and the rate of these changes, which is an important control on accommodation space created (Shanley and McCabe, 1993). Candidates for sequence boundaries in an alluvial setting can be unconformable surfaces that have experienced erosion, incision and long term subaerial exposure, as for example regional paleosols. Additionally, a basinward shift in facies, often represented by an abrupt contrast in the facies and architectural style, should be expected at a sequence boundary (Shanley and McCabe, 1993). The modest changes in facies across the stratigraphic column may suggest only small changes in base-level, with the largest changes in base-level represented by the flooding surfaces. Any of these flooding surfaces are candidates for a maximum flooding surface.

Sequence boundaries start to form at the initial stage of base-level fall and may continue to be formed during early slow base-level rise (Fig. 9.2 A). Simultaneously, erosion and sediment bypass may occur together with the formation of a prograding shoreface deposit (Zaitlin *et al.* 1994; Posamentier and Allen, 1999). Candidates for sequence boundaries in the study area are the lowermost paleosol (0 meters), the paleosol between the sections 1 and 2 and the paleosol between sections 2 and 3. All of these paleosols are difficult to trace and may not be regional, but are candidates since the alluvial architecture and sometimes the facies change across these surfaces. Thus several sequences appear to be present with several candidates for sequence boundaries and maximum flooding surfaces.

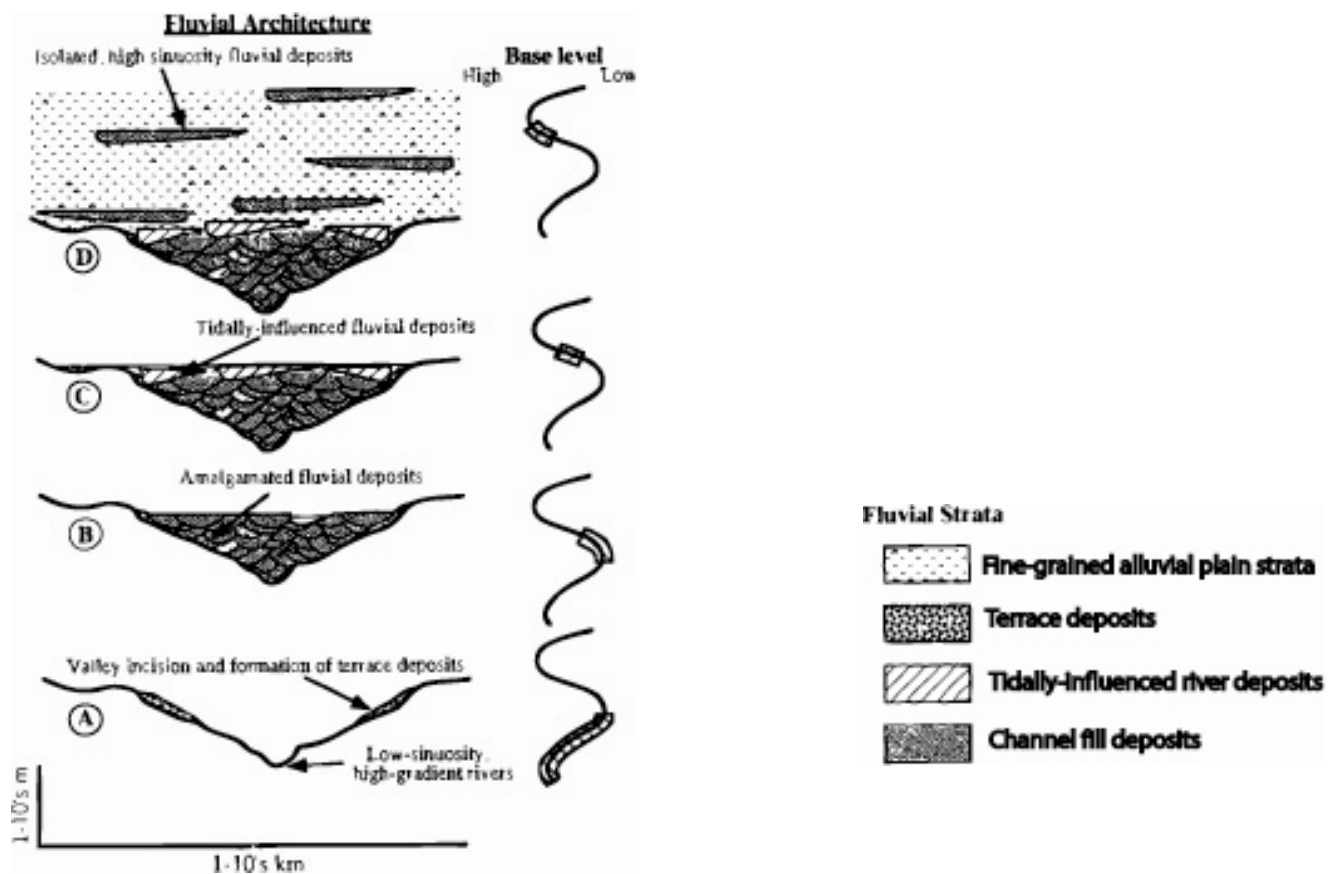


Fig.9.2: Illustration of relationship between fluvial architecture and base-level changes. A) Base-level fall to stillstand give rise to fluvial incision, sequence boundary development and deposition of a prograding lowstand wedge. B) Reduced rate of base-level fall to initial base-level rise result in aggradation and amalgamated fluvial deposits. C) Increased rates of base-level rise lead to retrograding shoreface parasequences, decreasing sand-mud ratio. This is the equivalent to the transgressive system tracts which is overlain by a maximum flooding surface that is temporally equivalent to tidally-influenced fluvial deposits. From Shanley and McCabe (1993).

Sandstone proportions in a fluvial depositional environment largely rely on the accommodation space for sediments and the supply of sediments. Base-level fluctuation is an important factor which controls the accommodation space, though other factors, like tectonics, are also essential controls in many places. In general, low sandstone proportion is associated with high accommodation space and little incision during rising and high base-level. High sandstone proportion is associated with incision and low accommodation space during low base-level or high tectonic subsidence (Bridge *et al.* 2000; Posamentier and Allen, 1999; Miall, 1996). Estuarine development may occur during sea-level rise after this stage.

As the base-level raises the fluvial deposits aggrade together with the aggrading/retrograding phase of the shoreface. At this point the channels switch rapidly, consuming floodplain fines by lateral erosion, resulting in amalgamation of channel sandstone bodies (Fig 9.2 B), as suggested in the model of (Shanley and McCabe, 1993), and high sand:gross ratio (Laure and Hovadik, 2006). The high degree of lateral stacking of elements as well as vertical stacking of bars and thick and extensive levee complex indicate an aggradational setting of stable or slowly rising relative sea-level (Komatsubara, 2004).

There is a general upward increase in sandstone body proportion and thickness in the stratigraphic column. Section 0 may be the equivalent stage of the marine lowstand systems tracts bounded below by a candidate sequence boundary, representing initial base-level rise with fluvial deposits. Section 1 has a majority of isolated sandstone units and high proportion of floodplain fines which can represent a rapid rise in base-level and increase in A/S, or the alluvial equivalent to highstand system tract corresponding to an aggrading shoreface (Shanley and McCabe, 1993). Section 2 show signs of low or initial base-level rise with a stable channel generating large point bar deposits and local paleosol development. Section 3 shows an aggradational setting with bars and levee complex which may indicate a stable or slowly rising base-level. Section 4 may record a decreasing rate in base-level rise where the lower part contains some isolated sandstone units, but also a small levee complex, with higher degree of amalgamation towards the top.

10 HETEROGENEITY

To determine the reservoir heterogeneity is significant in relevance to the oil recovery expected from the reservoir as the heterogeneity has a major impact on the reservoir properties of porosity and permeability. Heterogeneity occurs at several levels of scale and as different types of heterogeneity which commonly has a directional variation (Weber, 1986). In an unfaulted succession, as the one observed in the Lourinhã Formation, heterogeneity types can be observed at: 1) boundaries between genetic units, where boundaries between channel fill and adjacent elements of e.g. floodplain or crevasse splays will have a higher directional heterogeneity e.g. perpendicular to the channel axis than along the axis on this scale; 2 & 3) permeability zones and barriers (baffles) within a genetic unit, like a multistorey channel fill and IHS, which will most likely have a higher heterogeneity along the vertical axis or obliquely within the element; 4) laminations and cross-stratification, like mud drapes in cross-stratified sand and mudstone-sandstone laminae, which will have a higher heterogeneity along the vertical axis or obliquely on the facies scale; 5) and microscopic heterogeneity on the textural level of the grains and mineral composition.

The types of heterogeneity mentioned above are only 5 of a total of 7 which are included in Weber's (1986) classification scheme of reservoir heterogeneity types. Faulting and fracturing are the two remaining types of reservoir heterogeneity and are not included as they are not largely present in the Lourinhã Formation. In general, with the exception for faulting and fracturing, the 5 types of heterogeneity can be said to be an identification of depositional environments as the porosity and permeability properties are a function of the depositional environment and sedimentary facies which has later been modified by its diagenetic history (Nystuen and Fält, 1995; Weber, 1986).

There are several different ways of organizing the different levels of heterogeneity in a sedimentary succession. Aigner *et al.* (1998) suggested a heterogenic hierarchy which includes 5 levels reaching from microscale (first-order) up to both autogenic (megascala, fourth-order) and allogenic (gigascale, fifth-order) base-level changes. Jiao (2005) proposed a less detailed division of the heterogenic hierarchy where megascala is the upper

heterogenic level and here represents the depositional environment of architectural elements, which is included in the macroscale level in the hierarchical system of Aigner *et al.* (1998).

Miall (1996) introduced a fourth-order hierarchical system, quite similar to the system of Aigner *et al.* (1998), which will be applied here:

- 1) Megascale heterogeneity, which is caused by the architectural style and base-level fluctuations and includes the variations across sedimentary units within the entire basin.
- 2) Macroscale heterogeneity, which is caused by the various architectural elements and variability associated with the deposition of these;
- 3) Mesoscale heterogeneity, which is caused by depositional processes, bedding units sedimentary structures;
- 4) Microscale heterogeneity, which is caused by particle properties like grain size, texture and diagenetic processes, and are responsible for the petrophysical properties (porosity and permeability) of the rocks

(Fig. 10.1).

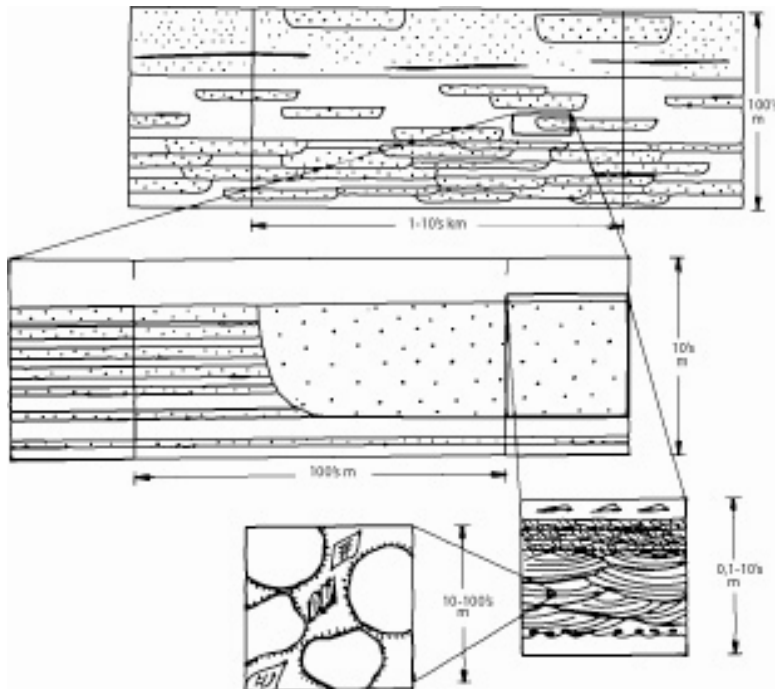


Fig. 10.1: Levels of heterogeneity; from Megascale to microscale. Modified form Weber (1986).

10.1 Megascale Heterogeneity

This level of heterogeneity is affected by the stacking pattern of the architectural elements and is thus closely related to properties described and discussed in the previous chapter (Ch. 9) and to sand:gross ratio. The general trend is an increasing sand:gross ratio and a decrease in compartmentalisation upwards in the stratigraphy. The lower part of the studied succession (up to Section 2) is characterized by floodplain fines with isolated minor sandstone bodies and large heterogeneity on this scale. Larger elements, better connectedness and amalgamation characterize the upper stratigraphic level. Thus the megascale heterogeneity decreases upwards in the stratigraphy. Mesoscale heterogeneity includes heterogeneity between generic elements and will have a higher directional heterogeneity e.g. perpendicular to the channel axis than along on this level.

10.2 Macroscale Heterogeneity

The heterogeneity on the macroscale level includes heterogeneity formed by the various lithology and geometry of architectural elements present. These elements represent depositional systems with differences in generic facies which may give rise to heterogeneity within the elements.

Most architectural elements are rather homogenous than heterolithic. The main element experiencing heterogeneity at this level is levee deposits (FA 3.1) where thin beds of mudstone, siltstone and sandstone alternate frequently. The large point bar element (FA 1.2) only shows thin mudstone beds or laminae on reactivation surfaces and at the transition zone to the associated channel (FA 1.1). However, the small point bar elements tend to display larger heterogeneities with e.g. centimetre to decimetre thick Inclined Heterolithic Strata (FA 4.2). Additionally, multistorey crevasse splays can have thin mudstone layers present between the separate lobes.

Elements with centimetres to decimetres thick Inclined Heterolithic Stratification (FA 4.1) are mainly present within Section 4 but also locally in Section 3. The IHS units have major impact on the reservoir heterogeneity with alternations of decimetre thick sandstone and mudstone beds, where the sandstone beds are commonly thicker than associated mudstone

beds. The IHS units are rather large scale heterogeneity compartments formed commonly in channels or point bars. The mudstone beds are locally, but not frequently, laterally persistent, thus some communication between sandstone beds occurs. Units consisting of IHS have multiple barriers and will reduce the ability for fluid to flow significantly. Although they in general will be poor conduits, variations occur with the thickness and lateral extent of the mudstone present.

10.3 Mesoscale Heterogeneity

This level of heterogeneity is at the level of facies, bedding units and sedimentary structures. Mesoscale heterogeneity is mainly caused by single and double mud drapes (facies A and C) in foresets and sandstone-mudstone laminae (facies D).

The mud drapes in cross-stratified units will normally not function as fluid flow barriers within these beds as they seldom are continuous across the whole vertical thickness. The toesets of these mud drapes may, however, be better preserved and can locally, though not frequently, function as vertical barriers or low permeable areas. Generally, this is not thought to have a major restriction on the fluid flow, though only where mudstone drapes seldom are present within the full thickness of these units.

Sandstone-mudstone laminae are fairly frequent, either as the main- or subordinate constituent in sandstone beds mainly present in Section 4 (FA 4.1), though also in other sections. The amount and lateral persistence of mud laminae can vary greatly. Beds, in which the amount and lateral extent of the mudstone laminae are large, are not thicker than 0,5 meters. Beds with minor mud content, or beds where sandstone-mudstone laminae are a subordinate component, are more common. The laminae may not affect the flow properties significantly where they are present in moderate and low amounts of the total volume of the sandstone bodies, but will most likely function as domains of very restricted flow. This type of heterogeneity may create fluid flow barriers where mudstone-sandstone laminae dominate the lithology.

Other heterogeneities on this scale include soft sediment deformed beds (facies M), but these are of minor significance as they seldom occur, and then at a minor scale.

10.4 Microscale Heterogeneity

On microscale, the heterogeneity is within the domain of grain size, texture and diagenetic processes which affect the petrophysical characteristics, like porosity and permeability, of the rock. Thin sections have been made from several architectural elements from different stratigraphic levels in the study area (see chapter 8).

The main components of the sandstone bodies in our study area are quartz, feldspar (alkali feldspar, plagioclase and leached feldspar), mica and calcite in addition to organic matter and mudstone particles. The mineral composition does not vary depending on facies or architectural element, only the amount of each component, in addition to porosity and permeability, vary. The amount of mudstone and cement is particularly important concerning the preservation of primary porosity and permeability.

The presence of calcite cement and mudstone appears to be decreasing upwards in the stratigraphy, thus giving better values for porosity and permeability, but this is probably an effect of the actual architecture elements commonly present at different levels. Overbank (FA 3) and floodplain sandstones (FA 2) are more heterogeneous on the microscale level than channel fill (FA 1), due to generally larger amount of mudstone and calcite cement. Nevertheless, the supposed channel element present at ~50 meters has a greater amount of calcite cement than what would be expected for such an element.

11 DEPOSITIONAL ENVIRONMENT

11.1 Processes

The deposits of the Lourinhã Formation are affected by fluvial-, tidal- and marine processes. It has a main fluvial characteristic which includes architectural elements of e.g. channel fill, bars, levee, floodplain and crevasse channels and splay deposits (see Ch. 7).

The fluvial deposits have an overall significant tidal influence, mainly recorded as tidal bundles and tidal bundle sequences, possibly also bipolar indicators like ripples climbing up foresets of cross-stratified sand. The intensity and significance of tidal signatures vary within the formation, depending on type of architectural element and stratigraphic level in which the tidal indicators occur. There is a general trend of higher frequency and more clear tidal signatures upwards in the stratigraphy. The uppermost stratigraphic level is apparently more tidally influenced with tidal deposits predominating in the Inclined Heterolithic Stratified (IHS) deposits of rhythmic mudstone-sandstone laminae and centimetre to decimetre thick alternating layers of sandstone and mudstone.

The tidal influence indicates a proximity to the coastline, i.e. within the paralic or marginal-marine depositional environment, and in a deltaic, estuarine or siliciclastic coastal sub-environment.

Tides can be divided into micro, meso and macro with 0-2 meters, 2-4 meters and >4 meters vertical range respectively (Boggs, 2001). The lateral extent, or the landward limit of tidal influence, depends on the landward slope, in addition to the tidal range. The tidal limit can reach tens to hundreds of kilometres inland if the slope is small enough. Equally, the coastline may move several tens to hundreds of kilometres landwards in response to an even minor relative sea-level rise if the slope gradient is low. The fluvial channels are likely to record tidal influence at greater landward distances than interfluvial areas due to downcutting.

Purely fluvial channel deposits with no or little tidal influence may signify deposition above or close to the bayline, i.e. the alluvial plain or the transitional area between the coastal plain and alluvial plain (Posamentier *et al.* 1988), while tidally influenced fluvial deposits indicate deposition seaward from this, on the coastal plain. These tidally influenced fluvial channel deposits can be e.g. on the delta plain or within the “straight-meandering-straight” fluvial dominating portion of a tidal estuary. Tidal deposits of tidal channels and intertidal flats are within the interdistributary areas of the lower delta- or coastal plain, or on the coastal plain adjacent to a tidal estuary, i.e. within the steeper sloped intertidal areas adjacent to distributary channels or estuaries.

The thin open marine intervals recorded within the formation and interpreted as marine flooding surfaces (Ch. 7) are less than one meter thick and do not appear to have a long term effect on the depositional environment and are thus thought to represent ephemeral events only.

In case of marine flooding the shoreline has crossed the depositional site represented by the study area and has retreated landward to the north relative to its previous position. A general estimation of the relative proximity of the shoreline can be made for each stratigraphic point in the measured sections, but will be quite unreliable and impossible to quantify without any additional data, e.g. true tidal range and landward slope.

The cause of a relative rise in sea-level can be debated, based on allogenic- and autogenic processes, where allogenic processes represent all events causing eustatic changes in sea-level, e.g. plate tectonics, climate, glaciations, whereas autogenic processes represent local variations in the basin, e.g. avulsion and lobe switching and minor subsidence due to compaction or salt movement.

11.2 Palaeocurrent Directions

Based on the palaeocurrent measurements obtained from channel infill deposits it is possible to give a rough estimate of the fluvial style. Since meandering rivers approximate a sine wave in the horizontal plane, it only tangents its true downstream direction by a few points, resulting in few palaeocurrent measurements which will represent this main direction of

fluvial flow. Meandering rivers will therefore have palaeocurrent measurements with a high standard deviations to the true downstream direction. On the contrary, braided rivers will have minor deviations and palaeocurrent measurements closer to the true palaeocurrent direction (Bluck, 1971).

The palaeocurrent measurements are primarily done on cross-stratification of individual dune structures and only a few on depositional surfaces of large bed forms. The palaeocurrent measurements therefore represent local migration direction of individual dunes and not the regional trend of the system itself. The orientation of cross-stratified units with double mud drapes indicates that the ebb currents have been dominating, with dune migration roughly towards south in the direction of open marine environment and with flood tidal currents directed towards the north.

78 palaeocurrent measurements have been recorded from the study area. This is not a vast amount of data and will not be statistically valid for regional palaeocurrent interpretation. However, the mean value for the 78 palaeocurrent measurements and from several individual architectural elements point towards the south-eastern direction (Fig. 11.1).

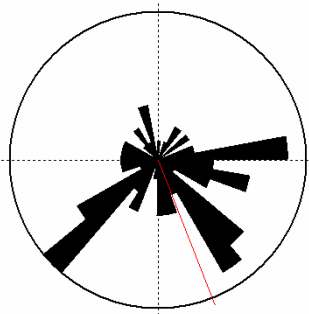


Fig. 11.1: A rose diagram showing the palaeocurrent directions measured in the studied succession of the Lourinãha Formation. The main directions lie within the eastern to south-western direction with the mean (red line) towards the south-east. The diagram also suggests a subordinate current direction towards the west to northeast. $n=78$.

The rose diagrams representing Section 4 and 3 appear to indicate bidirectional palaeocurrents. The rose diagram of Section 3 has a higher number of measurements, and the mean value, in a roughly south-eastern dominant direction. Section 4 appears to have more equal bipolarity in its diagram with a possible dominant direction towards the west. This may

signify a stronger tidal current compared to the power of the fluvial current. However, this may also be an effect of measurements within different architectural elements, e.g. levee and lateral accretionary elements, which combine various depositional systems with different local palaeocurrent trends. Considering only the measurements recorded in the lateral accretionary element in Section 4 the majority of the measurements point in an eastern direction. Further, the wide spread in the rose diagram may indicate a meandering system as mentioned above (Fig. 11.2 A and B).

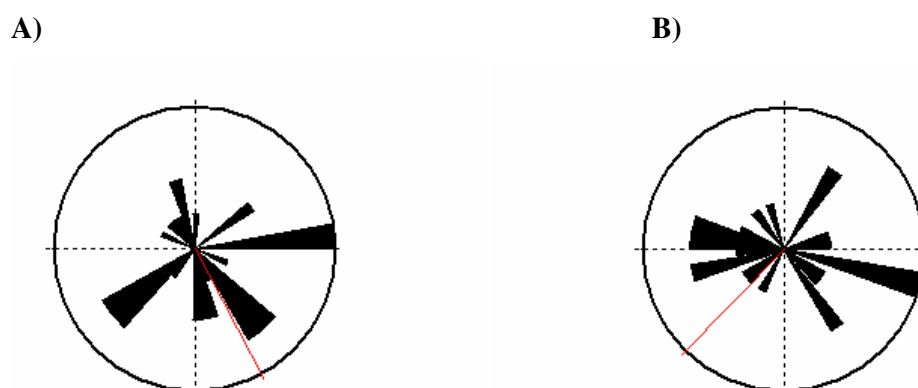


Fig. 11.2: A) Rose diagram of the palaeocurrent measurements from Section 3. $n = 32$.

B) Rose diagram of the palaeocurrent measurements from Section 4. $n = 25$.

The red line indicates the mean direction.

Nevertheless, the measurements are too few to give any clear and certain statistical value to draw definite conclusions from. The regional palaeocurrent direction is identified to be towards the southeast (Hill, 1989; Leinfelder and Wilson, 1989).

11.3 Autogenic and Allogenic Processes

Autogenic and allogenic processes refer to processes within the sedimentary system and external sedimentary processes respectively (Kim, 2006). Some of the most recognized autogenic processes are channel avulsion and lobe switching in addition to local tectonics like salt movement. Allogenic processes are associated with climate, glaciations, sediment supply, subsidence and regional tectonics like plate movement, rifting events and mountain chain formation etc. Both autogenic and allogenic processes may be responsible for

fluctuations in the coastline, though allogenic processes may be responsible for eustatic changes in sea-level. Autogenic processes will in general form local variations in magnitude and direction of shoreline migration due to e.g. relocation of depocenters (Kim, 2006).

As mentioned earlier, shoreline fluctuations are recorded in our study area by e.g. marine flooding surfaces and paleosols. The facies between the flooding surfaces and paleosols do not experience a great variation as the tidal signature is present throughout. Further, the beds recording the marine flooding surfaces are rather thin and likely representing a short time interval. Tectonic activity is thought to have ceased and be virtually nonexistent at this time (Late Kimmeridgian – Tithonian) (Leinfelder and Wilson, 1989). It is therefore reason to argue for the marine flooding surfaces to be only minor with limited coastline migration, resulting from autogenic processes rather than allogenic processes which cause larger eustatic changes in shoreline migration.

11.4 Estuarine versus Deltaic Deposits

It can sometimes be difficult to distinguish between deltaic- and estuarine deposits both theoretically and even more so in the field. There are various definitions and statements of estuaries and tide-dominated deltas to consider. Additionally, the recognition of ancient deposits in contrast to present day active examples of these systems may be problematic.

11.4.1 Previous Studies on Tidally Influenced Deposits

The most widely acknowledged definition of an estuary within sedimentary geology is from Dalrymple *et al.* (1992) which stated that an estuary is “the seaward portion of a drowned valley system which receives sediments from both fluvial and marine sources and which contains facies influenced by tide, wave and fluvial processes. The estuary is considered to extend from the landward limit of tidal facies at its head to the seaward limit of coastal facies at its mouth”. Nichols and Biggs (1985) stated that “estuaries form best where river valleys or coastal embayments become drowned or revived, by recent marine submergence”, though they did not use this characterization as a definition of an estuary. Some definitions of estuaries are based on the characteristic tidal influence, e.g. Meckel (1975) which claimed

that an estuary “is that lower segment of a river’s course which is appreciably affected by the tides”, and thus he included an estuary within the modern tide-dominated Colorado Delta. Additionally, there are other scientific directions which have used definitions based on e.g. salinity (e.g. biographers) (Elliott, 2002; Dyer, 1996), which not will be considered here.

Galloway (1975) classified deltas to be fluvial-, wave- and tide-dominated, though he also stated “that tide-dominated deltas tends to be estuarine to irregular in geometry” and that their framework facies were “estuarine fill and tidal sand ridges”. Walker (1992) disagreed with Galloway’s (1975) classification of tide-dominated deltas as he expressed that the tide-dominated deltas described in literature have little in common with other deltas concerning their morphological characteristics and would consider many of them as tidal estuaries instead. Walker (1992) actually went to the extreme and tore off the “tide-dominated” corner of Galloway’s (1975) triangular delta classification scheme, indicating that they are nonexistent. Many tide-dominated deltaic systems may not be recognized since their deltaic facies do not resemble those of other deltas (Coleman and Wright, 1975). Galloway (1975) also commented that interpretations of tide-dominated deltas in ancient deposits are virtually nonexistent in the literature (up to that time), and that the evolutionary trend and infill of these systems thus need to be better documented. Several studies have been focusing on tidal estuaries and tide-dominated deltas the last decades (see below 11.4.2).

The triangular deltaic classification scheme seems to hold for present day active systems, but its application has been questioned for ancient deposits of tide-dominated deltas. The restricted amount of literature on tide-dominated deltaic systems can be due to i) little occurrence and recording of these systems in the past, or ii) very low preservation potential of tidally influenced deposits during stable or falling relative sea-level, in contrary to a transgressive setting where tidally influenced facies are readily formed and preserved (Galloway, 1975). Many previously termed tide-dominated deltaic deposits have been questioned by others at a later stage to better be classified as estuarine (e.g. The Ord River Delta, Coleman and Wright (1975)) (Dalrymple, 1992; Bhattachayra and Walker, 1992).

The Fly River Delta has been described by Dalrymple (2003) as a tide-dominated delta which is also concluded by Harris (1994). Though additionally, Harris (1994) found evidence of transgressive estuarine facies in cores and described the Fly River as “tide-dominated “funnel-shaped” estuary together with an offshore prograding delta...”. Further he explained

this as an initial estuary, with clear incision shown on seismic, where an apparent pause in relative sea-level rise has resulted in progradation and delta development. Development from a transgressive estuary to prograding delta is not a uncommon feature after the initial incised valley has been filled (Dalrymple *et al.*1992).

Even though estuaries are transgressive- and deltas regressive systems the ideal sequences of upward fining or coarsening successions, respectively, may also be modified by local transgressive or regressive phases of deposition with respect to e.g. discharge position of distributaries within a delta where transgressive phases may prevail in the interdistributary bays, or channel erosion of underlying units which may remove part of the record (Meckel, 1975).

11.4.2 Recent Studies on Tidally Influenced Deposits

Several recent studies have been done on tide-dominated deltas and estuaries the last decade. Estuaries appear to be better documented in recent literature, or in the literature in general, than tide-dominated deltas. Some authors (Willis and Gabel, 2003; Willis and Gabel, 2001; Seidler and Steel, 2001; Willis, 1997) suggested this may reflect an interpretation bias based on the commonly assumed formation of tidally influenced facies during transgression, where embayments are created whose geometry amplify the tidal currents, and not during regression (Galloway, 1975). Although there is still a great deal of disagreements between authors about the criteria used, and to which extent they are correct in their interpretation of ancient tidally influenced deposits (Willis and Gabel, 2003; Higgs, 2002; Shanmugam and Poffenberger, 2002; Shanmugam *et al.* 2000,), there are several indicators the majority of authors seem to agree upon.

Some of the criteria needed to interpret the former existence of an estuarine, particularly tide-dominated, depositional environment should include:

- a basal regional unconformity which represent valley-incision, sequence boundary and subaerial exposure with possible root traces, desiccation cracks and paleosol development;
- estuaries can only form during transgression, thus a landward shift of facies is expected to record this;

- a usual deepening and fining upward vertical succession to also represent the transgressive nature of an estuary;
- a more heterolithic nature upwards as an effect of more rapid sea-level rise relative to rate of sediment supply;
- commonly bipolar indications and Inclined Heterolithic Stratified deposits (also present in the tide-dominated deltas)
- elongated tidal sand ridges or sand bars (also present in tide-dominated deltas)
- submarine tidal sand sheets, upper flow regime sand flat
- possible marsh deposits
- commonly a complex stack of estuarine fluvial fill representing multiple incision and erosion surfaces due to numerous minor cycles in relative sea-level

(Shanmugam *et al.* 2000; Zaitlin *et al.* 1994; Dalrymple *et al.* 1992).

Willis (1997) promoted the hypothesis of two depositional models for incised-valley fill which reflects differences in A/S; i) the flood-based valley-fill deposit, with rapid flooding of the incised valley, thus generating a thin fluvial transgressive unit and a thick highstand unit deposited during declining rate of relative sea-level rise, and ii) the flood-capped valley fill deposit, with lower rate of relative sea-level rise, thus generating a thicker transgressive unit which develop upwards from sheet like channels to more laterally amalgamated and heterolithic tidally influenced channel deposits, and a thin highstand unit. These two models represent a development from high to low A/S and a development from low to high A/S, respectively.

Tide-dominated deltas can be recognized by lacking many of the criteria mentioned above for estuaries and have some of the following additional criteria:

- evidence of progradation or prograding lobes;
- elongated tidal sand ridges or bars;
- deltas are associated with regression, thus a basinward shift in facies is expected to record this regression;
- a coarsening upward succession is also expected from marine mud to fluvial deposits;
- a dominance of ebb oriented stratification and inclining beds indicating strong fluvial sourced system;

(Willis and Gabel, 2003; Seidler and Steel, 2001; Ehlers and Chan, 1999; Willis, 1997)

Seidler and Steel (2001) proposed the idea that tide-dominated deltas usually form as a part of the lowstand prograding wedge at the turnaround from the lowstand- to transgressive systems tract during early sea-level rise. Thus the tidal influence is not only linked to transgression but also to lowstand regressive, prograding system. Tide-dominated deltas may though be connected to rising relative sea-level and an increase in accommodation space which does not exceed sediment supply in such that a prograding system is maintained.

The common confusion of the two systems is understandable due to the similar characteristics of tide-dominated facies like tidal sand ridges or bars, tidal channels, intertidal flats and generally large amount of Inclined Heterolithic Stratified deposits.

Misinterpretations have also been made due to high-relief erosion surfaces which do not necessarily represent valley incision, but can also develop in a tidal delta setting, e.g. by submarine scouring by tidal currents on the delta front (Willis and Gabel, 2001; Harris, 1994) rather than fluvial incision. Evidence or lack of evidence of subaerial exposure should be used to distinguish between these two erosional surfaces.

Although deposits originating from tide-dominated deltas may have similar facies as those formed in tidal estuaries (Dalrymple, 1992), the general trend of estuaries is associated with transgression and deltas with progradation of the coastline. Several authors emphasize that deltaic terminology can only be applied where there are evidence of such progradation (e.g. Bhattachayra and Walker (1992) and Cooper (1994)).

11.4.3 Discussion of the Depositional Environment of the Louriñha Formation

Due to the tidal influence recorded in the study area the depositional environment is expected to be associated with a tide-dominated delta or a tide-dominated estuary, which is the basis for the previous focus on these two systems. It appears, however, impossible to determine more specifically which of these two depositional environments these ancient deposits belong to based on the study area alone. The literature about tide-dominated deltas and estuaries are mainly from studies done in the more basinward regions of the systems, thus not within the fluvial dominated part of the present study area. The exception is a study by Ehlers and Chan (1999). They have interpreted ancient tidally influenced deposits to

represent the intertidal and supratidal region of a tide-dominated estuary. Their interpretation is, however, quite model dependant and does not include many of the common criteria suggested for tide-dominated estuaries (see 11.4.2). Additionally, they have interpreted the succession to evolve from intertidal to supratidal conditions, which is not consistent with transgression but rather regression. Their interpretation greatly relies on modern analogues and lack of prograding lobes and a prodelta. Due to the scepticism to their work, reluctance is preformed in applying this as an analogue.

The landward position of the actual study area makes it difficult to detect any upward fining/deepening or upward coarsening/shallowing trend, since prodelta- or transgressive mudstone is absent. Further, the study area does not show any great indication of basinward or landward shift in facies which can indicate transgression or progradation, but only a slight increase in tidal influence. However, caution has to be applied to interpret this in a matter of transgression as changes in tidal current strength are common due to minor changes in basin morphology as a result from variations in sediment supply and accommodation space (Willis and Gabel, 2001). As the morphology and particularly the width of the basin affect the tidal current strength, changes in tidal influence do not have to be related to sequence stratigraphic events (Willis and Gabel, 2003).

The study area extends ~2,5 km without any control on the third dimension. Thus any conclusion on depositional environment based on this study area alone is highly questionable. The area indicates deposition within the tidally influenced fluvial system, above the intertidal flat, which is present within both the tide-dominated estuary and delta. The criteria listed above are therefore not optimally applicable to this region, but more for basinward areas. Several paleosols (facies L/FA 2.2) are present within the succession, but the regional extent, and thus a valley-incision interpretation, is uncertain. The thin marine beds representing flooding surfaces (facies N/FA 5.1) are thought to represent event of short duration and probably indicate only minor relative sea-level rise. Thus, in a transgressive setting like an estuary it would be expected to see a more major and clearer transgressive trend, even for small relative sea-level rise. A plausible explanation for the observed marine flooding surfaces may be avulsion and lobe switching in a deltaic setting (see 11.3).

Nevertheless, information from other studies or a more extensive study within a larger area has to be applied before a valid conclusion on the depositional environment can be made.

Leinfelder and Wilson (1989) have interpreted the Louriña Formation to be part of a southward prograding slope based on seismic from this area. The evidence of progradation is a valid argument for a deltaic setting.

11.4.4 Summary of Discussion on the Depositional Environment

As the tide-dominated deltaic and estuarine ancient deposits have similar facies these have often been misinterpreted for each other. Overall, the interpretation of estuarine deposits have been favoured and easier accepted in the literature than tide-dominated deltaic ancient deposits, though this has been commented upon in recent years. The study area in which this paper is based upon lies within the tidally influenced fluvial dominating system which is present in both systems in question. The vertical succession does not show any particular indication of a landward or basinward shift in facies, but only an upward increase in tidal influence and heterolithic facies. Authors have commented upon the danger of interpreting this in a sequence stratigraphic matter without considering variations in the strength of the tidal current which commonly occur with changes in basin morphology. The regional extent of the several paleosols present in the succession has not been investigated, thus an interpretation of an incised valley is highly uncertain. The succession does not show any clear transgressive trends though have numerous minor marine flooding surfaces. These marine flooding surfaces probably only represent intermittent events in rise in relative sea-level, in contrary to a more continuous transgressive trend. Additionally, the flooding events are thought to represent only small rises in relative sea-level, whereas a more lasting effect of marine flooding should be expected to be present, also when only small changes in relative sea had taken place, if a transgression had occurred during the time represented by the actual studied section. The thin marine flooding surfaces are therefore possibly an effect of channel avulsion and lobe switching in a deltaic setting, causing submergence of abandoned lobes and associated distributary channels.

12 RESERVOIR MODELLING

An attempt have previously been made to understand the 3D geometry, lateral extent and sandstone body interconnectedness (Ch. 9) which to a large extent is the basis for the Petrel™ modelling. Due to the different architectural and fluvial styles present within the succession, 4 zones have been generated and modelled based on different parameters thought to represent the individual zones. Zone 1 consists of Section_0, Zone 2 consists of Section 1, Zone 3 consists of Section 2 and Zone 4 consists of Section 3 and 4 (Fig.12.1).

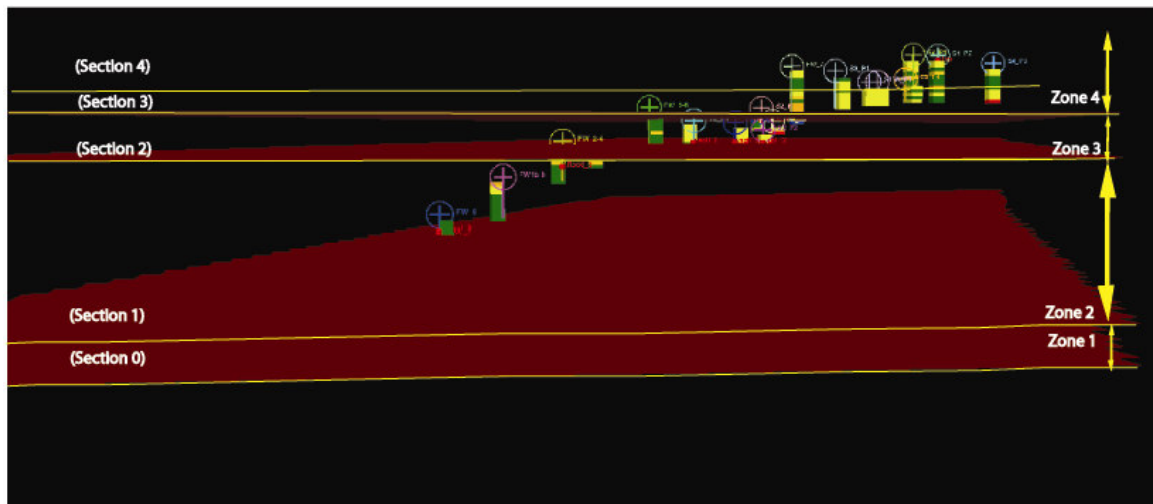


Fig. 12.1: Illustration of the upscaled logs and the partition of the study area into sections and zones. Yellow indicates sandstone while green indicate mudstone.

As the field area is along a 2D transect and the 3D control is absent, in addition to a regional tilt which limits the lateral extent at each stratigraphic level, the parameters, e.g. channel width, wavelength and amplitude, in which to apply to the individual zones are highly uncertain. Particularly parameters such as wavelength and amplitude, which are obtained in the third-dimension, are indecisive. The parameters will also be relative in many cases in respect to the other zones, e.g. concerning the sinuosity, wavelength and amplitude. Nevertheless, an attempt to improve the control and employ more accurate input in Petrel™ is vital to obtain a valid and realistic model as possible.

12.1 Parameters

Several authors have made attempts to quantify unknown parameters through empirical equations based on modern rivers and ancient deposits, which relate the unknown parameters, like palaeochannel width and channel-belt width to other, known or more easily derived parameters, like bankfull palaeochannel depth (e.g. Bridge and Tye, 2000; Bridge and Mackey, 1993; Lorenz *et al*, 1985; Leeder, 1973). Some of these equations are listed in Table 12.2 and 12.3.

The maximum bankfull channel depth is commonly an initial parameter, thus this should be estimated as accurately as possible from logs and out outcrop data as it has implications for further calculations. The maximum bankfull depth can be estimated from the thickness (decompacted) of complete channel bars (e.g. point bars, FA 1.2), channel fill sequences or the mean dune height.

Table 12.1: Lists of symbols used

D	Maximum bankfull depth
d_m	Mean bankfull depth
h_m	Mean dune height
L	Wavelength
S_n	sinuosity
SD	Standard deviation (log units)
cbw	Channel-belt width
W	Channel width

Table 12.2: Equations relating channel width, w, to maximum, d, and mean, d_m, channel depth.

Source	Equation Channel width	SD	Sn
Bridge and Mackey, 1993	(1) $w = 8.88 d_m^{1.82}$		>1.0
	(2) $w = 15.85 d_m^{1.58}$	0.44	
Leeder, 1973	(3) $w = 6.8 d^{1.54}$	0.35	> 1.7

Table 12.3: Equations relating channel-belt width, cbw, to channel width, w, maximum channel depth, d and mean bankfull channel depth.

Parameter/ Source	Channel width, w	Bankfull channel depth, d, d _m	SD	
Lorenz <i>et al</i> , 1985	(4) $cbw = 7.44 w^{1.01}$			
Bridge and Mackey, 1993	(5) $cbw = 6.89 w^{0.99}$	(6) $cbw = 192.01 d_m^{1.52}$ (7) $cbw = 45.76 d^{1.52}$	0.233 (5)	0.324 (6)

Additionally Leeder (1973) has estimated the wavelength for highly sinuous channels (Sn >1.7) with following relation to the bankfull channel width:

(8) $L = 10.9 w^{1.01}$

Standard deviations (SD) are commonly given in log units. Calculations of maximum and minimum channel width of twice the standard deviation (97 % confidence level) is at +/- 2*SD log units. The use of the log scale results in an asymmetric or skewed curve if

converted to the Gaussian curve where the addition of two standard deviations results in a greater numeric deviation than the subtraction of two standard deviations.

The empirical equations depend upon channel pattern parameters, like the sinuosity (Bridge and Tye, 2000), which commonly has been derived from modern rivers and should be applied with caution to ancient deposits. They are also derived only from fluvial channels and not channels within a paralic setting. These equations will thus only be used as a guidance to determine the parameters set for the modelling in addition to what is observed in the study area and from modern rivers through Google Earth™. Table 12.4 will list the resulting parameters which Petrel™ requires to perform the modelling in Zone 1-4.

The Petrel™ modelling is based on input data regarding the ancient channel deposits created from the fluvial system and not of stream channel geometry as no parameter which incorporates the shift of the channel across its channel-belt is included. It is therefore assumed that Petrel™ does not generate composite channel deposits with a more realistic channel-belt width if only channel parameters were to be utilized. Within a meandering system the channel-belt width will coincide with the meandering-belt width or amplitude, while in a braided system the channel-belt width will approximate the channel width (including bars) (Bridge and Mackey, 1993). Petrel™ also has no elements which characterize crevasse splays (FA 2.3) or point bar deposits (FA 1.2) to be included separately in the model with correct association to the system itself. However, crevasse splays is attempted to be modelled with another geometric unit (alluvial fan) in Zone 2.

Table 12.4: Zone 1: Representative parameters for modelling (intervals).

Parameter	Bankfull depth	Channel width	Channel-belt width	Amplitude	Wavelength	comments
Zone 1	3	50	200	1500	2180	Stacked channels. Low-medium A/S.
	4	100	650	2000	7000	
	5	300	1950	3500	20000	
Zone 2	1	40	200	250	1000	Also Crevasse. Splays. High A/S, base-level rise, 2D reservoir, sinuous?
	3	100	500	900	2000	
	4	250	800	2200	3000	
Zone 3	9	60	500	8000	6000	Sn>1.7, meandering. Low A/S
	12	320	2080	10000	25000	
	15	1500	9000	15500	50000	
Zone 4	4	100	550	2000	5000	Low sinuous to braided. Stacked channels
	6	500	900	4000	8000	
	9	2000	2500	6000	35000	

12.2 Stochastic Object Models

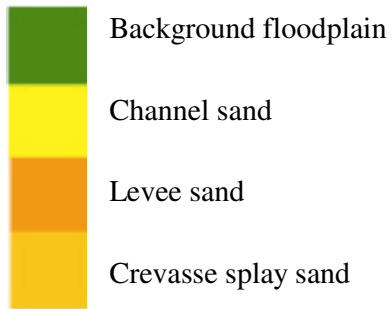


Fig 12.2: Legend for models.

Three runs with the input parameters listed in Table 12.4 generated the models shown in Fig. 12.3 - 12.5.

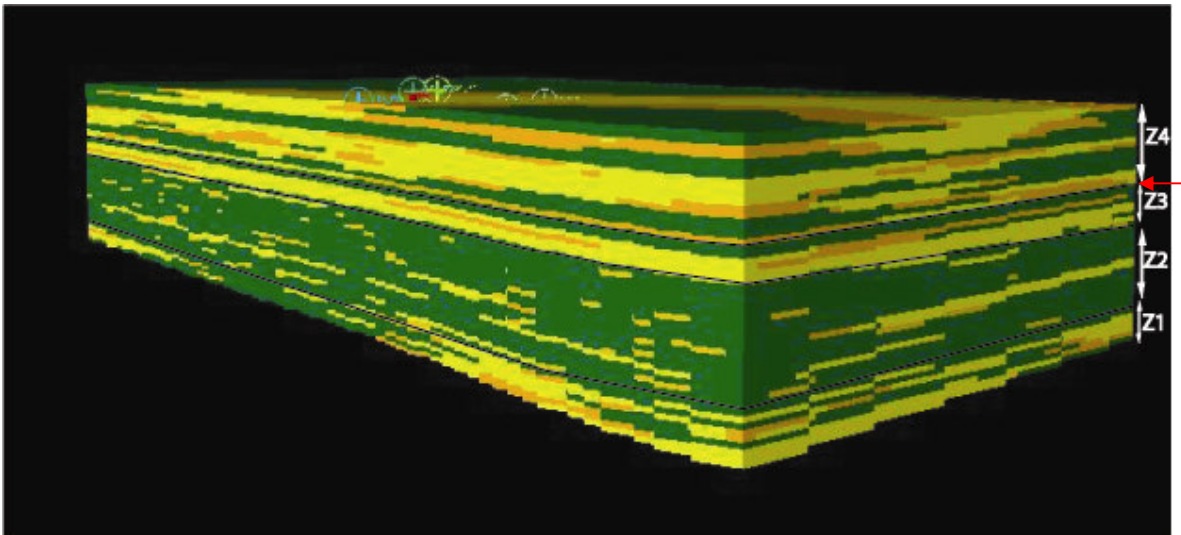


Fig. 12.3: Stochastic object model generated in Petrel™. Run 1. The red arrow indicates the level of a possible thin barrier.

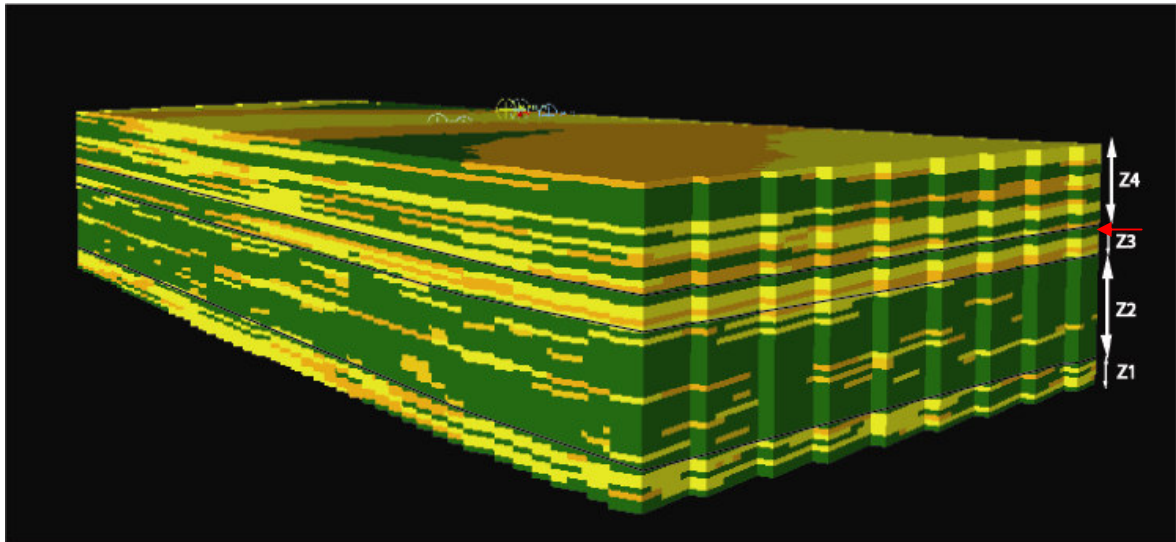


Fig. 12.4: Stochastic object model generated in Petrel™. Run 2. The red arrow indicates the level of a possible thin barrier.

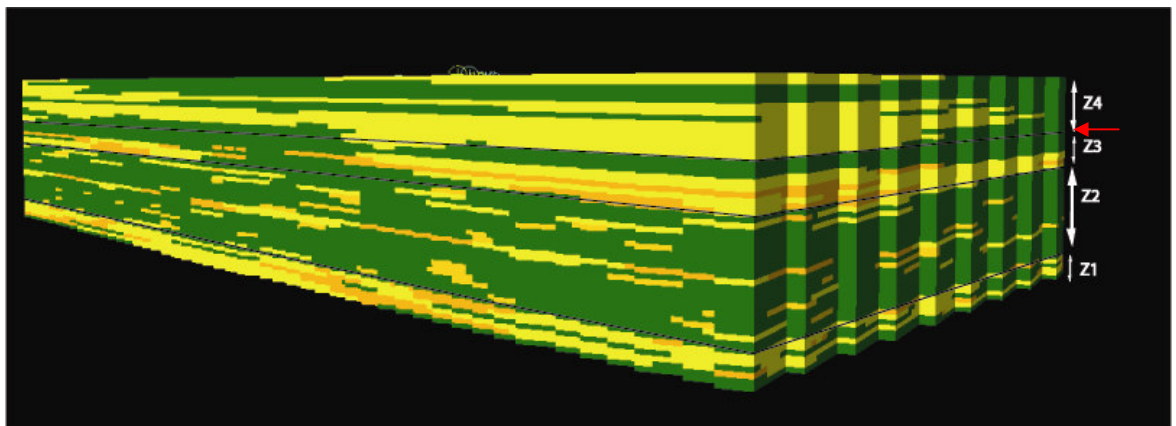


Fig. 12.5: Stochastic object model generated in Petrel™. Run 3. The red arrow indicates the level of a possible thin barrier.

These models show a high sandstone body interconnectedness in the upper part in Zone 3 and 4 and at base in Zone 1. This is expected due to the large sand:gross ratio in these sections (Ch. 9). Zone 1 is, however, very thin, but may be significant if the high interconnectedness is equally high at lower stratigraphic levels. Zone 2 is, however, dominated by background floodplain with little interconnectedness in both vertical and lateral direction. This interval may thus function as a vertical barrier between the two intervals of higher prosperity. All 3 models also have a thin floodplain interval between Zone

3 and 4 (indicated by the red arrows), which coincides with an interval containing a flooding surface. This interval of floodplain mudstone may function as a fluid flow barrier. The lower barrier zone contains 3 flooding surfaces which indicate rapid base-level rise (Ch. 9).

Fig. 12.6 – 12.9 show some horizontal slices at different stratigraphic levels. The software generates the models with a set sand:gross ratio calculated from the upscaled logs for each zone. The sand:gross ratio can, however, vary greatly at different levels within the zones. It is difficult to see the fluvial geometry in some horizontal slices, though this is expected since it is attempted to model the channel-belt and stacked fluvial deposits and not the actual fluvial channels that have generated the deposits. In general, the input parameters estimated in Table 4 appear to generate models in concurrence with what should be expected according to chapter 9.

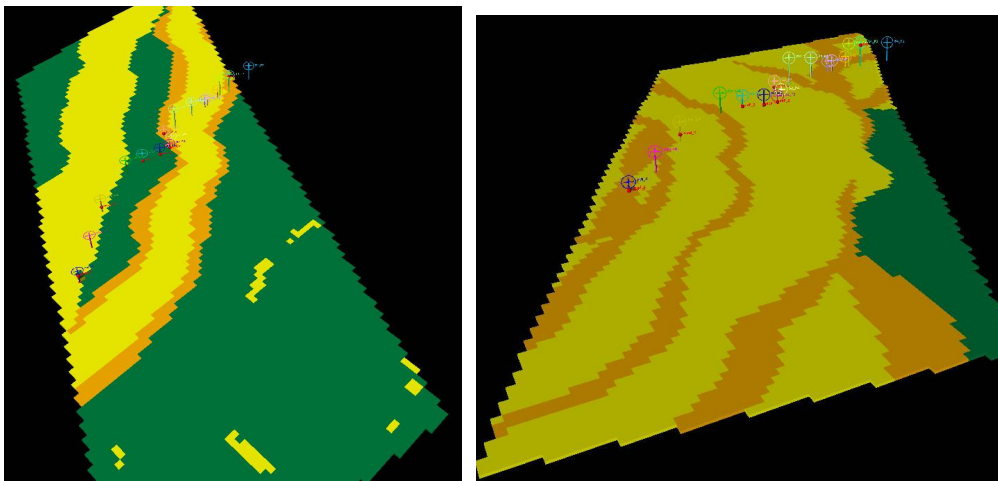


Fig. 12.6: Different stratigraphic levels within Zone 1. Left: low sand:gross ratio with individual channel geometry present. Right: high sand:gross ratio and stacked fluvial deposits in a channel-belt.

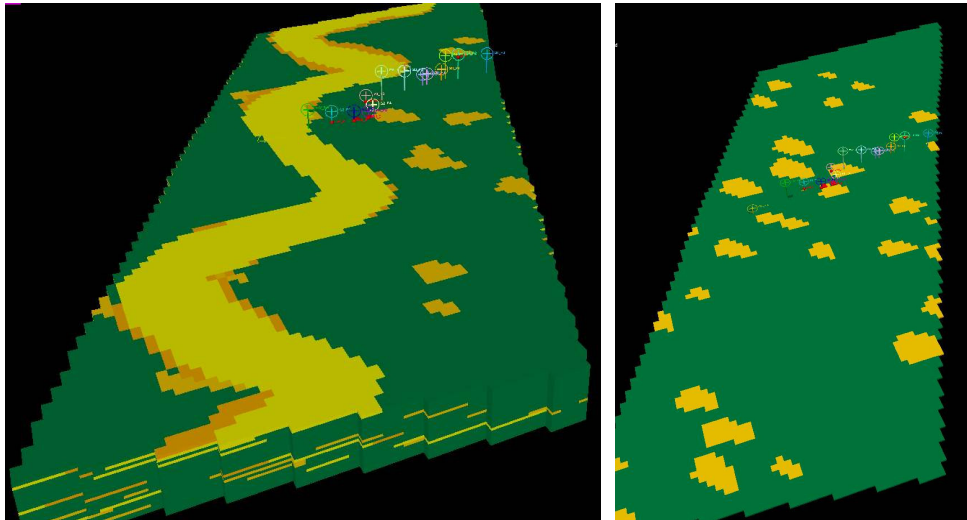


Fig. 12.7: Different stratigraphic levels within Zone 2. Left: medium sand:gross ratio with an individual channel which appears to represent the largest sandstone body within Section 1 (Log FW_1b, 43-51 m) well. Right: very low sand:gross ratio. Only crevasse splays are present at this stratigraphic level. Several flooding surfaces are present in this zone, but not indicated in the model.

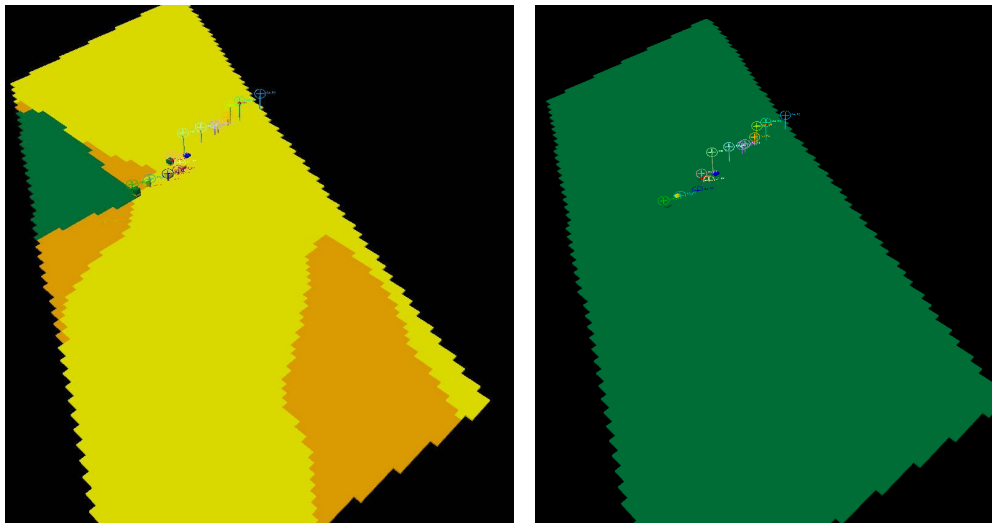


Fig. 12.8: Different stratigraphic levels within Zone 3. Left: high sand:gross ratio showing a channel-belt of laterally stacked fluvial deposits. Right: Background floodplain deposits which may function as a barrier. A flooding surface is present in this interval, though not indicated in the model

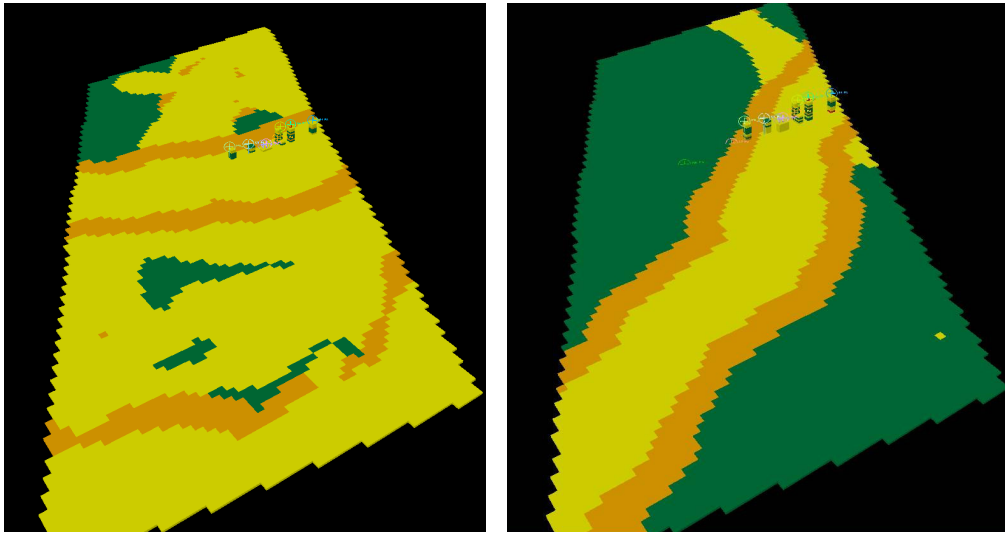


Fig. 12.9: Different stratigraphic levels within Zone 4. Left: high sand:gross ratio showing a channel-belt of laterally stacked fluvial deposits. Right: medium sand:gross with a single channel geometry unit of low sinuosity.

13 RESERVOIR EVALUATION

The reservoir potential is determined mainly by two factors or processes i) depositional factors and ii) diagenetic factors. The depositional factors include primarily the depositional environment and geometry which control the architectural elements and the orientation and stacking of these, in addition to the energy levels resulting in different facies and facies associations with strong control on the initial petrophysical characteristics of porosity, permeability and sorting of the sediments. Levels of heterogeneity (Ch. 10) and interconnectedness compose a large role when evaluating the reservoir potential with respect to the depositional factors. Diagenetic factors involve post-depositional processes of mechanical- and chemical compaction (Ch. 8). Particularly chemical compaction of precipitation of carbonate cement and authigenic minerals is an important issue within the study area.

A proper setting with source rock, cap rock and trap is assumed when evaluating the upper Lourifãha Formation as a possible reservoir.

13.1 Depositional Factors

Depositional environment and geometry

The fluvial depositional environment and architectural style will firstly generate a reservoir which needs to be evaluated on the megascale and macroscale heterogeneity levels (Ch. 8) with respect to sand:gross ratio and interconnectedness of the architectural elements (Ch. 9), the architectural elements themselves and different types of heterogeneity (Ch. 8).

The stochastic reservoir models indicate a 2D reservoir on the megascale heterogeneity level where Zone 2 functions as a vertical barrier and where a probable minor vertical barrier is present between Zone 3 and 4. The barriers are associated with flooding surfaces and rapid base-level rise. The sand:gross ratio is optimistic in the reservoir intervals, i.e. Zone 1, 3 and 4, and insures well interconnectedness between the architectural elements. Thus the lower

and upper parts of the model can, alternatively, be viewed as 3D reservoirs separated by an interval of 2D reservoir properties. The 3D reservoirs will have some heterogeneity between the architectural elements as these are embedded within background floodplain (1st type heterogeneity). This heterogeneity is larger in cross sectional view than in the axial direction of the channels and channel-belts, and zones on low permeability (2nd type heterogeneity) may be expected between the architectural elements despite well interconnectedness.

On the macroscale heterogeneity level, heterogeneity within genetic units (3rd type heterogeneity) is evaluated. This appears to increase upwards in the stratigraphy where multistorey channels (FA 1.1), reactivation surfaces within point bars (FA 1.2) and particularly IHS units (FA 4) are important architectural elements.

Facies and petrophysical characteristics

The initial petrophysical parameters are largely controlled by the energy levels responsible for the individual facies. A high energy level will in general result in removal of mud and deposition of well sorted sand with optimistic primary petrophysical values. Facies expected to have good prosperity on the mesoscale and macroscale heterogeneity levels are e.g. dune structures (facies A and B) or upper stage plane parallel stratified sandstone (facies E) commonly deposited in channel fill elements (FA 1), while mud drapes in cross-stratified sandstone (facies C) and lower stage plane parallel sandstone (facies D) will increase the heterogeneity on this level (4th type heterogeneity). The heterogeneity on the mesoscale level seems to increase upwards in the stratigraphy with an increase of clearer tidal signatures like double mud drapes.

The channel sandstone at base of the succession is finer-grained with a large portion of ripple lamination (facies F) which represents lower energy levels and reduced capability to remove the mud on the microscale level. Further, thin sections show an increase in porosity and permeability due to less carbonate cement upwards in the stratigraphy. The highest counted porosity is 22,5 % which is within reservoir range. This sandstone sample is taken from an IHS unit with type 3 heterogeneity. The porosity should be of minimum 10% in unfractured sandstone deposits to be considered of reservoir properties for an oil prone reservoir (Bjørlykke, 2001). This is a problem in the actual study area as some of the larger, cleaner and supposed promising sandstone elements show very low porosity due to carbonate cement.

A fluvial depositional environment may generate stacked reservoirs with impermeable barriers like the one represented in Zone 2. Fluvial paralic systems commonly generate spatially small reservoirs ($< 10 \text{ km}^2$) which are commonly stacked (Reynolds, 1999), though also larger reservoirs ($< 100 \text{ km}^2$). The depositional environment also gives rise to spatial variations and possible reservoirs downstream or upstream of the studied area. In case of either an estuarine- or tide-dominated deltaic depositional system, tidal ridges or sand bars are expected in the seaward direction which may compose reservoir properties (e.g. Sacha Field Oriente Basin, Equador, Shanmugam *et al*, 2000).

13.2 Diagenetic Factors

Thin sections from sampled rocks reveal a high degree of chemical compaction by both precipitation of carbonate cement and authigenic kaolinite. The reservoir properties are highly reduced by this process and could not, in its present stage, function as a producible reservoir despite promising sand:gross ratio and interconnectedness in parts of the study area. There are, however, possibilities that these effects are *partially* results of surface factors resulting from present day exposure.

Authigenic kaolinite

Authigenic kaolinite is precipitated from in the pores after dissolution of feldspar and mica by flushing of meteoric water (Ch. 8). Precipitation of authigenic kaolinite has a strong effect on the permeability as it commonly precipitates in the pore throats.

Due to the depositional setting, which includes deposition by meteoric water and a continental environment, fluvial sediments will be flushed by meteoric water after deposition, thus some leaching of feldspar and precipitation of authigenic minerals is expected. However, in case of imagined rapid marine burial, e.g. by marine transgression, the reservoir will experience less flux of meteoric water and following leaching and precipitation of authigenic kaolinite. Since the study area has not been buried deep it is assumed to be exposed to meteoric flushing throughout time.

Carbonate cement

The thin sections reveal a large variety in the amount of carbonate cement present in the individual architectural elements. Within separate channel fill elements it ranges from virtually none to 22,5 % porosity. This is largely linked to carbonate cement as the high porosity sandstone has less than 2 % while the point bar element has > 20 %. One should therefore expect a reason for this spread in quantity of carbonate cement within such a small interval and similar depositional elements. A possible explanation for this is the present position and climate of the deposits. The high porosity sandstone is positioned at the top of the cliff while the low porosity point bar deposits are positioned near the ocean surface which experience strong tides. The calcite may thus be a present day surface feature from exposure to carbonate saturated sea water and following evaporation and precipitation of carbonate cement.

In such a case the porosity is expected to reach ~20 % or more and will be within the range of a producible reservoir even when buried.

13.3 Summary: Reservoir evaluation

Reservoir evaluation involves both the depositional environment and diagenetic processes. The reservoir can be separated into 2 or 3 levels of high connectedness between sandstone bodies with one thick unproducibile interval and one thin possible barrier. The areas of high connectedness experience heterogeneity on macro- and mesoscale, though these are normally not thought to represent major fluid flow barriers.

Due to low porosity and permeability values observed in thin sections the reservoir is not producible. High porosity values are observed on top of the cliff wall with normally lower values near the beach within similar depositional units, thus a possible cause of carbonate cement from precipitation of carbonate saturated sea water is proposed to explain the great variations. If this is the case a supposed buried reservoir will have optimistic values of porosity even with further diagenesis during burial.

Authigenic kaolinite will most likely be present within such a depositional environment which initially includes meteoric water, though the amount may be of less quantity if the

reservoir were buried rapidly by marine deposits, which is a plausible scenario in a paralic setting, and thus experience less flux by meteoric water.

13.4 Application as analogue to Statfjord Formation, North Sea

Analogue studies are important and highly used to improve the control of subsurface reservoirs. The Statfjord Formation, which is a hydrocarbon bearing formation in the Statfjord and Snorre Fields in the North Sea, represents mainly braided, low sinuous paralic fluvial sandstones and mudstone where paleosols horizons are present and marine fossils have been recorded in the mudstone (Nystuen and Fält, 1995). By this, it has an immediate resemblance to the Lourinhã Formation, thus this study can be used as an analogue study to some extent. However, there is no decisive data which state that the Lourinhã Formation is deposited in incised valleys and this conclusion has not been reached in this study, though it may be the case. The matter of correct paralic setting may not be the most important question with relevance to this study as an analogue study as the large scale geometry is uncertain and the study area is within the fluvial realm, which may be somewhat similar for both estuarine and tide-dominated delta. To apply this study as a good analogue the matter of interest could be on a smaller scale than the regional, possibly on the level of architectural elements or heterogeneity. Further detailed comparison between the Lourinhã Formation and the Statfjord Formation, or other fluvial to marginal-marine reservoir formations, has been beyond the scope of this project.

14 CONCLUSIONS

- (1) The Louriñha Formation is deposited in a paralic setting which are mainly fluvial controlled, but influenced by tidal processes. The depositional environment is thought to be the fluvial portion of either a tide-dominated delta or estuary.
- (2) Sandstone bodies consist of 1st-order derived granitic detritus of low maturity. The source area is interpreted to be the Hercynian Basement Horsts at the north-western margin of the Lusitanian Basin, presently exposed as the Berlengas and Ferilhões Islands.
- (3) The modelled succession can be separated into 2 or 3 reservoir zones of high connectedness between sandstone bodies, with one thick unproducibile zone composing a fluid flow barrier and one thin possible barrier. Zones of high connectedness experience heterogeneity on macro- and mesoscale, though these are normally not thought to represent major fluid flow barriers. The permeability and porosity, however, makes the majority of the Louriñha reservoir unproducibile in its present stage.
- (4) No quartz overgrowth has been identified, and by this reason the burial depth had not been more than ~3 km. The sandstones show high degree of calcite cement, leaching of feldspar and mica, and formation of authigenic kaolinite. Due to pore-filling minerals, porosity is generally low, but is above 20 % in some channel sandstone bodies. In subsurface, below the zone of flushing meteoric water, porosity and hence also permeability may be better than in the studied sections. The extensive calcite cement may also be a present day surface feature from flux of carbonate saturated sea water and carbonate precipitation during exposure in a warm climate.
- (5) The application of the Louriñha Formation as an analogue to the Statfjord Formation in the North Sea area, or to other fluvial to paralic reservoir sandstone bodies, may be limited due to poor 3D control and regional data. However, the Louriñha Formation is considered a suitable analogue for the Statfjord Formation on the scale of architectural elements and macroscale heterogeneity.

15 REFERENCES

- Adams, A.E., McKenzie, W.S. and Guliford, C. (1984) Atlas of Sedimentary Rocks under the Microscope, pp. 104, Longman Group.
- Aigner, T, Heinz, J, Hornung, J and Aspöck, U. (1998) A hierarchical process-approach to reservoir heterogeneity; examples from outcrop analogues. *Bulletin du Centre de recherches Elf Exploration Production*, **22**, 1-11.
- Allen, J.R.L. (1984) Sedimentary structures, their character and physical basis. *Developments in Sedimentology*, 30, pp. 663, Elsevier.
- Alves T.M., Manuppella, G., Gawthorpe, R.L. Hunt, D.W. and Monteiro, J.H. (2003) The depositional evolution of diapir- and fault-bounded rift basins: examples from the Lusitanian Basin of West Iberia. *Sedimentary Geology*, **162**, 273-303.
- Azereido, A.C., Wright, V.P. and Ramalho, M.M. (2002) The Middle-Late Jurassic forced regression and disconformity in central Portugal: eustatic, tectonic and climatic effects on a carbonate ramp system. *Sedimentology*, **49**, 1339-1370.
- Bhattacharya, J.P. and Walker, R.G. (1992) Deltas. In: *Facies Models; response to sea level change* (Ed. by Walker, R.G. and James, N.P.), pp. 157-177. Geological Association of Canada.
- Bjørlykke, K. (1983) Diagenetic reactions in sandstone. In: *Sediment Diagenesis* (Ed. by Parker, A. and Sellwood, B.W.), pp. 169-213.
- Bjørlykke, K. (1998) Clay minerals diagenesis in sedimentary basins – a key to the prediction of rock properties. Examples from the North Sea Basin. *Clay Minerals*, **33**, 15-34.
- Bjørlykke, K (2001) *Sedimentology og Petroleumsgologi*. pp.334, Gyldendal yrkesopplæring, Oslo.
- Bluck, B.J. (1971) Sedimentation in the meandering River Endrick. *Scottish Journal of Geology*, **7**, 93-138.
- Boggs, S. jr, (2001) *Principles of Sedimentology and Stratigraphy*. pp. 726, Prentice Hall.
- Bridge, J.S. (1985) Paleochannel patterns inferred from alluvial deposits; a critical evaluation. *Journal of Sedimentary Petrology*, **55**, 579-589.
- Bridge, J.S. and Mackey, S.D. (1993) A theoretical study of fluvial sandstone body dimensions. In: *The Geological Modelling of Hydrocarbon Reservoirs and Outcrop*

- Analogues* (Ed. by Flint, S.S. and Bryant, I.D.), pp. 213-236, *Special Publication*, 15, International Association of Sedimentologists (IAS).
- Bridge, J.S. and Tye, R.S. (2000) Interpreting the dimensions of ancient fluvial channel bars, channels and channel belts from wireline-logs and cores. *AAPG Bulletin*, **84**, 1205-1228.
- Bridge, J.S. (2003) *Rivers and Floodplain; Forms, Processes, and Sedimentary Record*. pp. 491, Blackwell Science Ltd.
- Bridge, J.S., Jalfin, G.A. and Georgieff, S.M. (2000) Geometry, lithofacies, and spatial distribution of Cretaceous fluvial sandstone bodies, San Jorge Basin, Argentina: Outcrop analogue for the hydrocarbon-bearing Chubut Group. *Journal of Sedimentary Research*, **70**, 341-349.
- Coleman, J.M. and Wright, L.D. (1975) Modern river deltas; variability of processes and sand bodies. In: *Deltas, Models for Exploration* (Ed. by Brussard, M.L.), pp. 99-149, Houston Geological Society.
- Collinson, J.D. (1996) Alluvial Sediments. In: *Sedimentary Environments: Processes, Facies and Stratigraphy* (Ed. by Reading, H.G.), pp. 37-82. Blackwell Science Ltd.
- Cooper, J.A.G. (1994) Sedimentary processes in the river-dominated Mvoti Estuary, South Africa. *Geomorphology*, **9**, 271-300.
- Dalrymple, R.W., Zaitlin, B.A. and Boyd, R. (1992) Estuarine facies models; conceptual basis and stratigraphic implications. *Journal of Sedimentary Petrology*, **62**, 1130-1146.
- Dalrymple, R.W. (1992) Tidal depositional system. In: *Facies Models; response to sea level change* (Ed. by Walker, R.G. and James, N.P.), pp. 195-218. Geological Society of Canada.
- Dalrymple, R.W., Baker, E.K., Harris, P.T. and Hughes, M.G. (2003) Sedimentology and stratigraphy of a tide-dominated, foreland-basin delta (Fly River Papua New Guinea). In: *Tropical Deltas of Southeast Asia – Sedimentology, Stratigraphy and Petroleum Geology* (Ed. by Hasan, S.F., Nummedal, D., Patrice, I., Herman, D. and Posamentier, H.W.), pp. 147-173, *Special Publication Society for Sedimentary Geology*, **76**.
- Demko, T.M., Currie B.S. and Nicoll, K.A. (2004) Regional paleoclimatic and stratigraphic implications of paleosols and fluvial/overbank architecture in the Morrison Formation (Upper Jurassic), Western Interior, USA. *Sedimentary Geology*, **167**, 115-135.
- Doyle, P. (2004) *Understanding Fossils; An Introduction to Invertebrate Palaeontology*.

- Wiley, pp. 409.
- Dyer, K.R. (1996) The definition of the Severn Estuary. *Proceedings*, **56**, 53-66.
- Ehlers, T.A. and Chan, M.A. (1999) Tidal sedimentology and estuarine deposition of the Proterozoic Big Cottonwood Formation, Utah. *Journal of Sedimentary Research*, **69**, 1169-1180.
- Elliott, M. (2002) The need for definitions in understanding estuaries. *Estuarine, coastal and shelf science*, **55**, 815-827.
- Emery, D. and Meyers, K.J. (1996) *Sequence Stratigraphy*. pp. 111-177. Balckwell Science Ltd.
- Ferguson, R.J. (1999) Levee morphology and sedimentology along the lower Tuross River, south-eastern Australia. *Sedimentology*, **46**, 627-648.
- Fürsich, F.T. and Werner, W. (1986) Benthic associations and their environmental significance in the Lusitanian Basin (Upper Jurassic, Portugal). *Neues Jahrbuch für Geologie und Paläontologie, Abhandlungen*, **172**: 271-329.
- Gahr, M. (2005) Response of Lower Toarcian (Lower Jurassic) macrobenthos of the Iberian Peninsula to sea level changes and mass extinction. *Journal of Iberian geology*, **31**, 197-215.
- Galloway, W.E. (1975) Process framework for describing the morphologic and stratigraphic evolution of deltaic depositional systems. In: *Deltas; Models for Exploration* (Ed. by Broussard, M.L.), pp. 87-98, Houston Geological Society.
- Harms, J.C., Southard, J.B., Spearing, D.R. and Walker, R.G. (1975) Depositional environments from primary sedimentary structures and stratification sequences. *SEPM Short Course No. 2*, pp. 161, Dallas 1975, Society of Economic Paleontologists & Mineralogists.
- Harris, P.T. (1994) Incised Valleys and Backstepping Deltaic Deposits in a Foreland-Basin Setting, Torres Strait and Gulf of Papua, Australia. In: *Incised-Valley Systems; Origin and Sedimentary Sequences* (Ed. by Dalrymple, R.W., Boyd, R. and Zaitlin, B.A.), pp. 97-108, *SEPM Special publications*, **51**. Society of Sedimentary Geology.
- Higgs, R. (2002) Tide-dominated estuarine facies in the Hollin And Napo ("T" and "U") formations (Cretaceous), Sacha field, Oriente Basin, Equador: Discussion. *AAPG Bulletin*, **86**, 329-334.
- Hill, G.E. (1989) Distal Alluvial-fan sediments from the Upper Jurassic of Portugal – Controls on their cyclicity and channel formation. *Journal of the Geological Society*, **146**, 539-555.

- Jiao, Y.Q. (2005) Architectural units and heterogeneity of channel reservoirs in the Karamay Formation, outcrop area of Karamay oil field, Junggar basin, northwest China. *AAPG Bulletin*, **89**, 529-545.
- Kim, W. (2006) Shoreline response to autogenic processes of sediment storage and release in the fluvial system. *Journal of Geophysical Research*, **111**, F04013.
- Komatsubara, J. (2004) Fluvial architecture and sequence stratigraphy of the Eocene to Oligocene Iwaki Formation, northeast Japan: channel-fills related to the sea-level change. *Sedimentary Geology*, **168**, 109-123.
- Kullerud, K. (Author) and Svendsen, L.E. (Ass. Producer) (2003) Fjellkjededannelse. Retrieved 04.01.2007 from <http://www.ig.uit.no/~kaarek/elaer/geo101/flash/fjellkjeder.swf>
- Laure, D.K. and Hovadik, J. (2006) Connectivity of channelized reservoirs: a modelling approach. *Petroleum Geoscience*, **12**, 291-308.
- Leeder, M.R. (1973) Fluvial fining-upwards cycles and the magnitude of palaeochannels. *Geological Magazine*, **110**, 265-276.
- Leinfelder, R.R. (1987) Multifactorial control of sedimentation patterns in the ocean marginal basin; the Lusitanian Basin (Portugal) during the Kimmeridgian and Tithonian. *Geologische Rundschau*, **76**, 599-631.
- Leinfelder, R.R. and Wilson, R.L.C. (1989) Seismic and Sedimentological Features of Oxfordian- Kimmeridgian Syn-Rift Sediments on the Eastern Margin of the Lusitanian Basin. *Geologische Rundschau*, **78**, 81-104.
- Leinfelder, R.R. and Wilson, R.C.L. (1998) Third-order sequences in an Upper Jurassic rift-related second-order sequence, central Lusitanian Basin, Portugal. In: *Mesozoic and Cenozoic Sequence Stratigraphy of European Basins* (Ed. by de Garciánsky, P.C., Hardenbol, J., Thierry, J. and Vail, P.R.), pp. 507-525, *SEPM Special Publication*, **60**, Society of Sedimentary Geology.
- Lorenz, J.C., Heinze, D.M., Clark, J.A. and Searls, C.A. (1986) Determinations of Widths of Meander-Belt Sandstone Reservoirs from Vertical Downhole Data, Mesaverde Group, Piceance Creek Basin, Colorado. *AAPG Bulletin*, **69**, 710-721.
- Mechel, L.D. (1975) Holocene Sand Bodies on the Colorado Delta Area, Northern Gulf of California. In: *Deltas; Models for Exploration* (Ed. by Boussard, M.L.), pp. 239-265, Houston Geological Society.
- Miall, A.D. (1977) *Fluvial Sedimentology: note to accompany a lecture series on fluvial sedimentology, held at the Calgary Inn, 19th October 1977*. Canadian Society of

- Petroleum Geologists.
- Miall, A.D. (1978) Fluvial Sedimentology; a historical review. In: *Fluvial Sedimentology*. (Ed. by Miall, A.D.), pp. 1-47, Memoir Canadian Society of Petroleum Geologists, **5**.
- Miall, A.D. (1985) Architectural-element analysis – A new method of facies analysis applied to fluvial deposits. *Earth-science Reviews*, **22**, 261-308.
- Miall, A.D. (1992) Alluvial Deposits. In: *Facies Models; response to sea level change* (Ed. by Walker, R.G. and James, N.P.), pp. 119-142, Geological Association of Canada.
- Miall, A.D. (1996) The Geology of Fluvial Deposits: Sedimentary Facies, Basin Analysis, and Petroleum Geology. pp. 582, Springer.
- Miall, A.D. (2006) How do we identify big rivers? And How big is big? *Sedimentary Geology*, **186**, 39-50.
- Nichols, M.M. and Biggs, R.B. (1985) Estuaries. In: *Coastal Sedimentary Environments* (Ed. by Davis, R.A. Jr.), pp.77-186, Springer-Verlag.
- Nio, S.D. and Yang, C. (1991) Diagnostic attributes of clastic tidal deposits; a review. In: *Clastic Tidal Sedimentology* (Ed. by Smith, D.G., Reinson, G.E., Zaitlin, B.A. and Rahmani, R.A.), pp. 3-27, *Memoir Canadian Society of Petroleum Geologists*, **16**.
- Nystuen, J.P and Fält, L.M (1995) Upper Triassic-Lower Jurassic reservoir rocks in the Tampen Spur area, Norwegian North Sea. In: *Petroleum: Exploration and Exploitation in Norway* (Ed. by Hanslien, S.) pp. 135-179, *NPF Special Publication 4*, Elsevier, Amsterdam.
- Posamentier, H.W. and Allen, G.P. (1999) Chapter 2: Fundamental Concepts of Sequence Stratigraphy. In: *Siliciclastic sequence stratigraphy – Concepts and applications. SEPM Concepts in Sedimentology and Paleontology Series*, **7**, p. 9-51. Society for Sedimentary Geology.
- Posamentier, H.W., Jervey, M.T. and Vail, P.R. (1988) Eustatic controls on clastic deposition 1 – Conceptual framework. In: *Sea-level Changes: An Intergrated Approach* (Ed. by Wilgus, C.K., Hastings, B.S., Kendall, C.G.S.C., Posamentier, H.W., Ross, C.A. and Van Wagoner, J.C.), pp.109-154. *SEPM Special Publication*, **42**, The Society of Economic Paleontologists and Mineralogists.
- Puigdefabregas, C. (1973) Miocene point-bar deposits in the Ebro Basin, northern Spain. *Sedimentology*, **20**, 133-144.
- Puigdefabregas, C. and van Vliet, A. (1978) Meandering stream deposits from the Tertiary of the southern Pyrenees. In: *Fluvial Sedimentology*. (Ed. by Miall, A.D.), pp. 469-485, *Memoir Canadian Society of Petroleum Geologists*, **5**.

- Rabata, L.A., Gingras, M.K., Rasanen, M.E. and Barberi, M. (2006) Tidal channel deposits on a delta plain from the Upper Miocene Nauta Formation, Maranon Foreland Sub-basin, Peru. *Sedimentology*, **53**, 971-1013.
- Rasmussen, E.S., Lomholt, S., Andersen, C. and Vejbæk, O.V. (1998) Aspects of the structural evolution of the Lusitanian Basin in Portugal and the shelf and slope area offshore Portugal. *Tectonophysics*, **300**, 199-225.
- Reading, H.G. and Collinson, J.D. (1996) Clastic coasts. In: *Sedimentary Environments: Processes, Facies and Stratigraphy* (Ed. by Reading, H.G.), pp. 154-231, Blackwell Science Ltd.
- Reynolds, A.D. (1999) Dimensions of Paralic Sandstone Bodies. *APG Bulletin*, **83**, p. 211-229.
- Seidler, L. and Steel, R. (2001) Pinch-out style and position of tidally influenced strata in a regressive-transgressive wave-dominated deltaic sandbody, Twentymile Sandstone, Mesaverde Group, NW Colorado. *Sedimentology*, **48**, 399-414.
- Shanley, K.W. and McCabe, P.J. (1993) Alluvial architecture in a sequence stratigraphic framework; a case study from the Upper Cretaceous of southern Utah, USA. In: *The Geological Modelling of Hydrocarbon Reservoirs and Outcrop Analogues* (Ed. by Flint, S.S. and Bryant, I.D.), pp. 21-55. *Special Publication*, **15**, International Association of Sedimentologists (IAS).
- Shanley, K.W. McCabe, P.J. and Hettinger, R.D. (1992) Tidal influence in Cretaceous fluvial strata from Utah, USA – A key to sequence stratigraphic interpretation. *Sedimentology*, **39**, 905-930.
- Shanmugam, G. and Poffenberger, M. (2002) Tide-dominated estuarine facies in the Hollin and Napo (“T” and “U”) formations (Cretaceous), Sacha field, Oriente Basin, Ecuador: Reply. *AAPG Bulletin*, **86**, 335-340.
- Shanmugam, G., Poffenberger, M. and Álva, J.T. (2000) Tide-dominated estuarine facies in the Hollin and Napo (“T” and “U”) formations (Cretaceous), Sacha field, Oriente Basin, Ecuador. *AAPG Bulletin*, **84**, 652-682.
- Smith, D.G. (1988) Modern point bar deposits analogues to the Athabasca Oil Sands, Alberta, Canada. In: *Tidal-influenced Sedimentary Environments and Facies* (Ed. by de Boer, P.L., van Gelder, A. and Nio, S.D.), pp.417-432, Reidel, New York.
- Stapel, G., Cloetingh, S. and Pronk, B. (1996) Quantitative subsidence analysis of the Mesozoic evolution of the Lusitanian Basin (Western Iberian margin). *Tectonophysics*, **266**, 493-507.

- Thomas, R.G., Smith, D.G., Wood, J.M., Visser, J., Calverly Range, A.E. and Koster Emlyn, H. (1987) Inclined Heterolithic Stratification; terminology, description, interpretation and significance. *Sedimentary Geology*, **53**,123-179.
- Visser, M.J. (1980) Neap-spring cycles reflected in Holocene subtidal large-scale bedform deposits; a preliminary note. *Geology*, **8**, 543-546.
- Walker, R.G. (1992) Facies, Facies Models and Modern Stratigraphic Concepts. In: *Facies Models, response to relative sea level change* (Ed. by Walker, R.G. and James, N.P), pp. 1-14, Geological Association of Canada.
- Weber, K.J. (1986) How Heterogeneity Affects Oil Recovery. In: *Reservoir Characterization* (Ed. by Lake, L.W. and Carroll, H.B.), pp. 487-544, *Proceedings of the Reservoir Characterization Technical Conference Dallas, Texas 1985*, Academic Press Inc. Ltd, London.
- Willis, B.J. (1997) Architecture of fluvial-dominated valley-fill deposits in the Cretaceous Fall River Formation, *Sedimentology*, **44**, 735-757.
- Willis, B.J. and Gabel, S.L (2001) Sharp-based, tide-dominated deltas of the Sego Sandstone, Book Cliffs, Utah, USA. *Sedimentology*, **48**, 479-506.
- Willis, B.J. and Gabel, S.L. (2003) Formation of deep incision into tide-dominated river deltas: Implications for the stratigraphy of the Sego Sandstone, Book Cliffs, Utah, USA. *Journal of Sedimentary Research*, **73**, 246-263.
- Wilson, R.C.L., Hiscott, R.N., Willis, M.G. and Gradstein, F.M. (1989) The Lusitanian Basin of west-central Portugal; Mesozoic and Tertiary tectonic; stratigraphic, and subsidence history. *AAPG Memoir*, **46**, 341-361.
- Zaitlin, B.A., Dalrymple, R.W. and Boyd, R. (1994) The Stratigraphic Organization of Incised-Valley Systems Associated with Relative Sea-level Change. In: *Incised-Valley Systems; Origin and Sedimentary Sequences* (Ed. by Dalrymple, R.W., Boyd, R. and Zaitlin, B.A.) *SEPM Special Publication*, **51**, 45-60, Society of Sedimentary Geology.

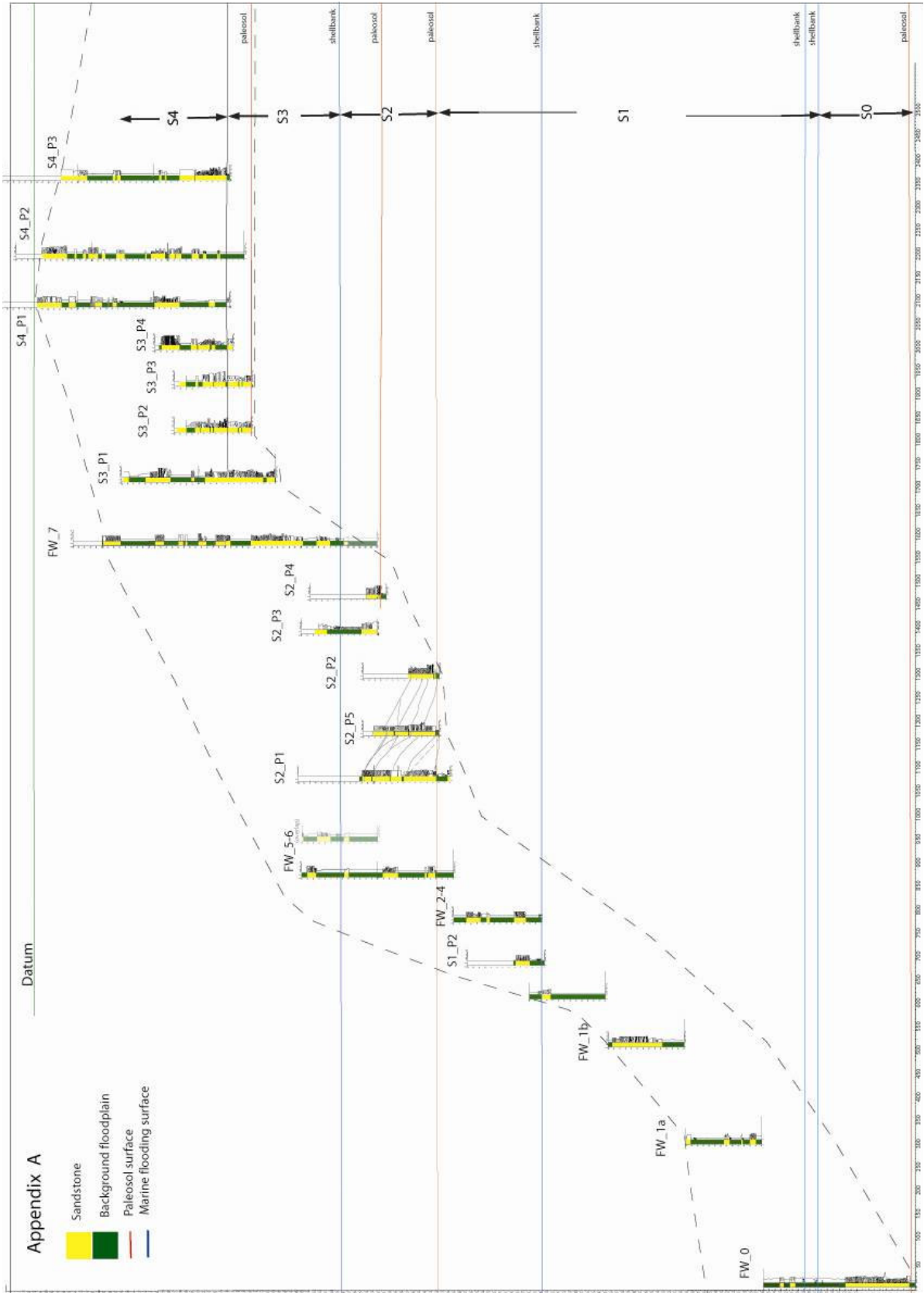
16 APPENDIX

Appendix A: Illustration of the logs-positions in the study

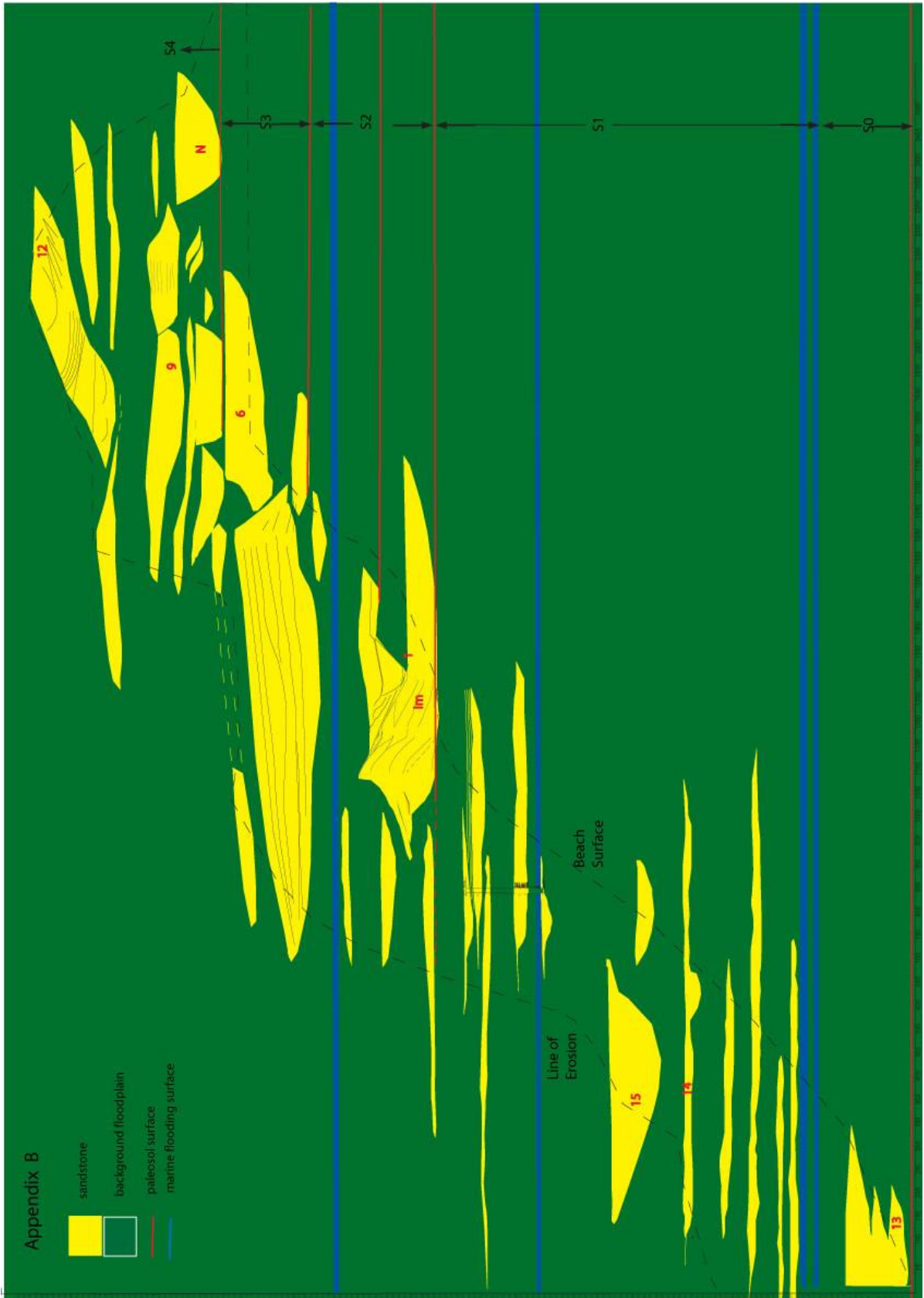
Appendix B: Illustration of the sandstone bodies in the study are

Appendix C: Logs

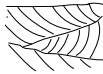
APPENDIX A





APPENDIX B




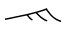
LEGEND FOR SEDIMENTARY LOGS


- Cross-stratified sandstone 


- Planar cross-stratified sandstone 


- Cross-stratified sandstone with double mud drapes 


- Mudstone-sandstone laminae 


- Ripple laminated sandstone 


- Climbing ripples 


- Soft sediment deformed sandstone 


- Shell fragments 






- Root structures 

- Calcrete nodules 

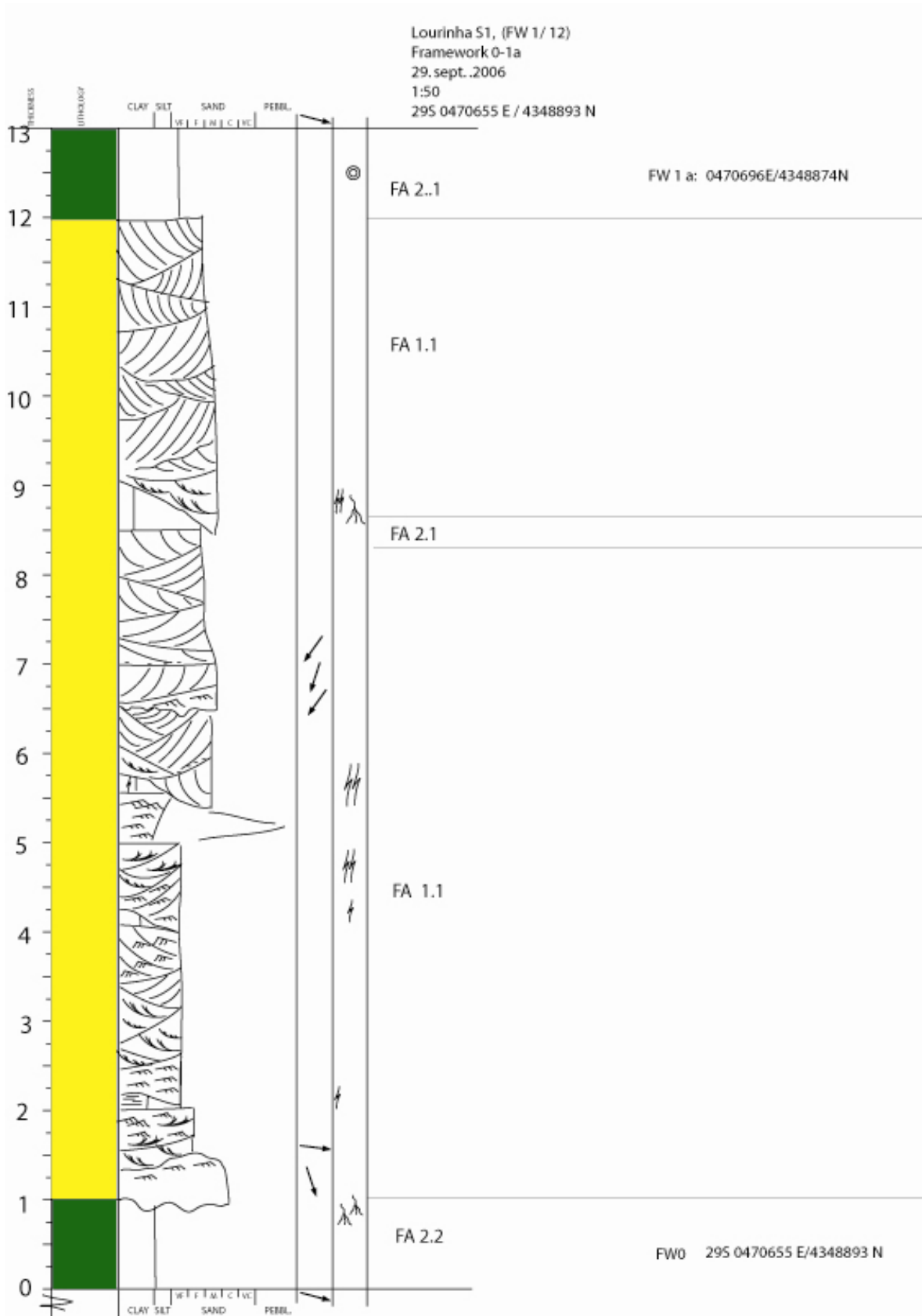
- Mud rip up clasts 

- Coal fragments 

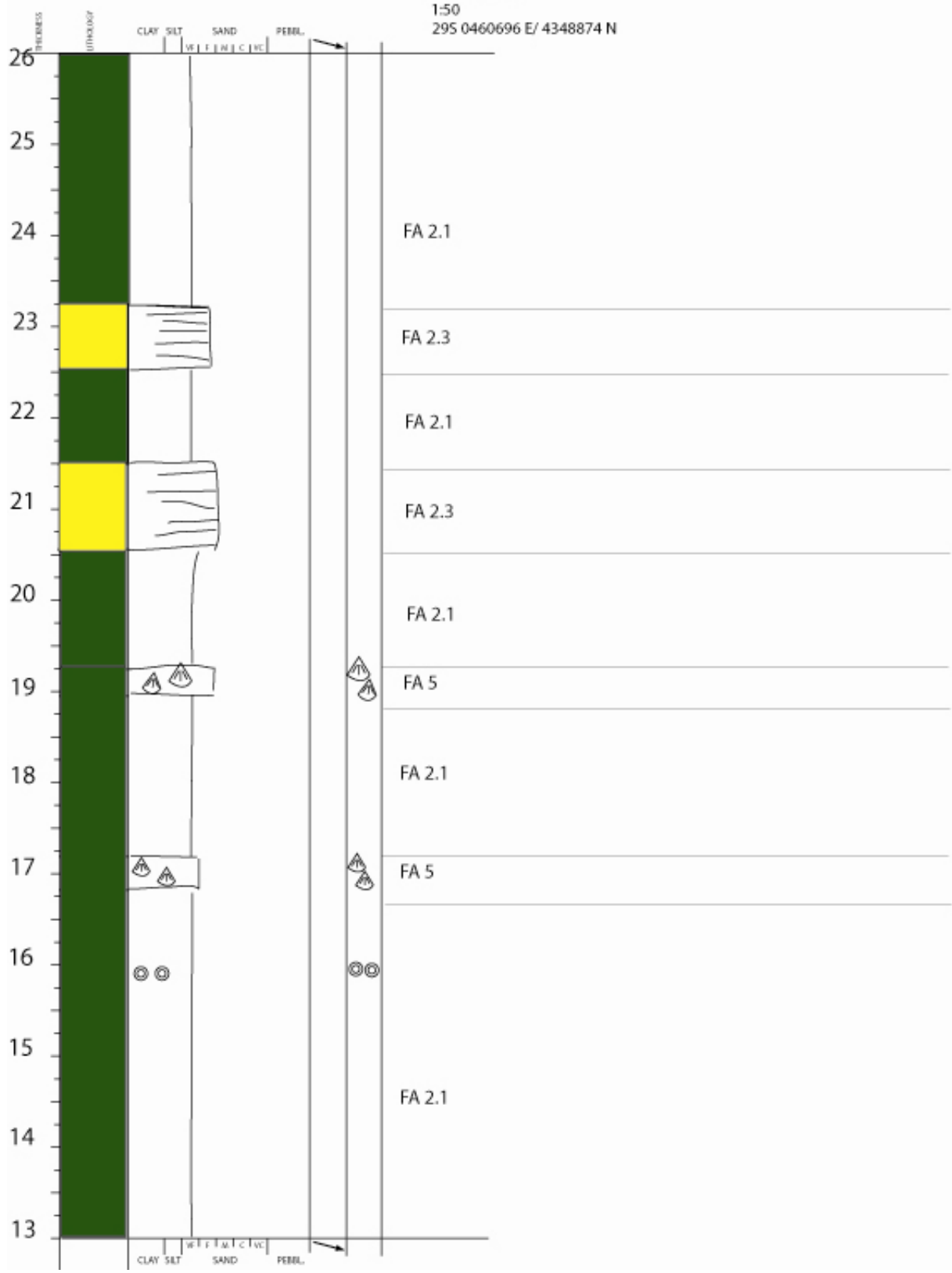
- Dinosaur footprints 

- Dessication cracks 
- Pebbles, ekstrabasinal 
- Mud conglomerate 
- Sandstone 
- Background floodplain mud 

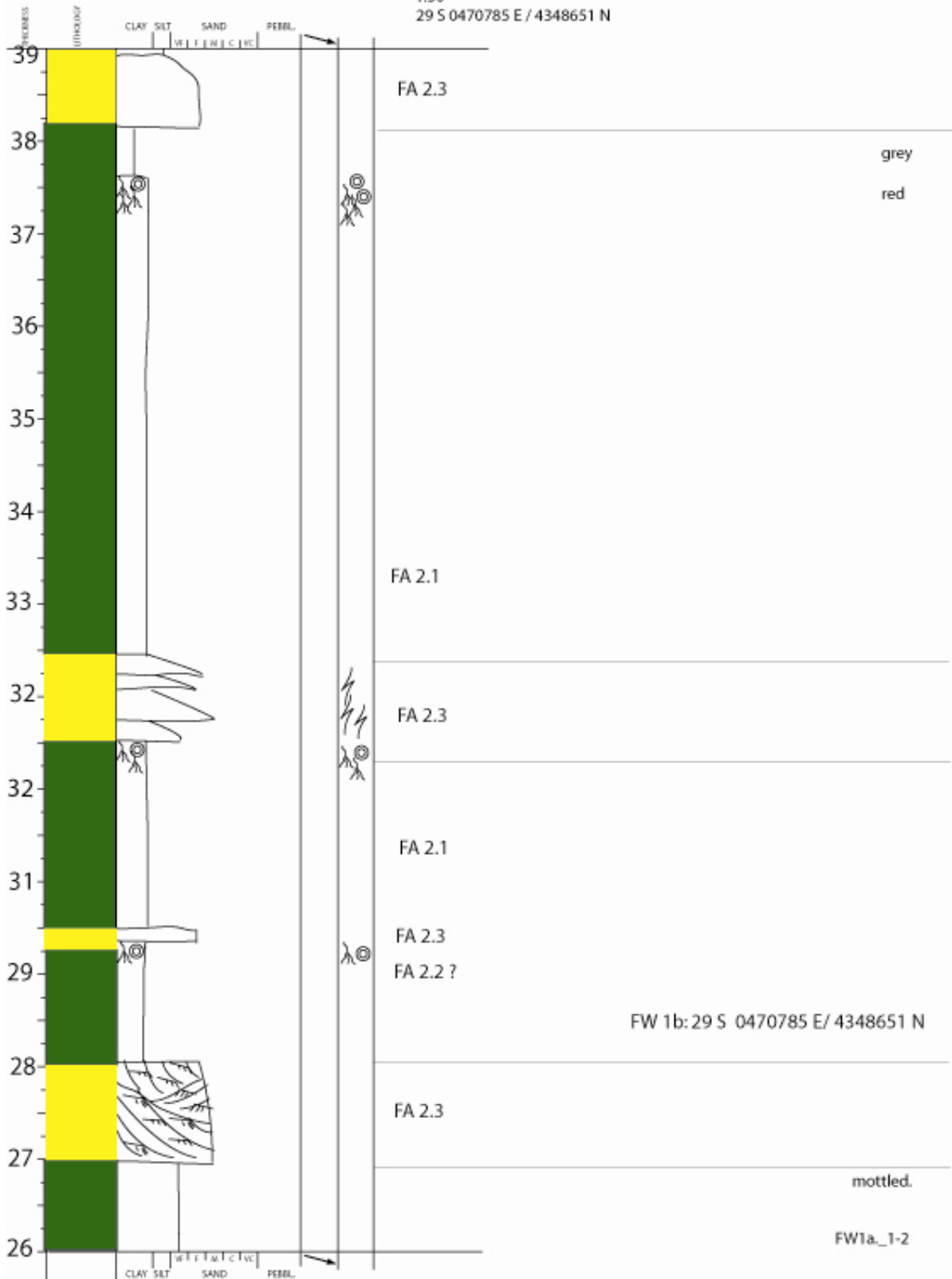
FRAMEWORK / STRATIGRAPHY LOGS



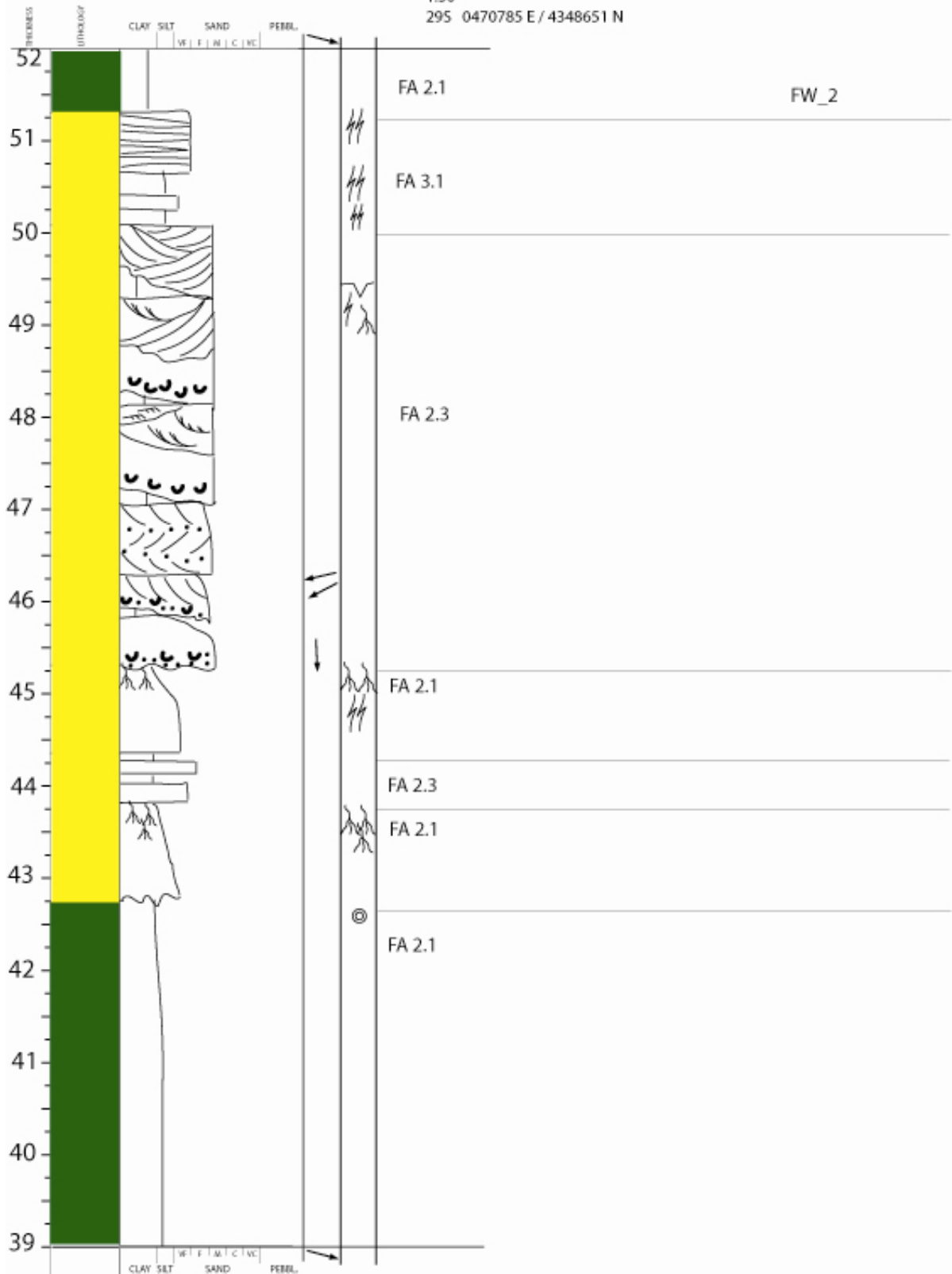
Lourinha S1, (FW 2/12)
 Framework_1a-1b
 30. sept 2006
 1:50
 29S 0460696 E/ 4348874 N

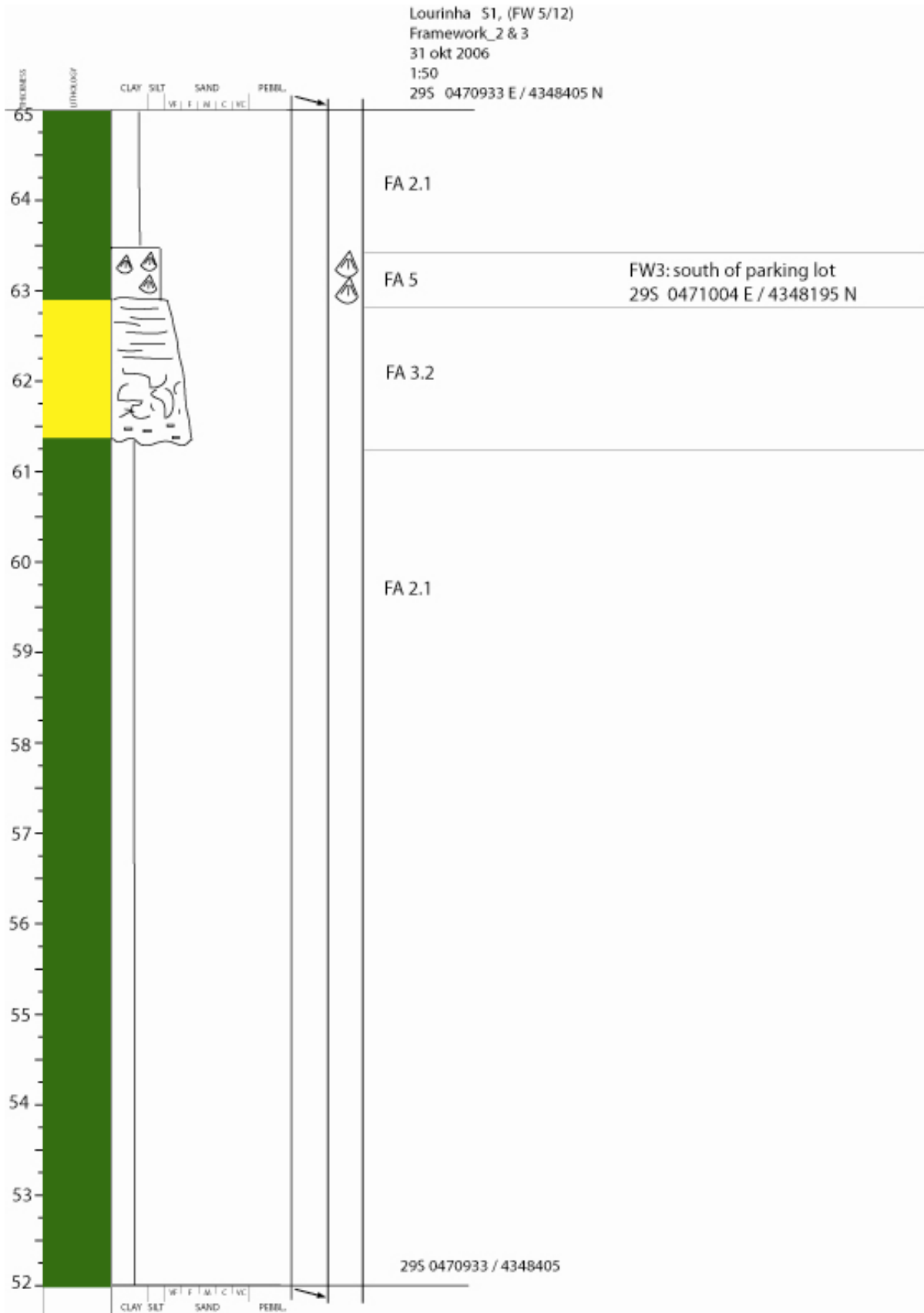


Lourinha S1, (FW 3/12)
 Framework_1a-1b
 30. sept 2006
 1:50
 29 S 0470785 E / 4348651 N

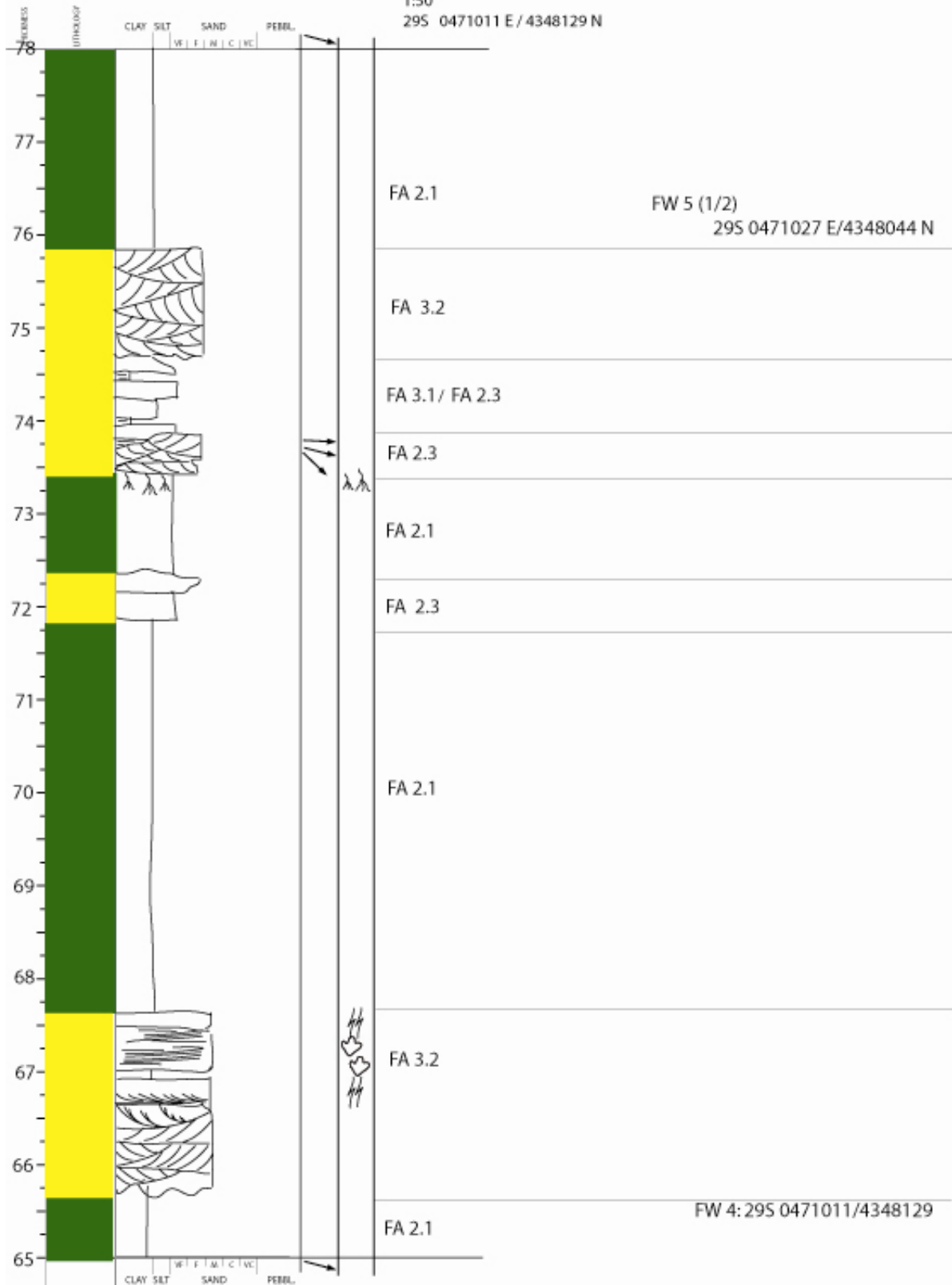


Lourinha S1, (FW 4/12)
 Framework_1b.
 30 sept 2006
 1:50
 295 0470785 E / 4348651 N

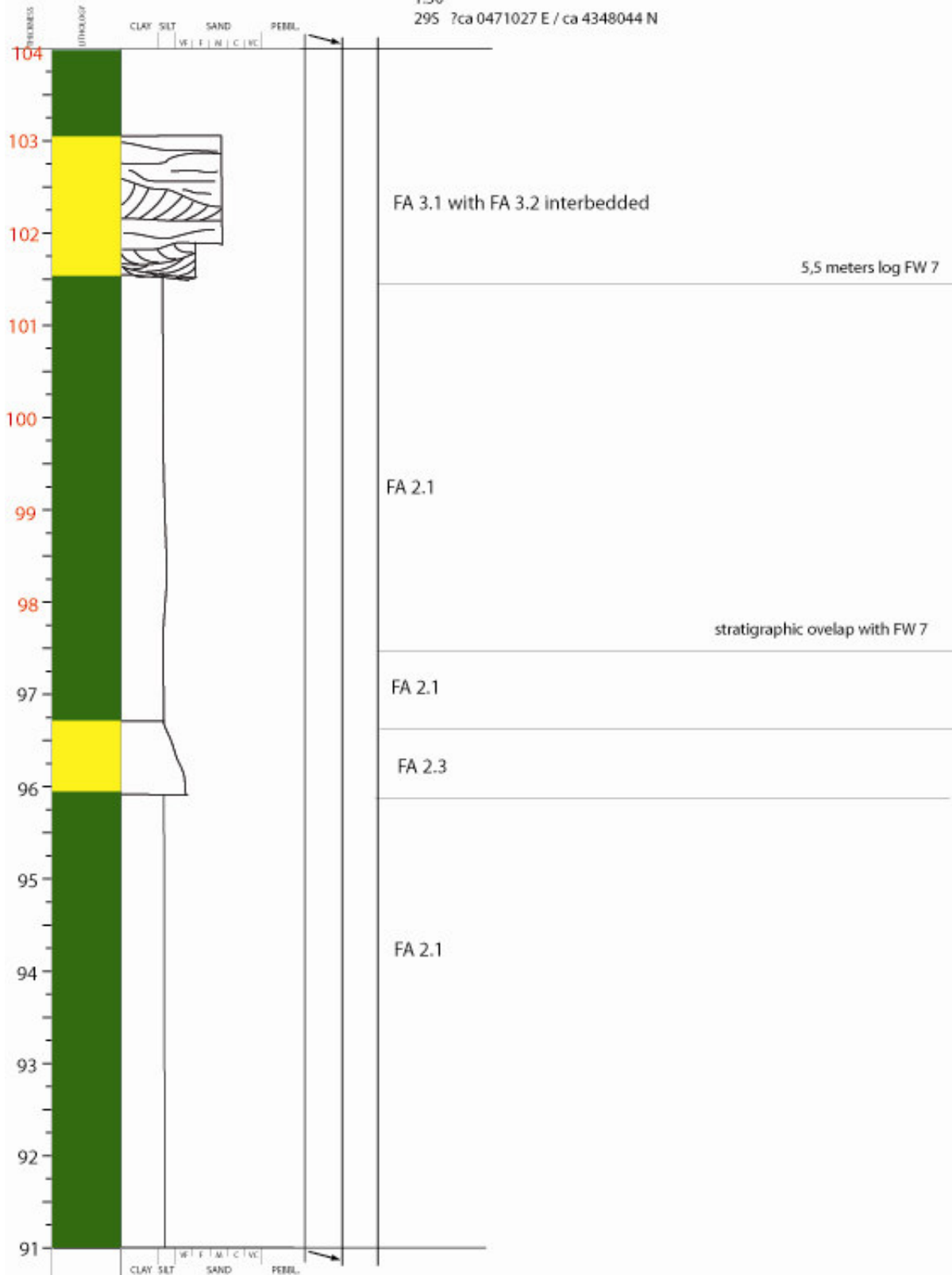




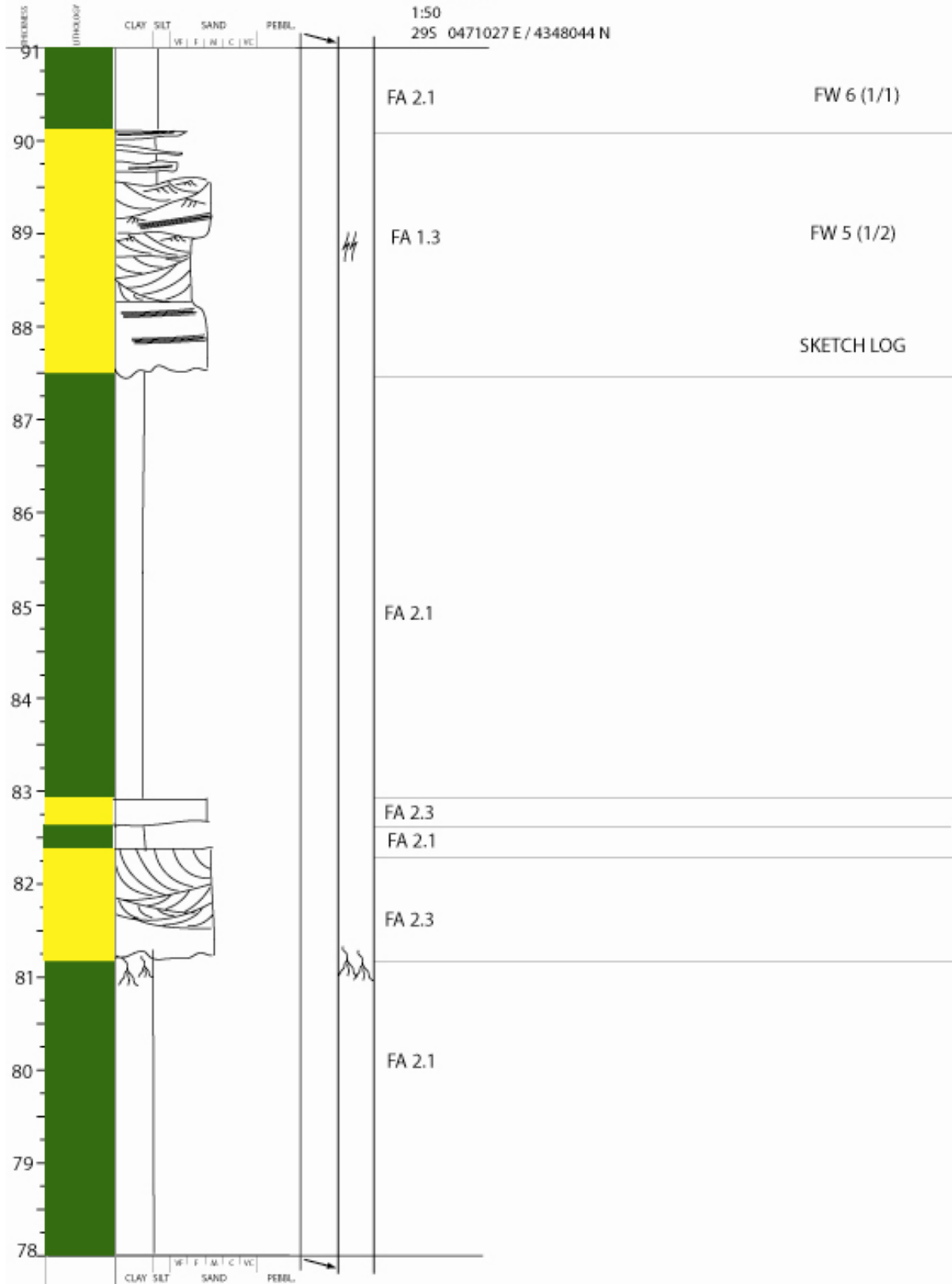
Lourinha S1, (FW 6/12)
 Framework_4
 1. okt 2006
 1:50
 29S 0471011 E/4348129 N



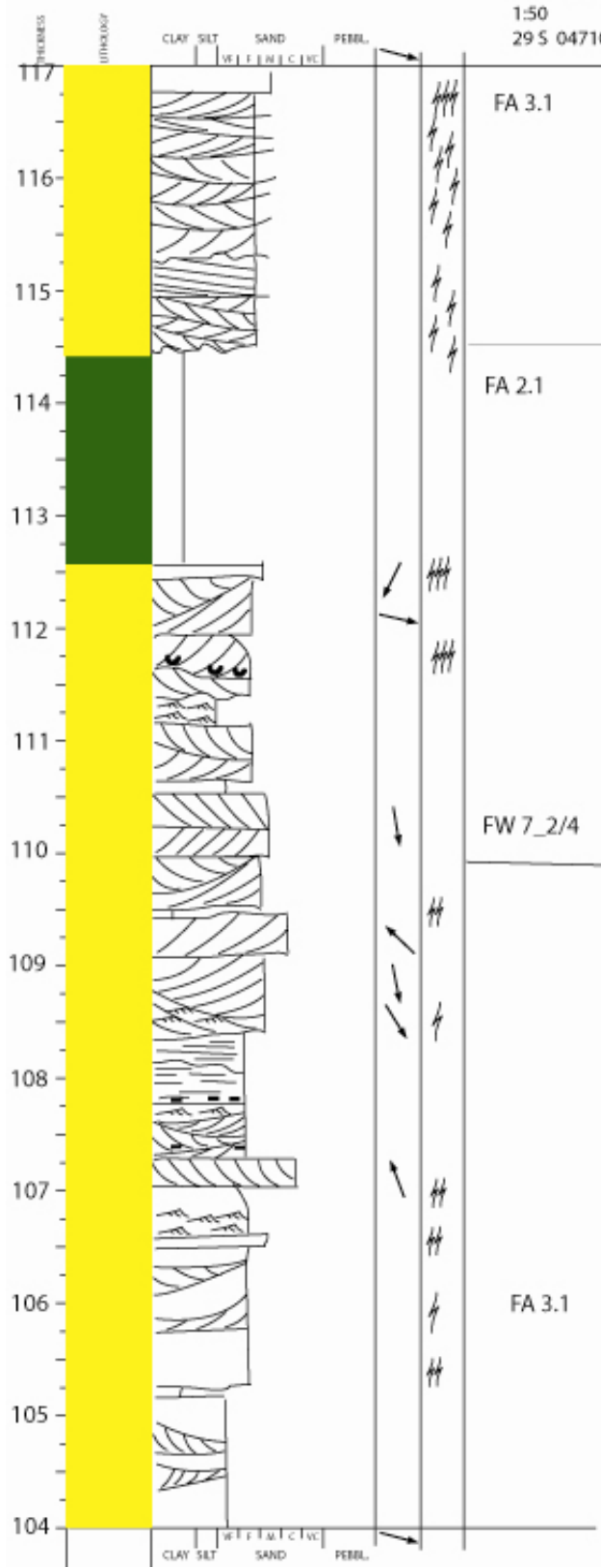
Lourinha S1, (FW 7/12)
 overlap Framework_6
 1. okt 2006
 1:50
 295 °ca 0471027 E / ca 4348044 N



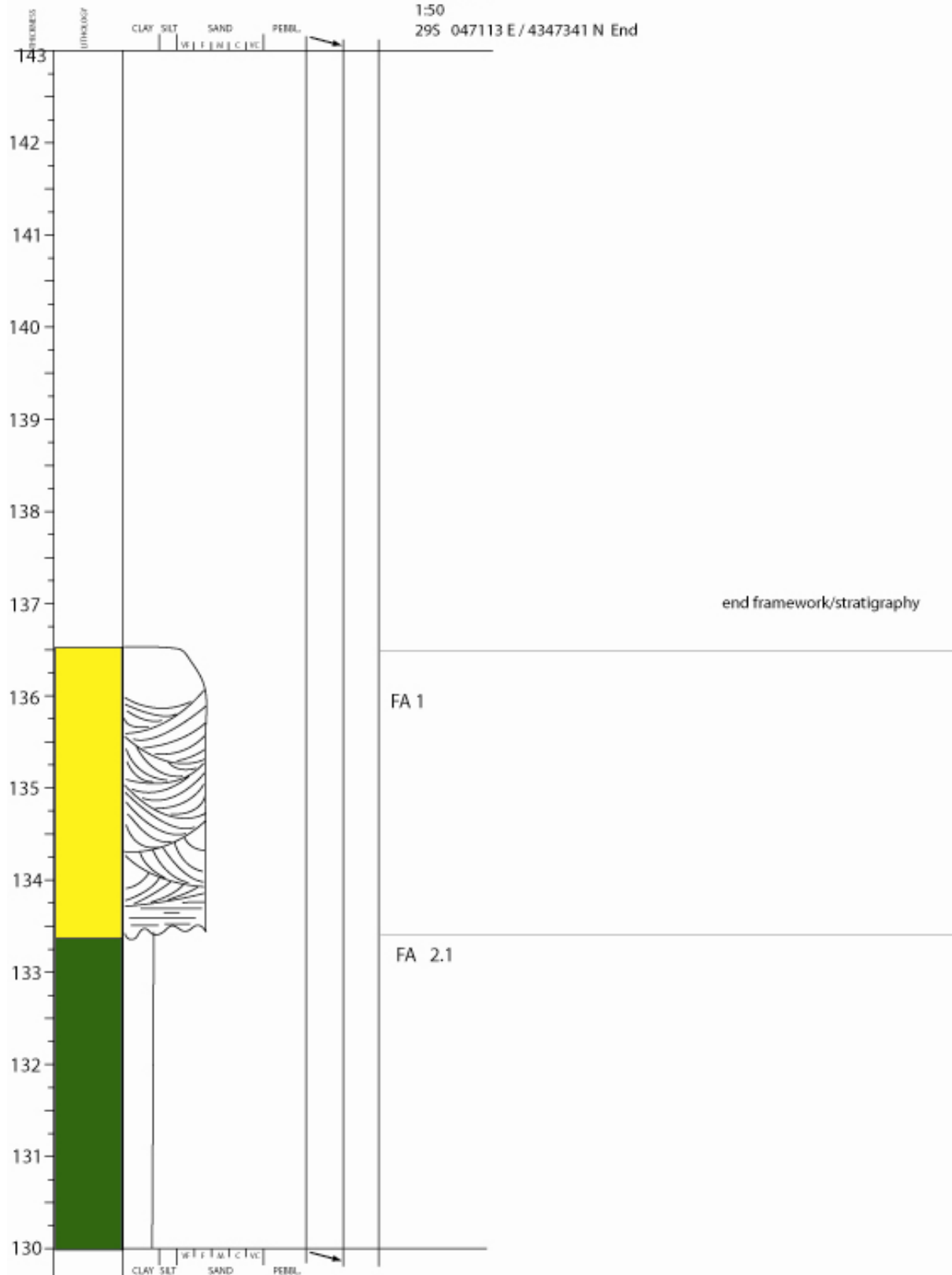
Lourinha S3, (FW 8/12)
 Framework_5 & 6
 1. okt 2006
 1:50
 29S 0471027 E / 4348044 N



Lourinha S3, (FW 10/12)
Framework_7, 1 & 2/4
5. okt 2006
1:50
29 S 0471080 E / 4347434 N

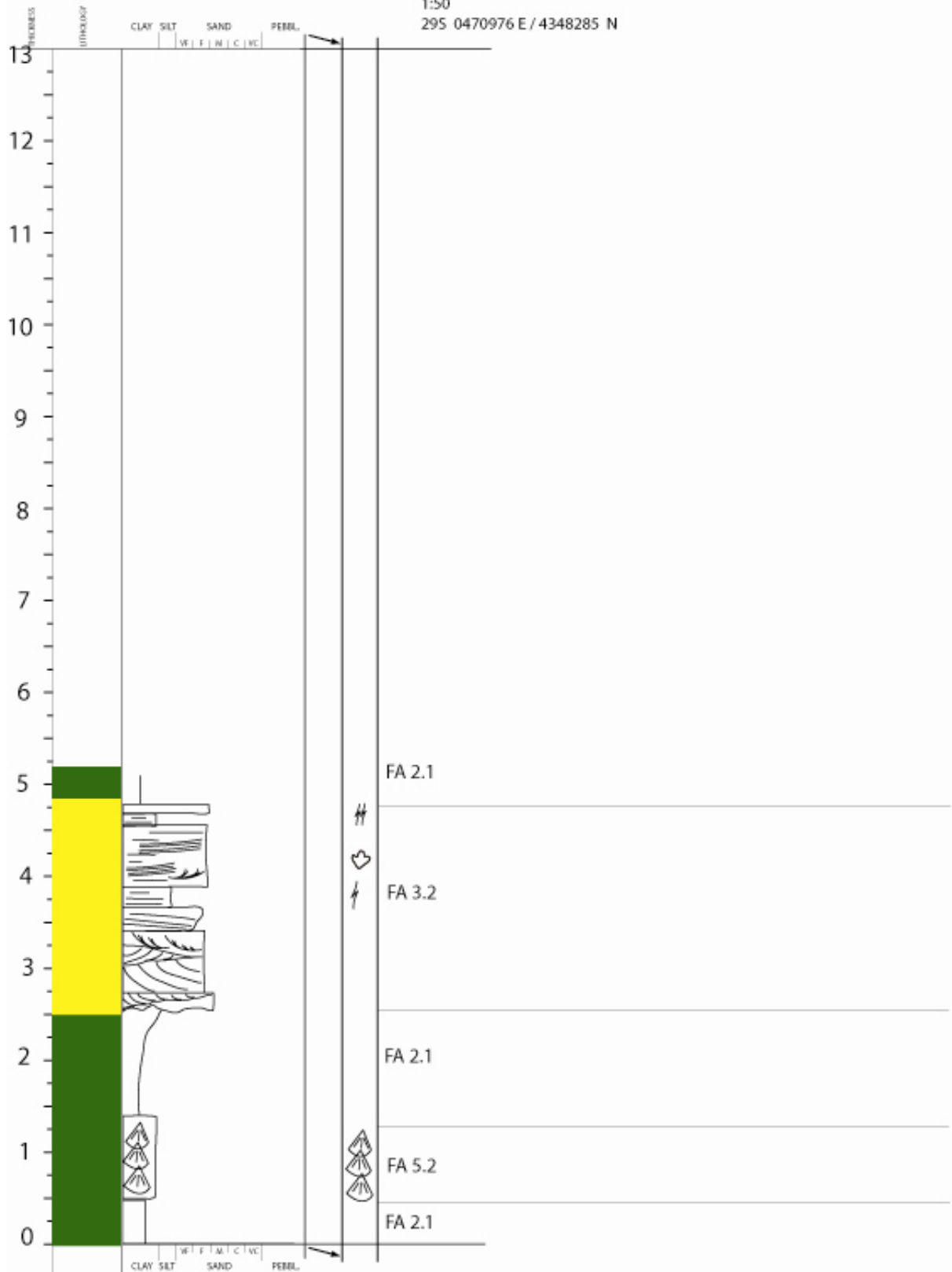


Lourinha S3, (FW 12/12)
Framework_7, 3 & 4/4
5. okt 2006
1:50
295 047113 E / 4347341 N End

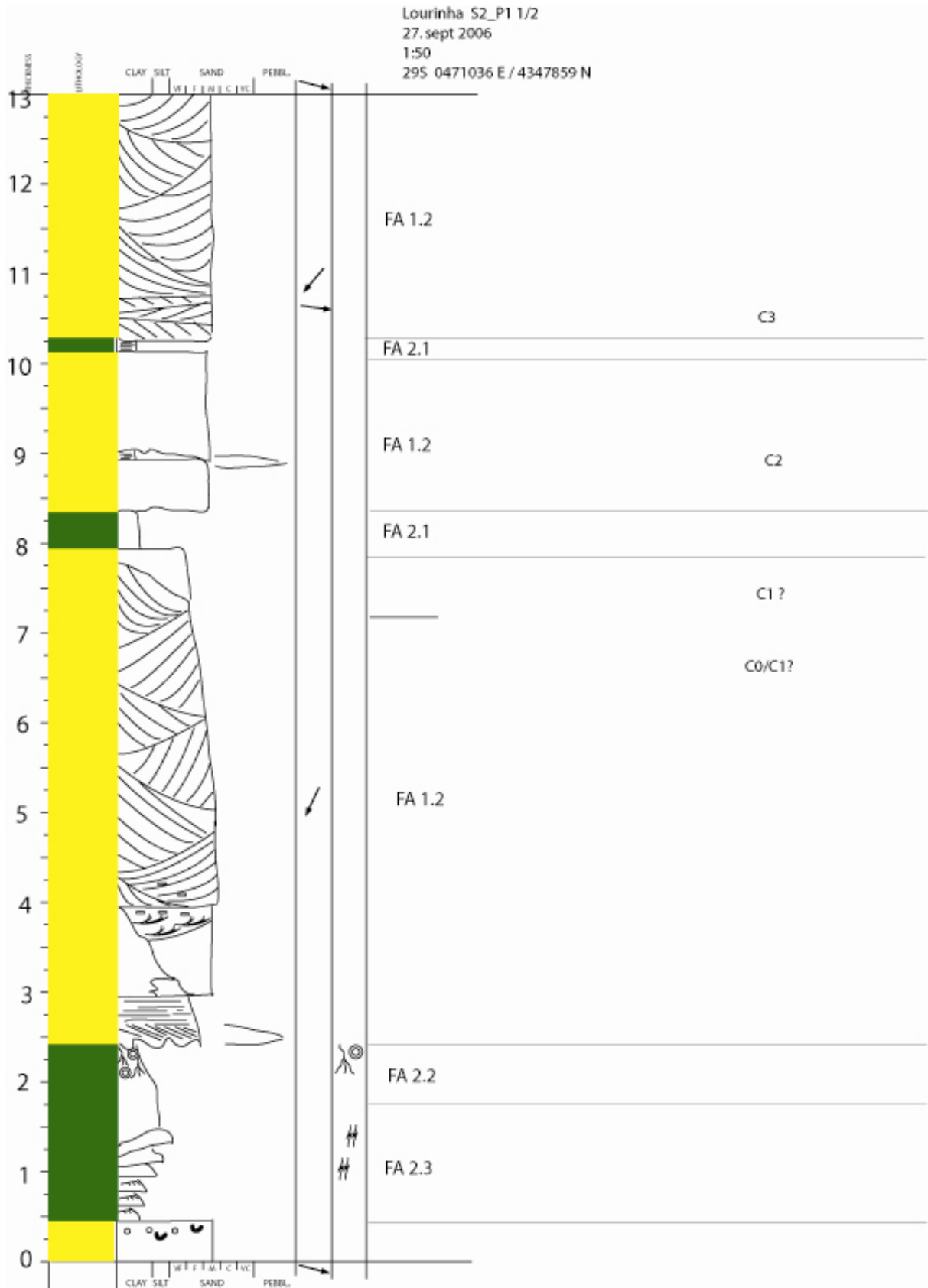


Log S1_P2

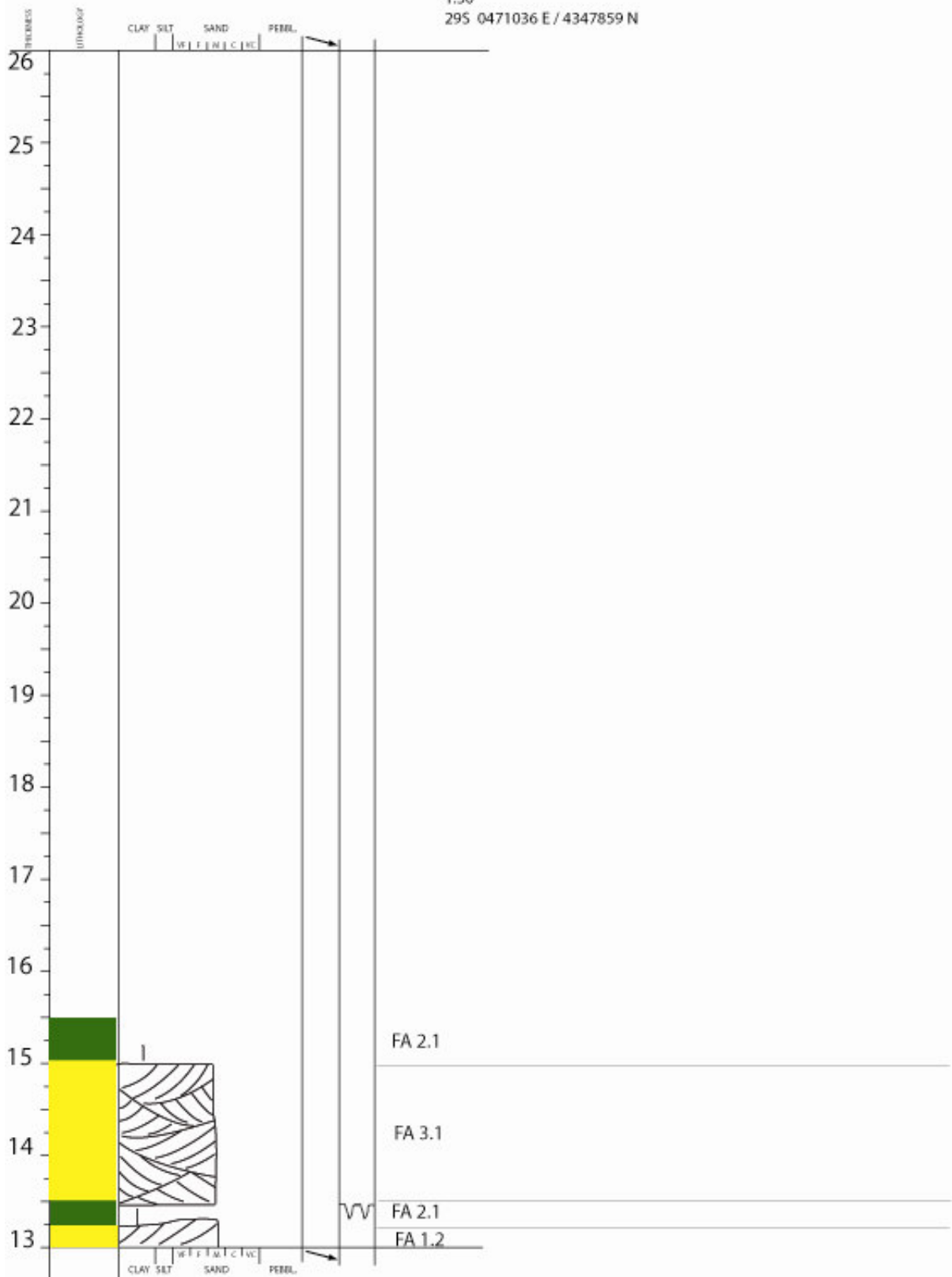
Lourinha S1_P2 1/1
03 okt. 2006
1:50
295 0470976 E / 4348285 N



Log S2_P1

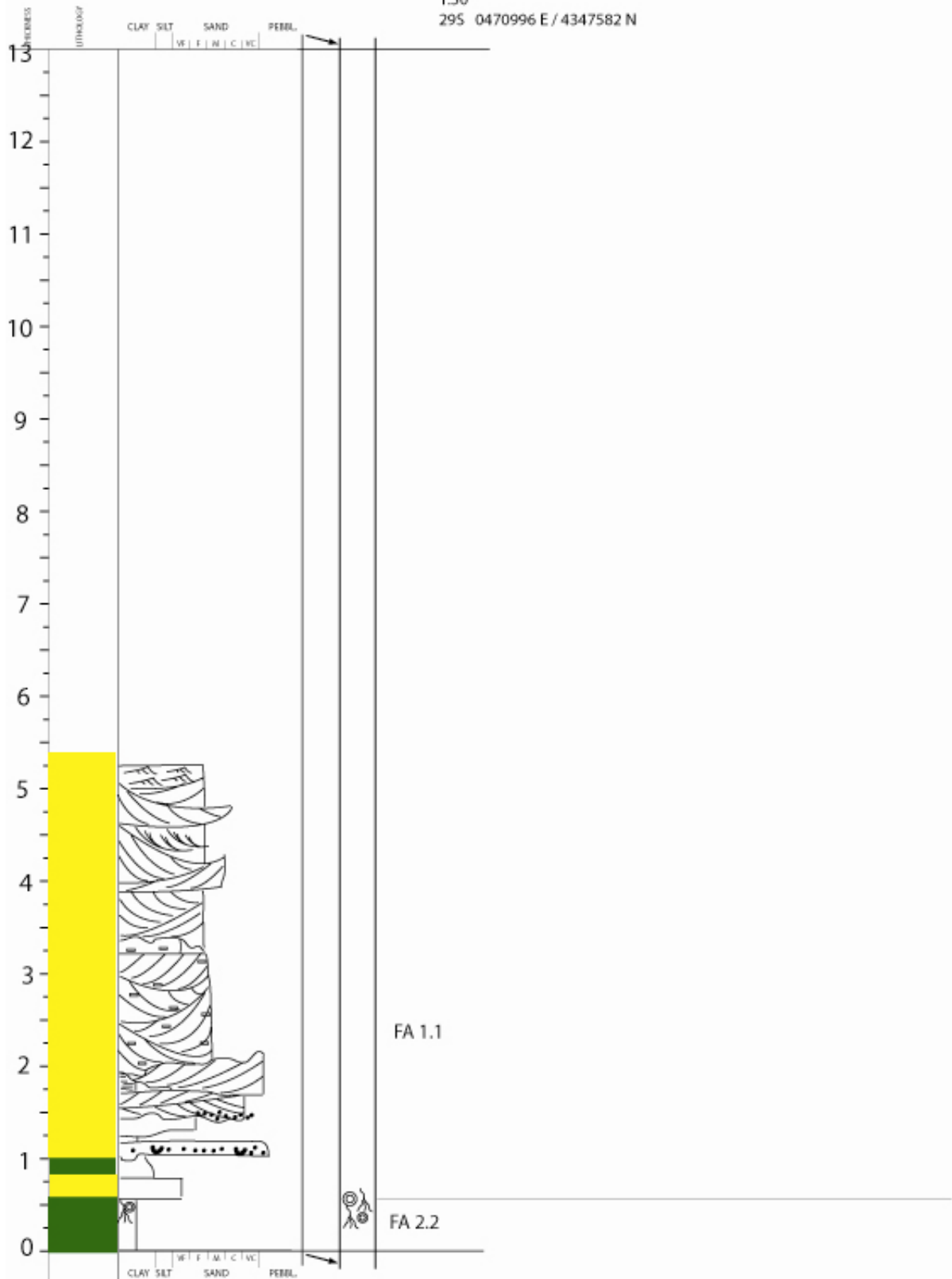


Lourinha S2_P1 3/3
27. sept 2006
1:50
295 0471036 E / 4347859 N

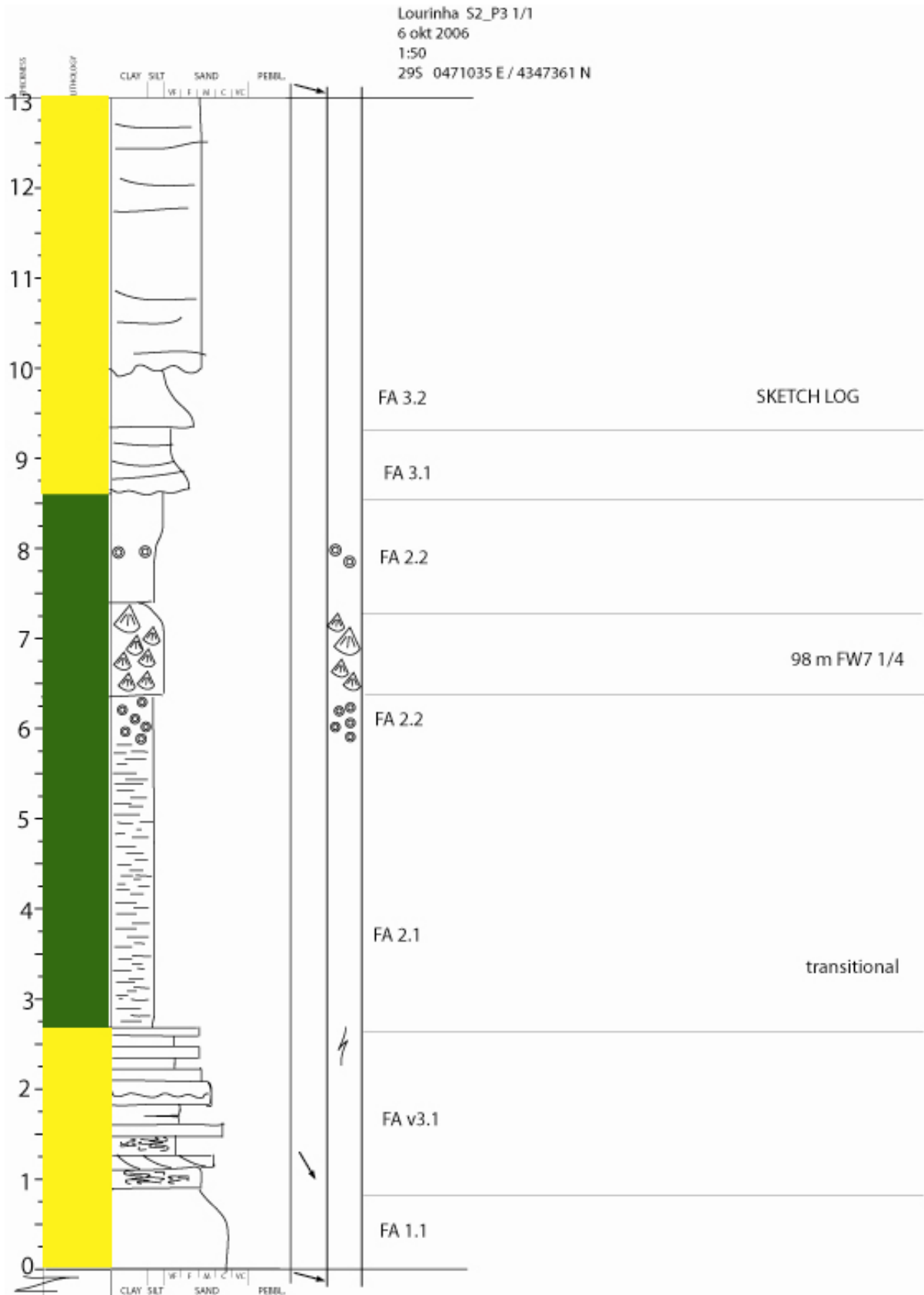


Log S2_P2

Lourinha S2_P2 1/1
6. sept 2006
1:50
29S 0470996 E / 4347582 N

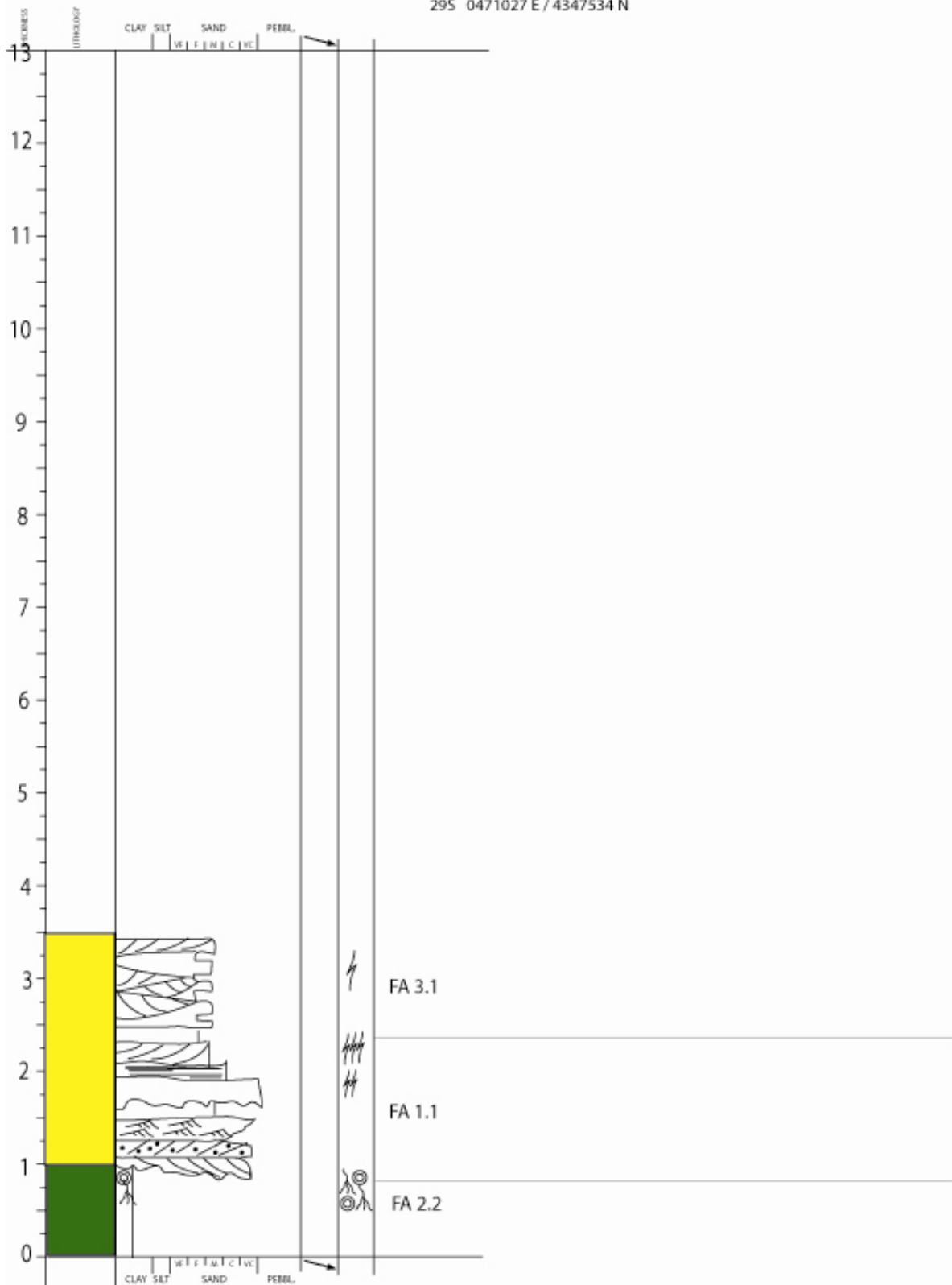


Log S2_P3

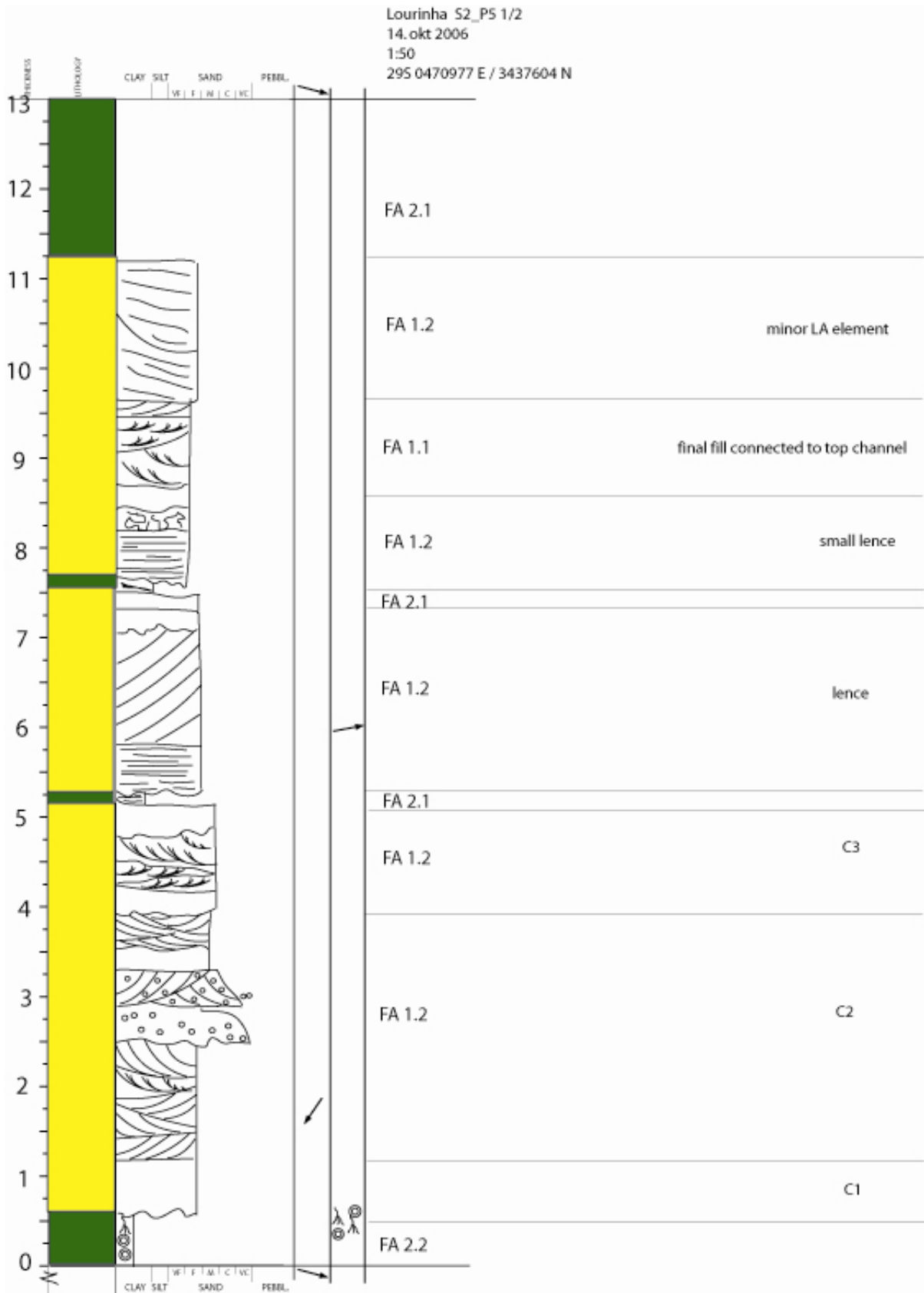


Log S2_P4

Lourinha S2_P4 1/1
5. okt 2006
1:50
29S 0471027 E / 4347534 N

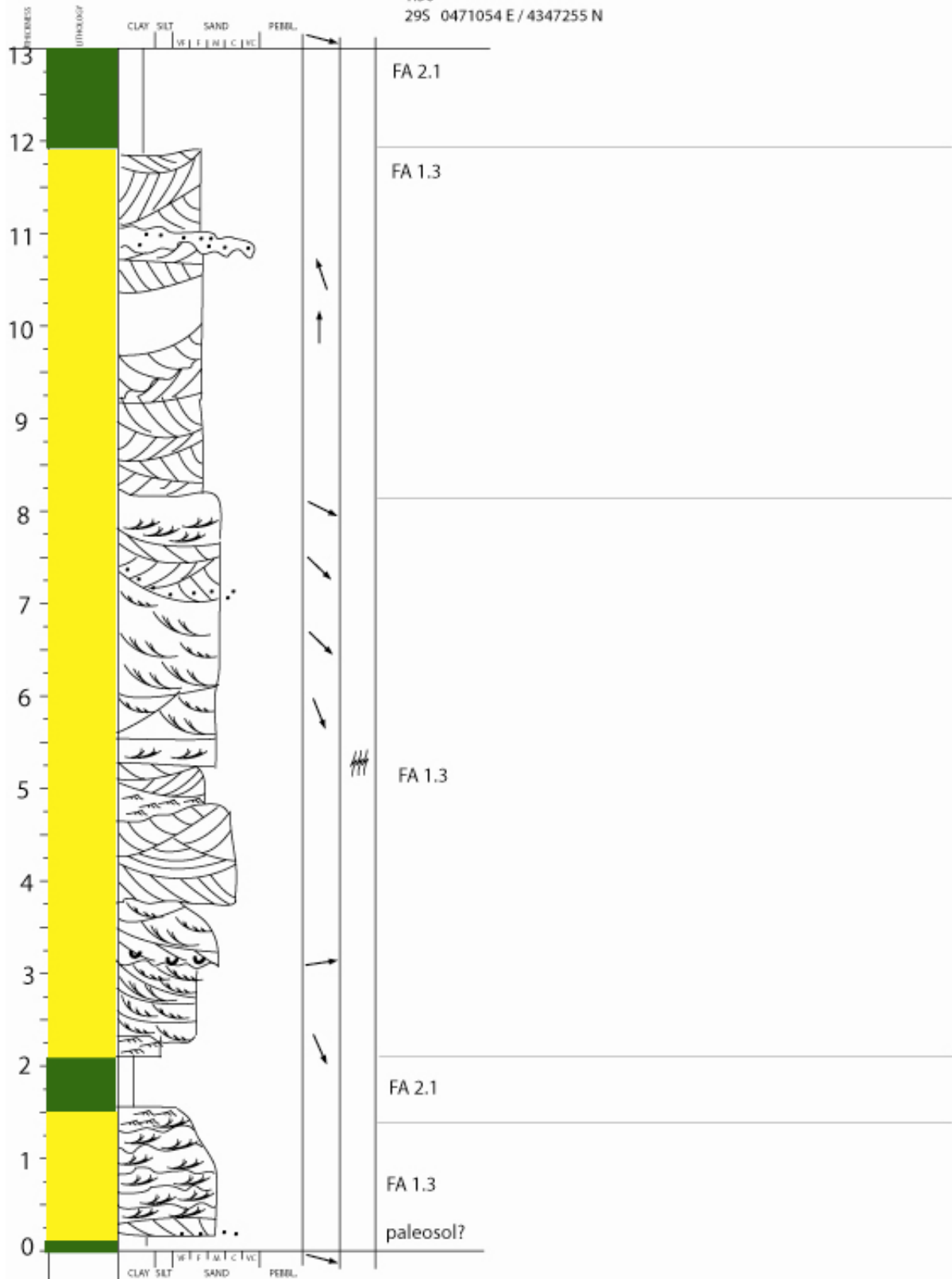


Log S2_P5

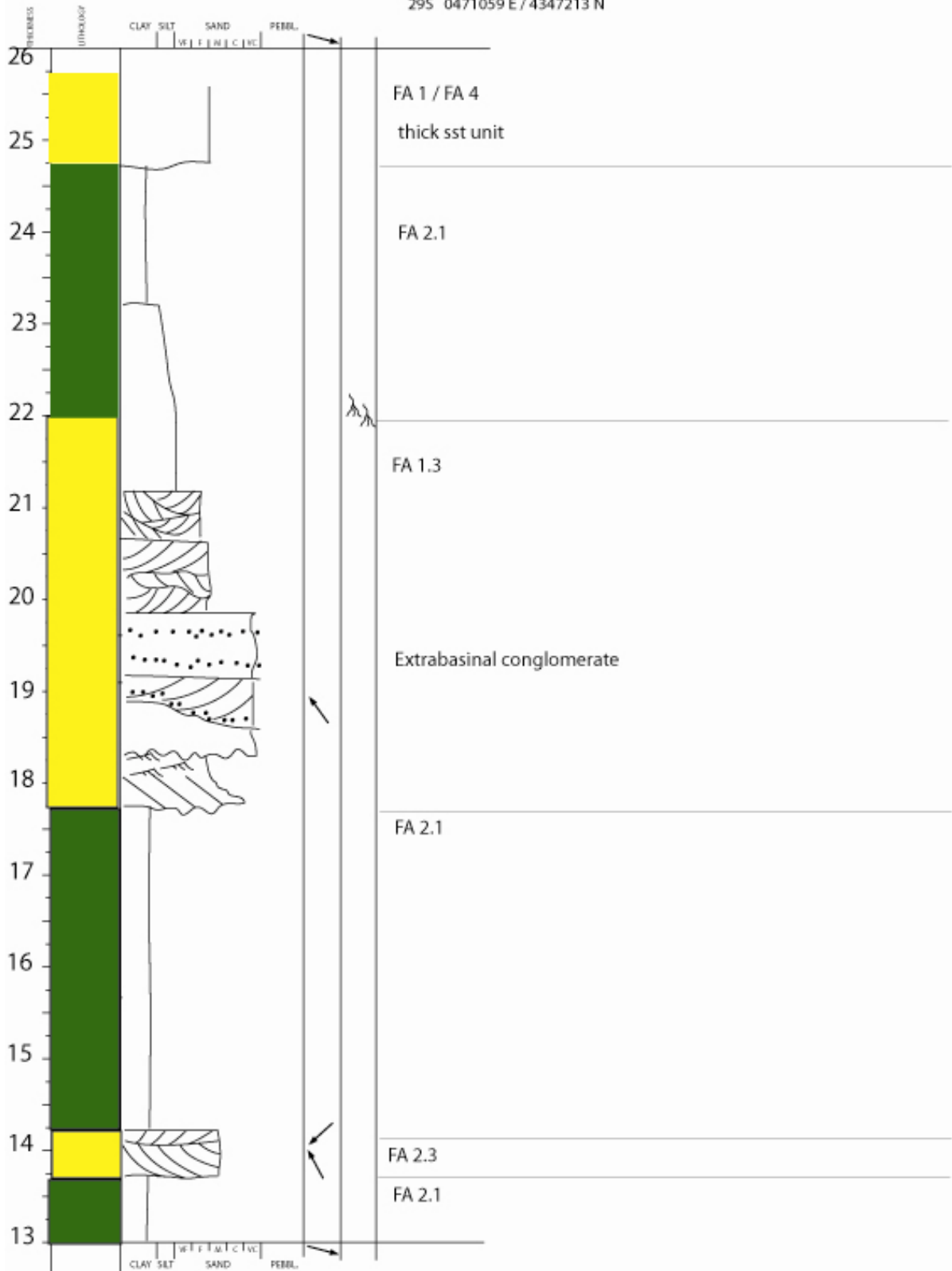


Log S3_P1

Lourinha S3_P1 1/2
 3. okt 2006
 1:50
 29S 0471054 E / 4347255 N

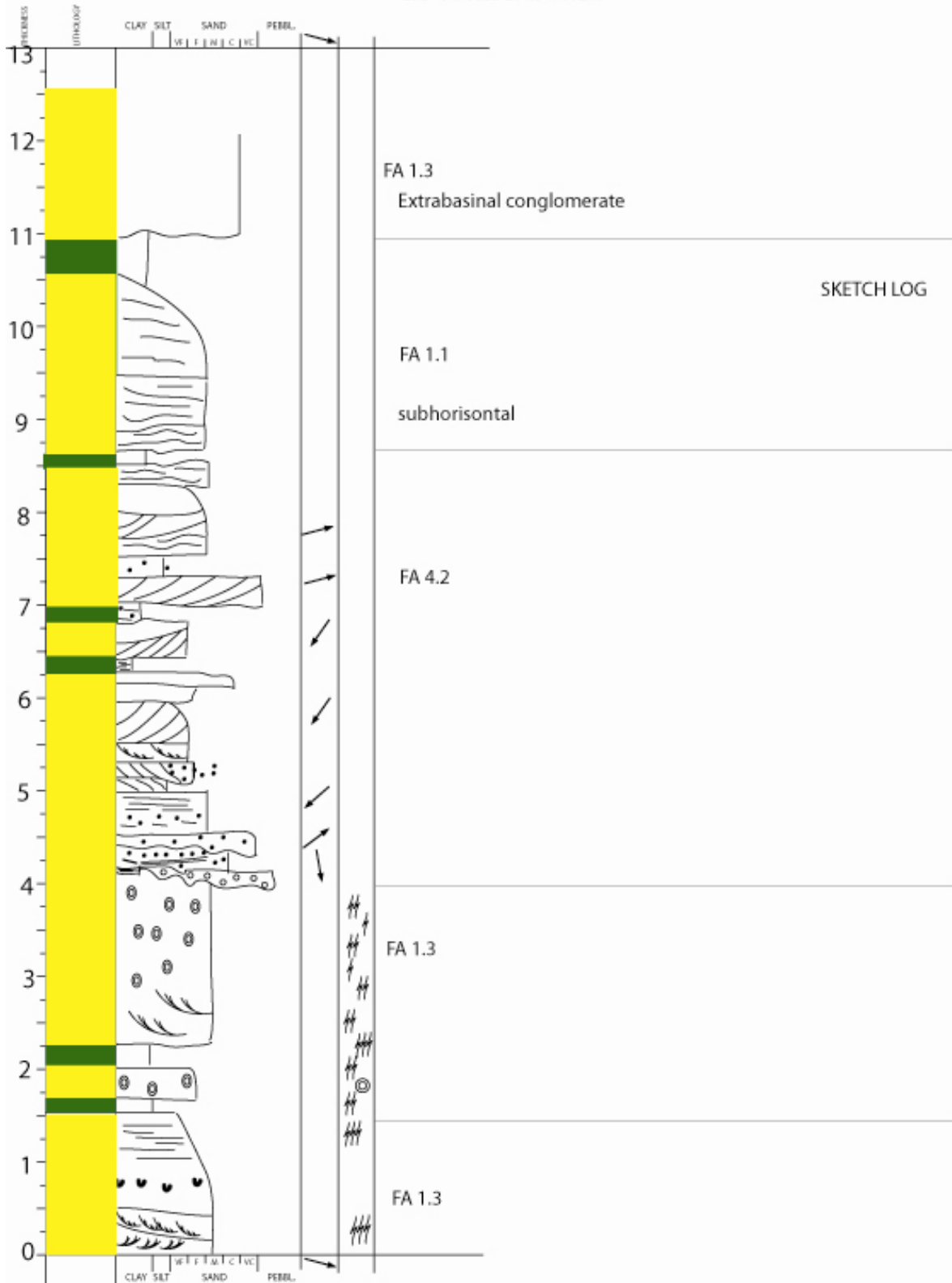


Lourinha S3_P1 2/2
 8. okt 2006
 1:50
 29S 0471059 E / 4347213 N



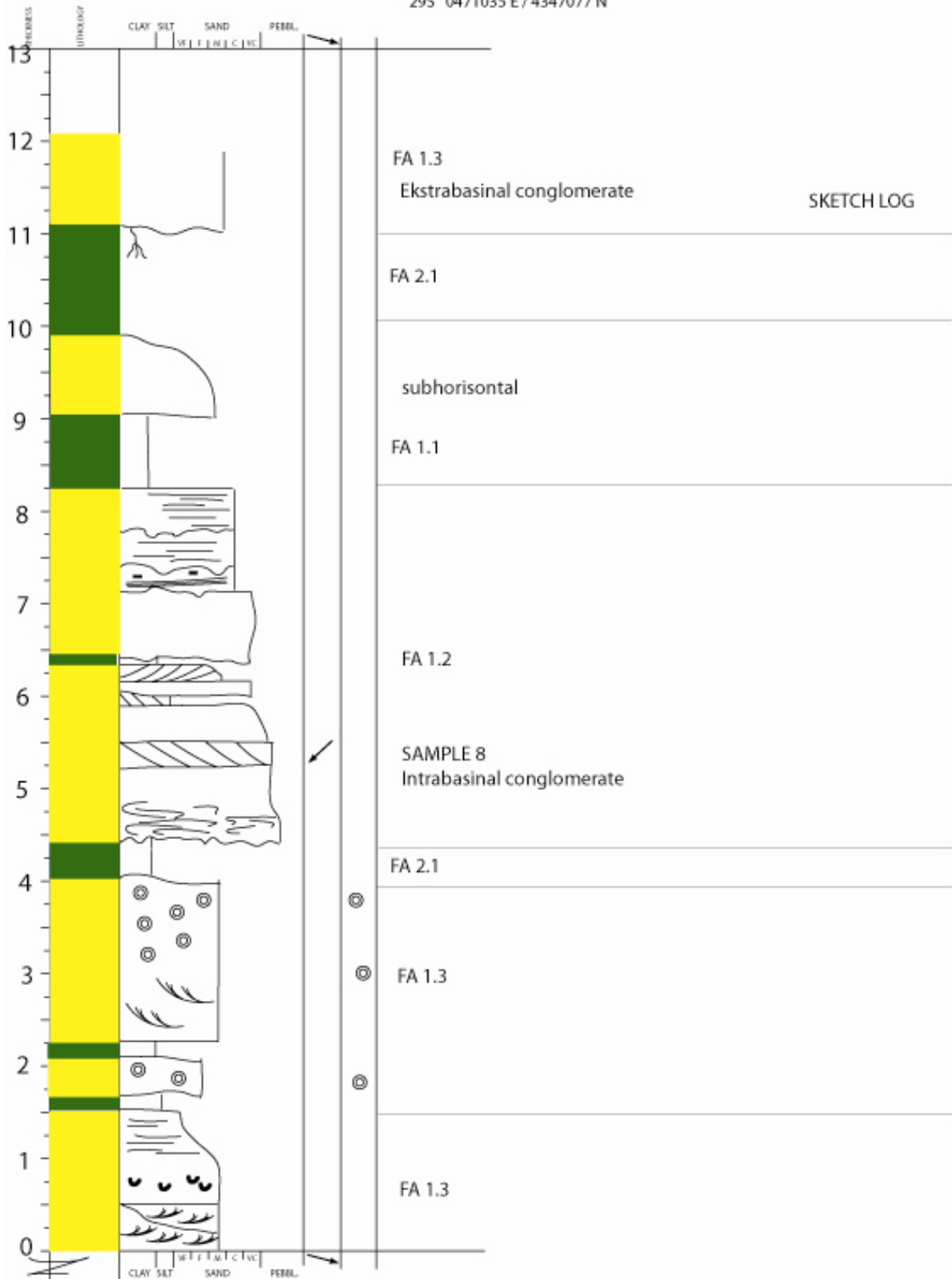
Log S3_P2

Lourinha S3_P2 1/1
 9. okt 2006
 1:50
 295 0471035 E / 4347112 N

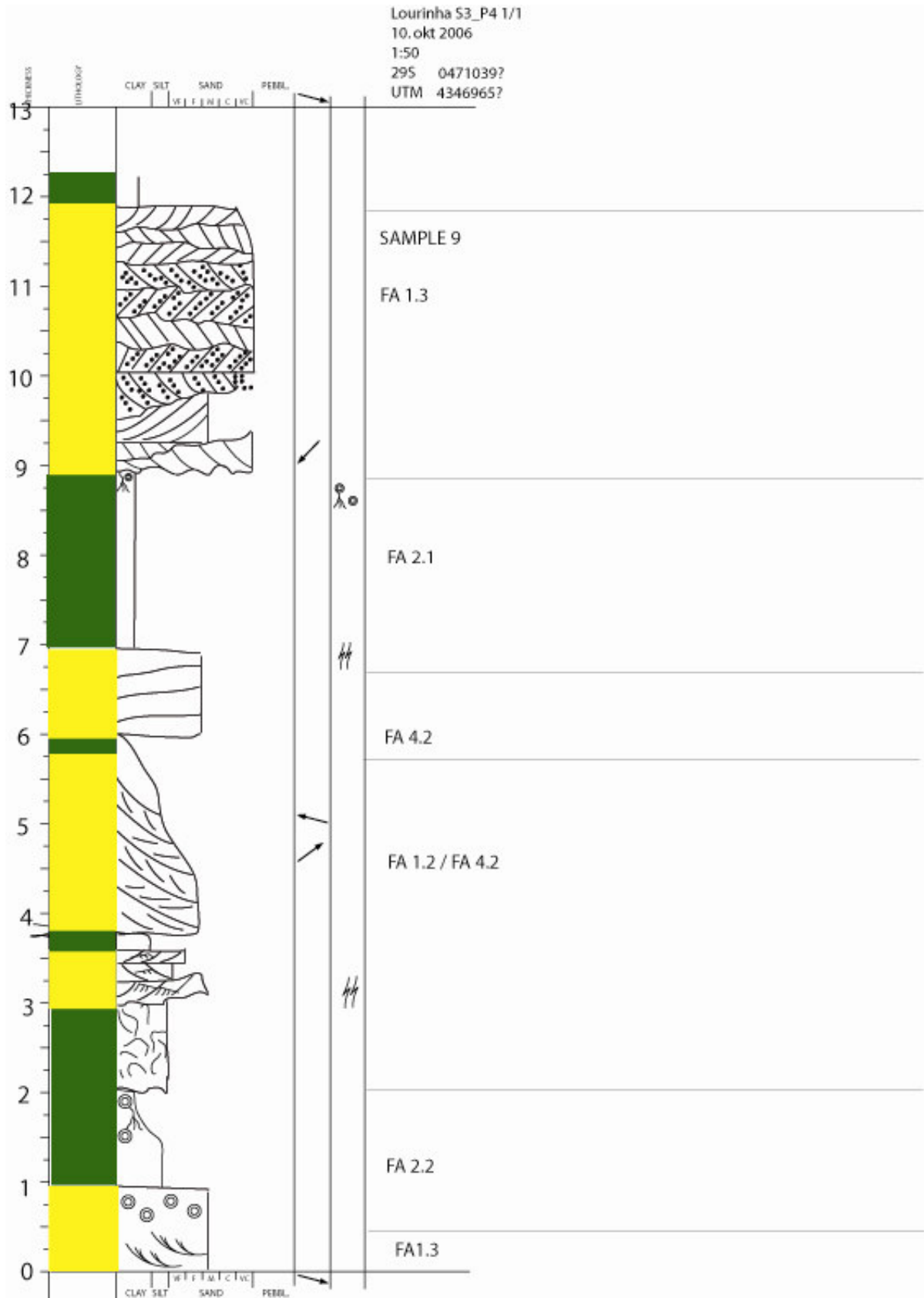


S3_P3

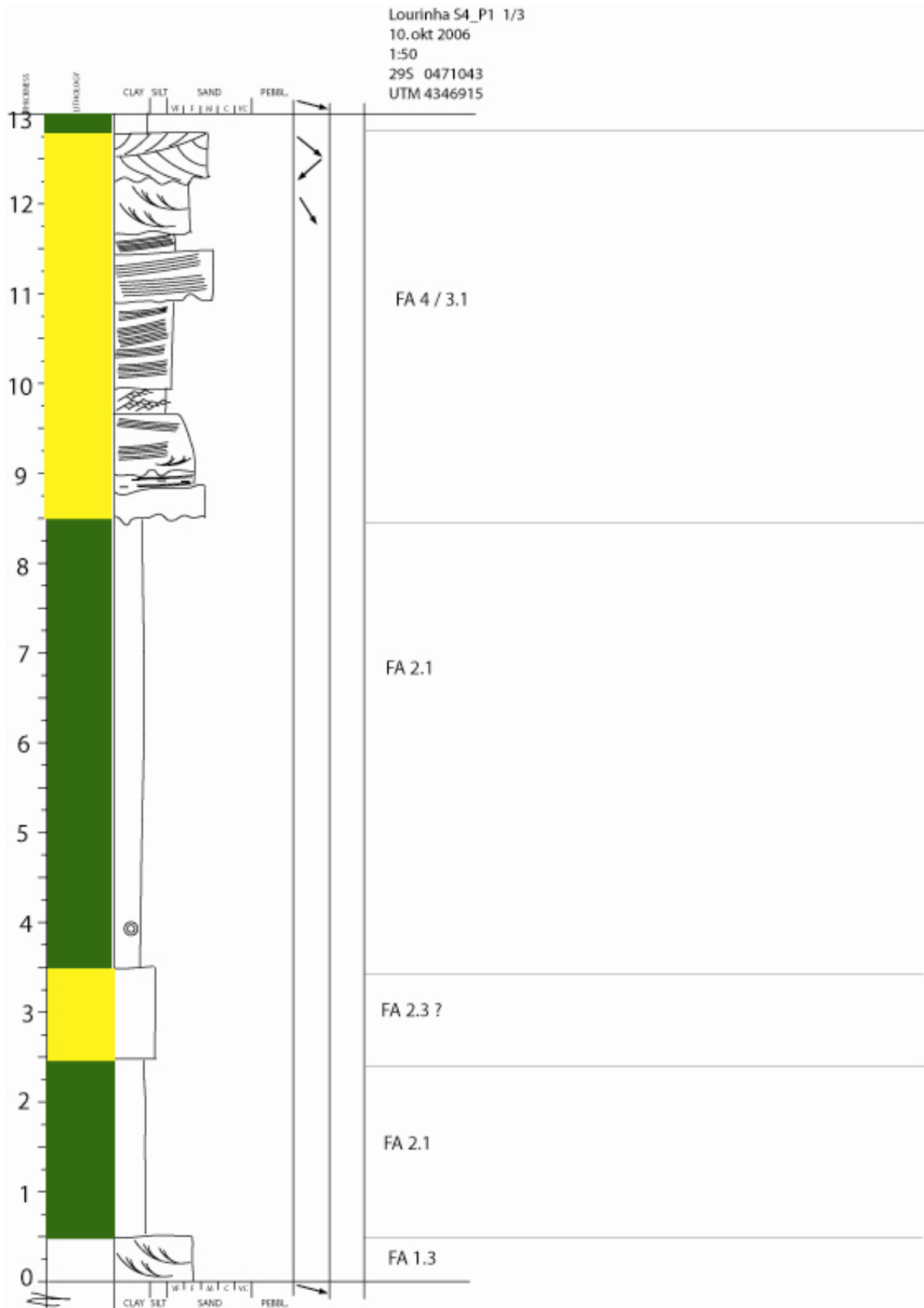
Lourinha S3_P3 1/1
 9. okt 2006
 1:50
 295 0471035 E / 4347077 N



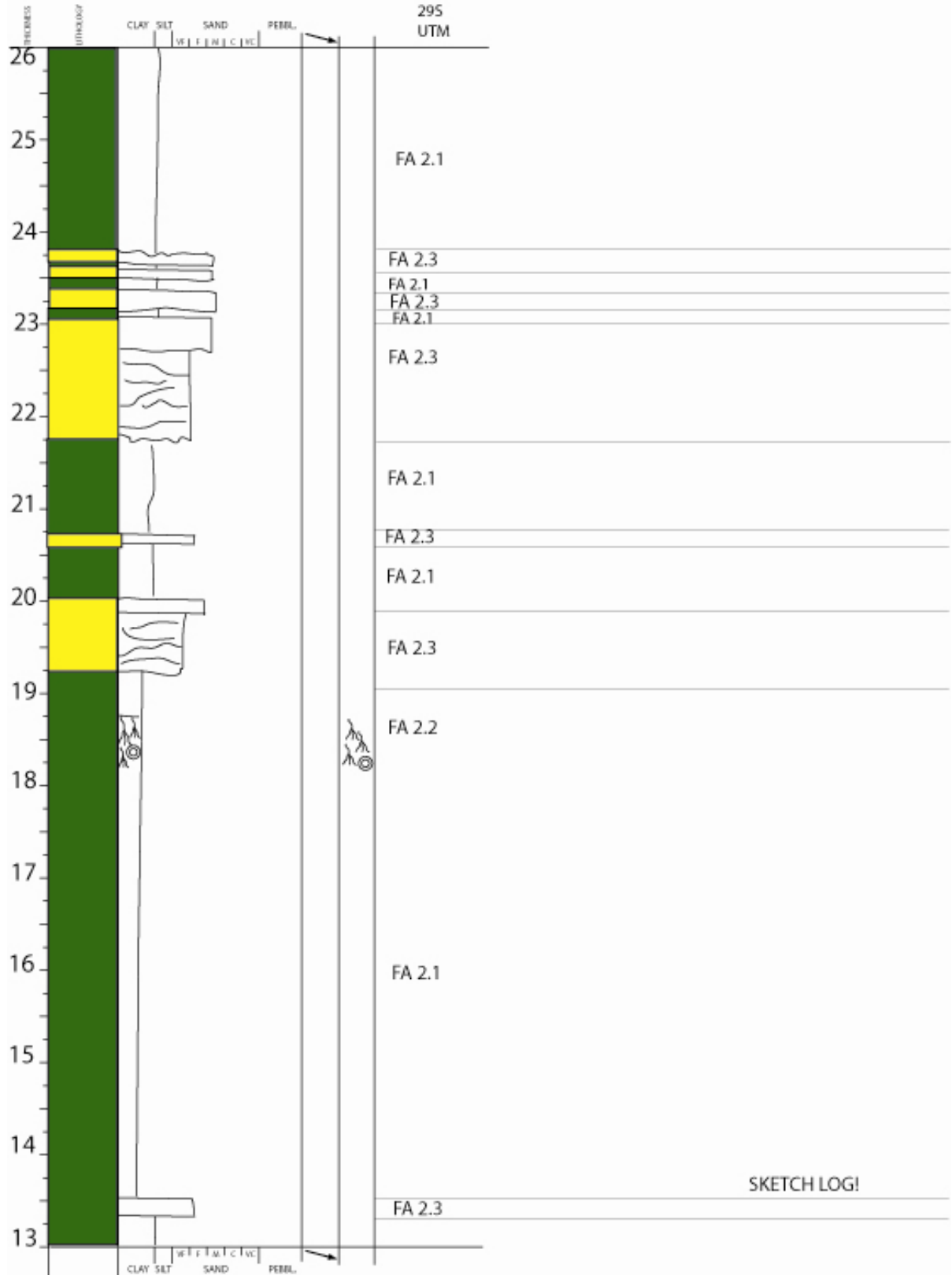
Log S3_P4



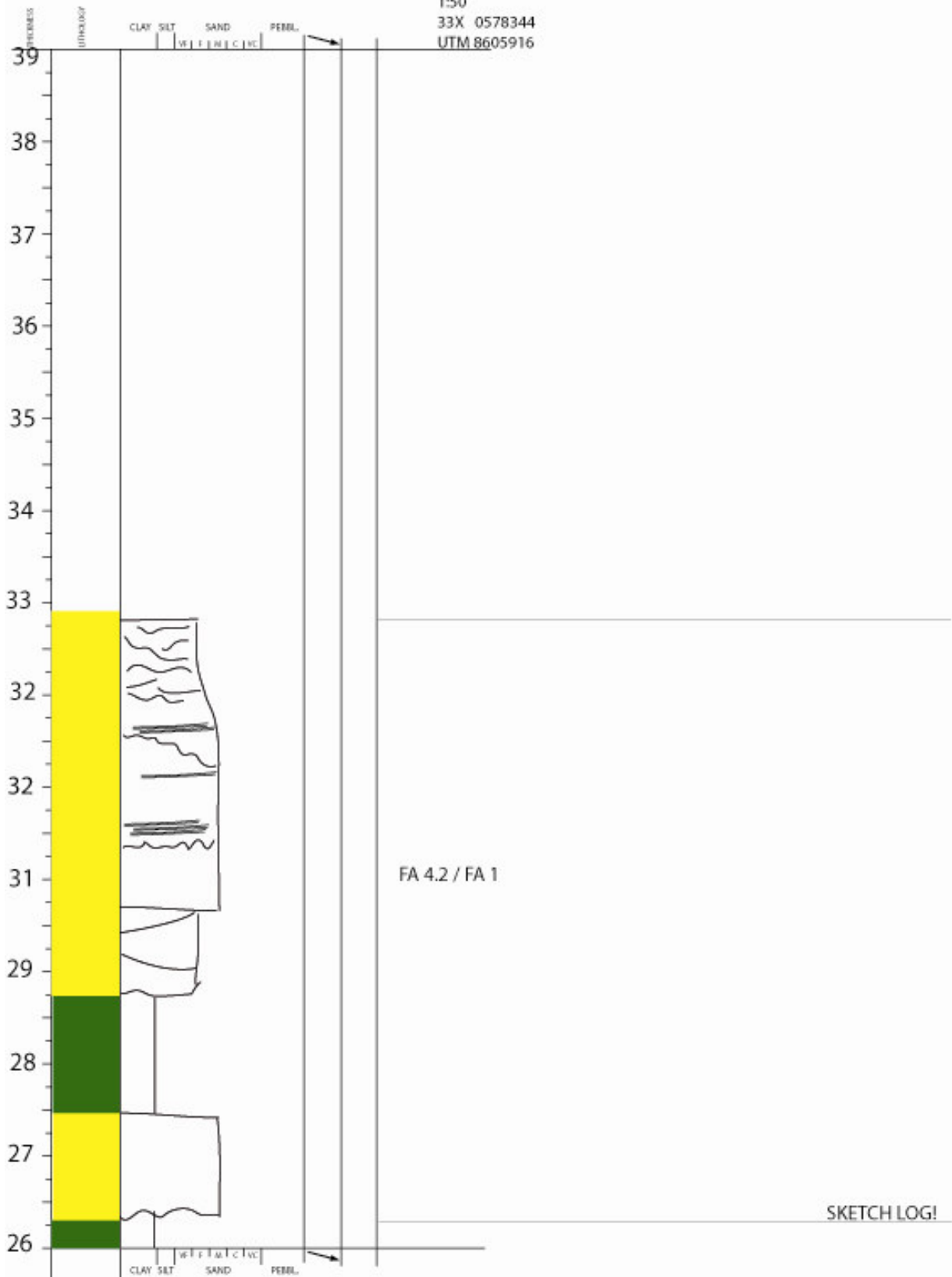
Log S4_P1



Lourinha S4_P1 2/3
 10. okt 2006
 1:50
 295
 UTM

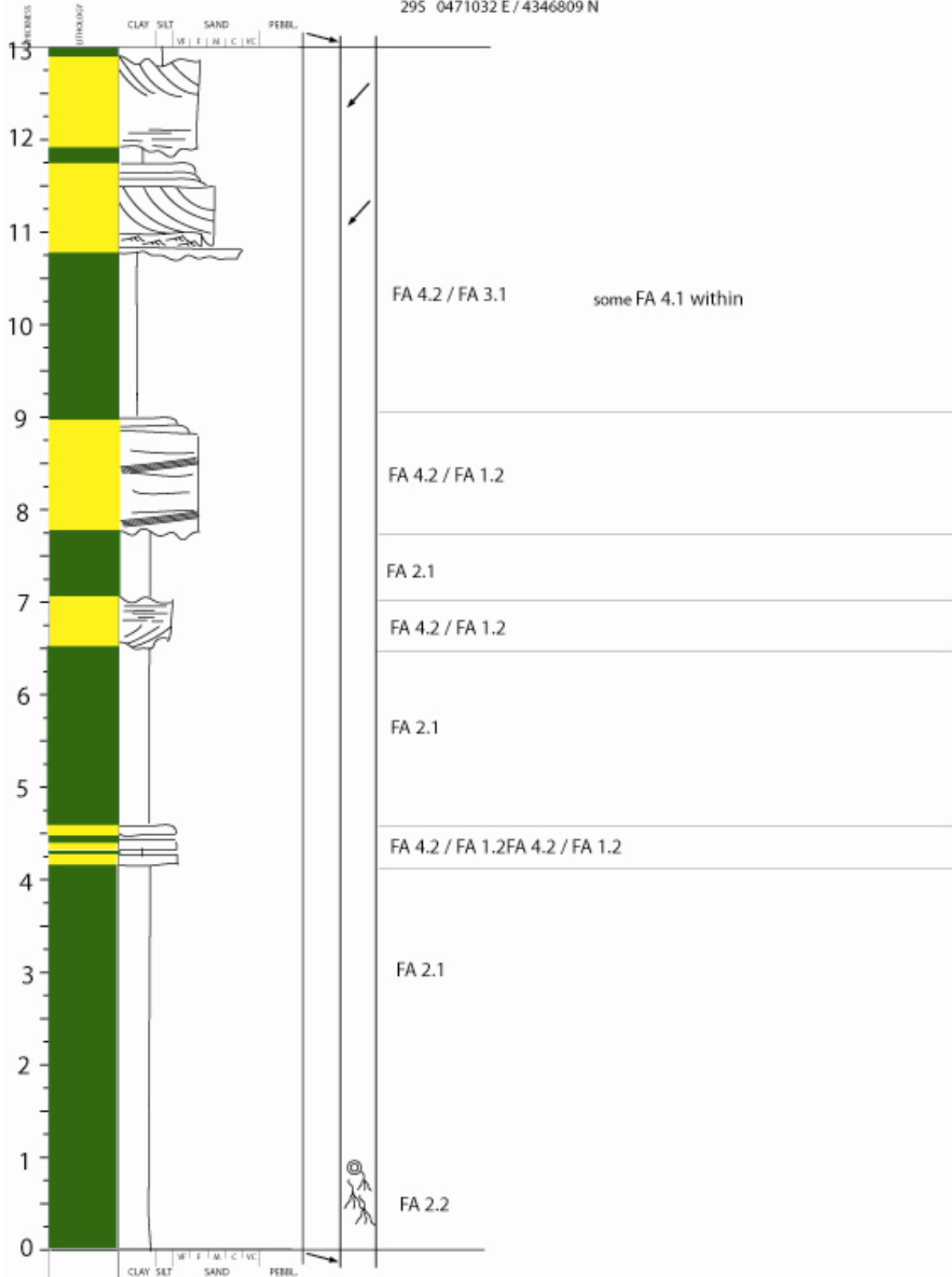


Lourinha 3/3
3. okt 2006
1:50
33X 0578344
UTM 8605916

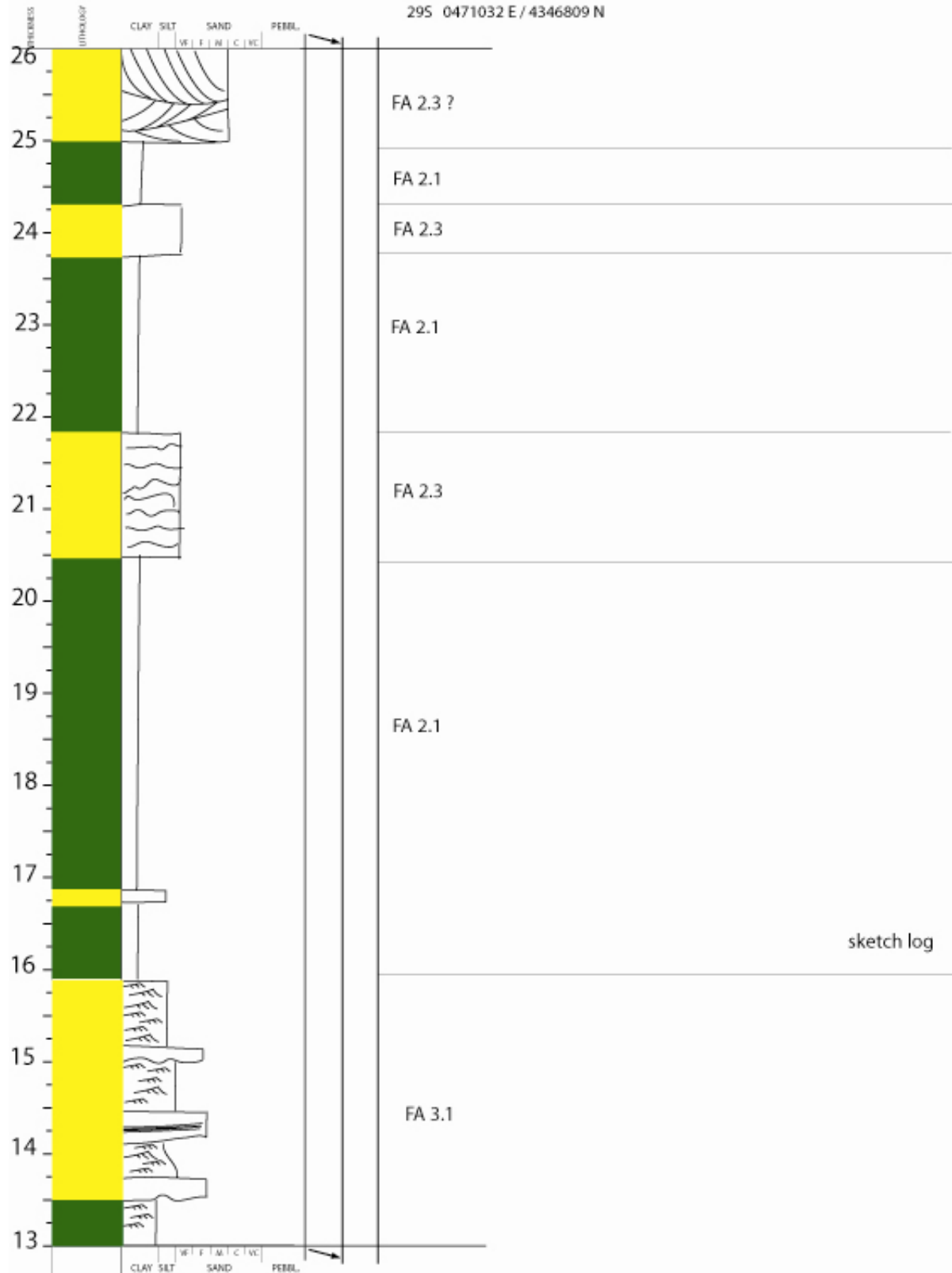


Log S4_P2

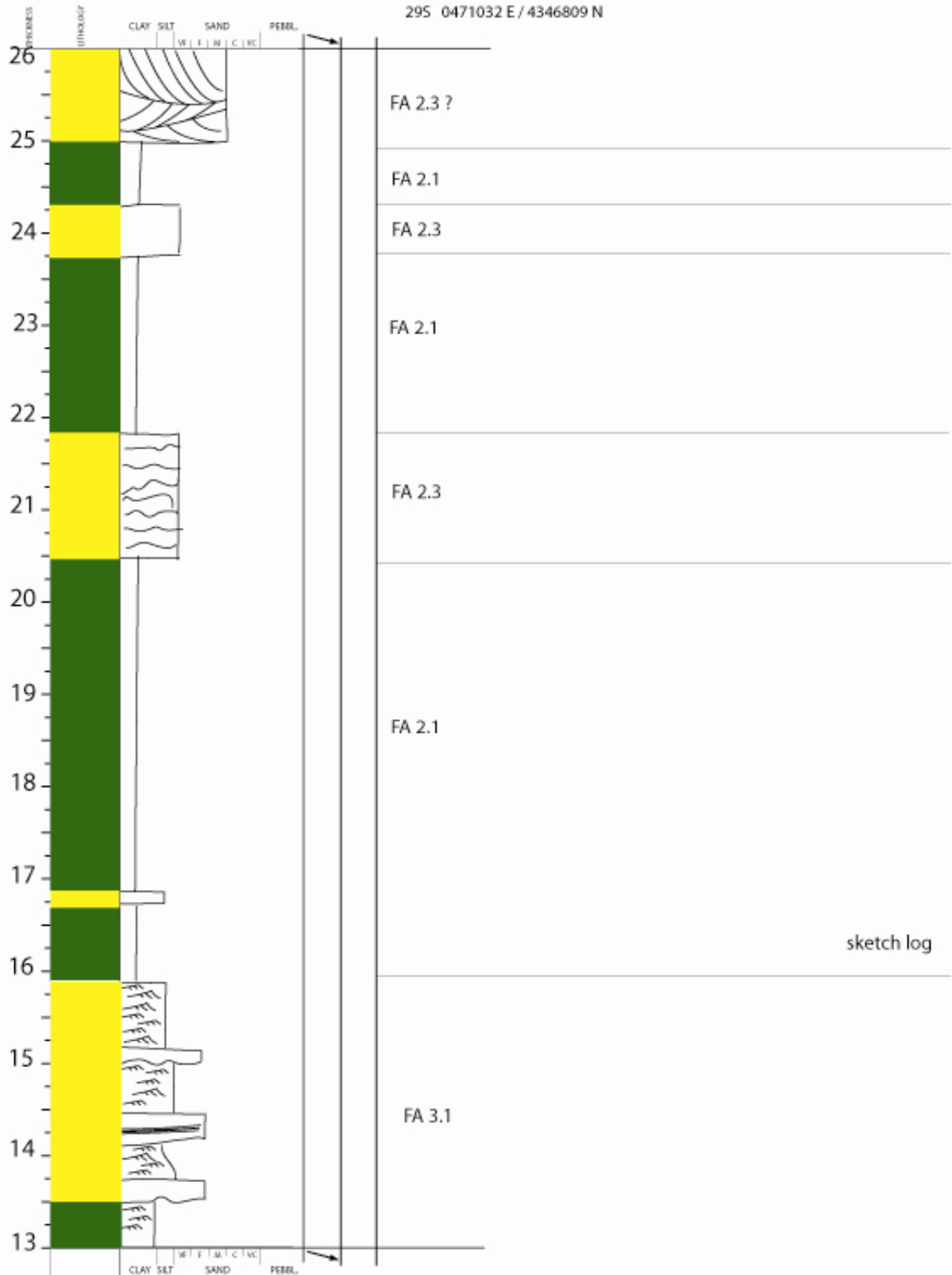
Lourinha S4_P2 1/3
 8. okt. 2006
 1:50
 295 0471032 E / 4346809 N



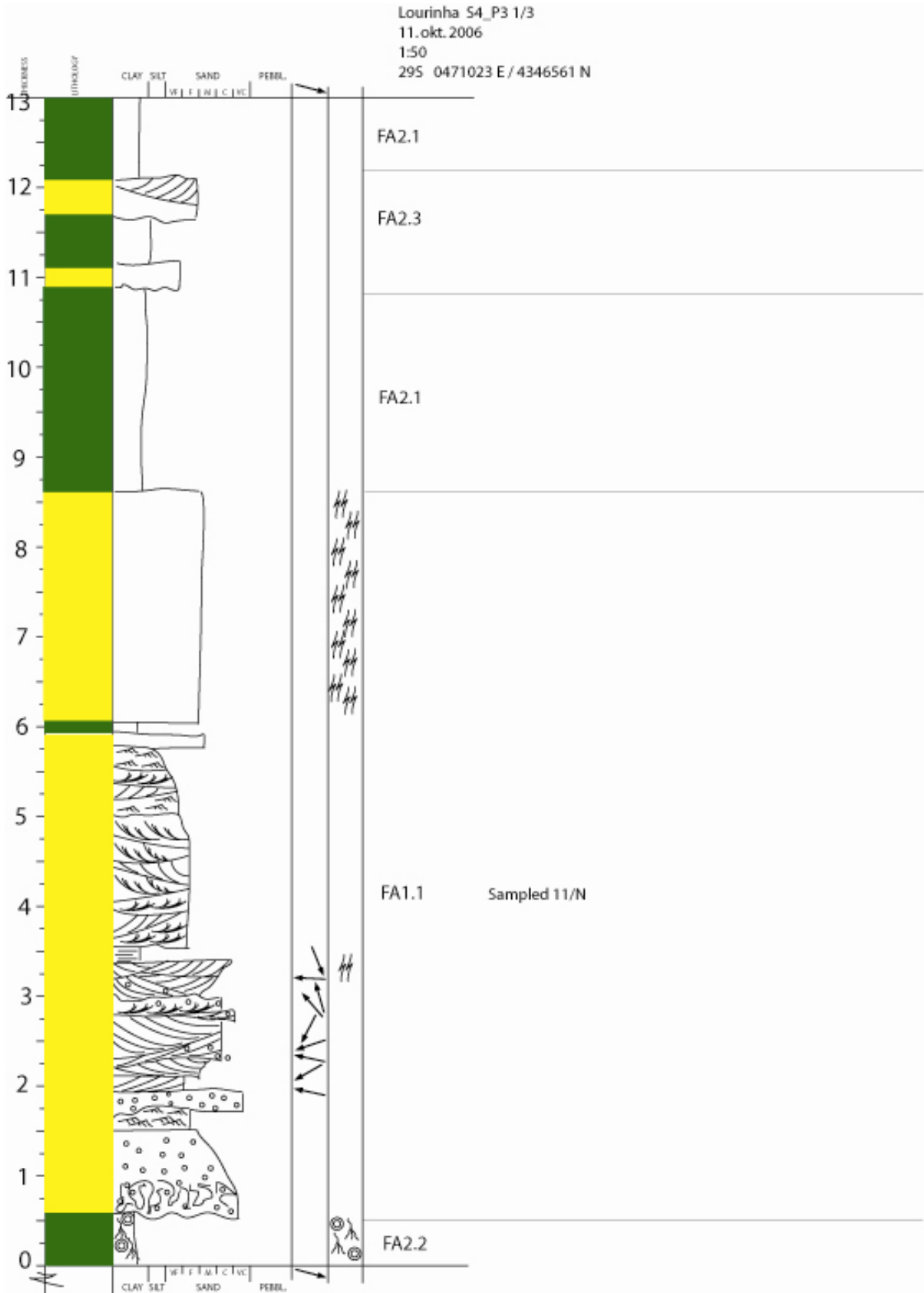
Lourinha S4_P2 2/3
 8.okt.2006
 1:50
 29S 0471032 E / 4346809 N



Lourinha S4_P2 2/3
 8.okt.2006
 1:50
 29S 0471032 E / 4346809 N



Log S4_P3



Lourinha S4_P3 2/3
11.okt.2006
1:50
29S 0471023 E / 4346561 N

